

Cranfield University

Matthew Moxon

Thermodynamic analysis of the Brayton-cycle gas-turbine under equilibrium chemistry assumptions

School of Engineering

PhD

Academic year: 2010/2011

Supervisor: Professor Riti Singh

July 2011

ABSTRACT

- A design-point thermodynamic model of the Brayton-cycle gas-turbine under assumptions of perfect chemical equilibrium is described.
- This approach is novel to the best knowledge of the author.
- The model uniquely derives an optimum work balance between power turbine and nozzle as a function of flight conditions and propulsor efficiency.
- The model may easily be expanded to allow analysis and comparison of arbitrary cycles using any combination of fuel and oxidizer.
- The model allows the consideration of engines under a variety of conditions, from sea level/static to >20 km altitude and flight Mach numbers greater than 4.
- Isentropic or polytropic turbomachinery component efficiency standards may be used independently for compressor, gas generator turbine and power turbine.
- With a methodology based on the paper by M.V. Casey, “Accounting for losses” (2007), and using Bridgman’s partial differentials, the model uniquely describes the properties of a gas turbine solely by reference to the properties of the gas mixture passing through the engine.
- Turbine cooling is modelled using a method put forward by Kurzke. Turbohaft, turboprop, separate exhaust turbofan and turbojet engines may be modelled. Where applicable, optimisation of the power turbine and exhaust nozzle work split for flight conditions and component performances is automatically undertaken.
- The model is implemented via a VB.net code, which calculates thermodynamic states and controls the NASA CEA code for the calculation of thermodynamic properties at those states. Microsoft Excel[®] is used as a graphical user interface.
- It is explained that comprehensive design-point cycle analysis may allow novel approaches to off-design analysis, including engine health management, and that further development may allow the automation of cycle design, possibly leading to the discovery of opportunities for novel cycles.

ACKNOWLEDGEMENTS

This work would not have been possible without the generous help and support of many people. As I write this at the literal, as well as the figurative, eleventh hour, I am all-too aware of the risk that I might inadvertently forget somebody – for this I can only offer my humble apologies.

My parents have provided me with constant support for all 27 years of my life; but for their love and support I could not possibly have stayed the course.

My tentative steps into the field of software engineering were guided by my life-long friend John Hewson; if the code described herein is good, it is because he taught me well.

The University in general and my supervisor, Professor Riti Singh, in particular deserve my thanks, firstly for giving me the opportunity to pursue a PhD, secondly for the freedom they have given me, and thirdly for tolerating me for almost four years since my first arrival in August 2007 (is it really that long ago?). I hope that this thesis was worth the wait!

I would also like to thank Professor Doug Probert for his generosity in reading several drafts of my thesis, and providing advice on writing style (as well as the kind gift of his book on the subject). Needless to say, whatever stylistic *faux pas* remain are entirely my responsibility!

In the first year of my PhD, Dr Eric Goodger was kind enough to give me a copy of his book *Transport Fuels Technology*, which contains the clearest general description of thermodynamics that I have found, and for which I am most grateful.

My supervisor's secretaries, (in chronological order) Rachel Smith, Sam Broe and Charlotte Donald have also gone far above and beyond the call of duty in helping me to understand what to do, where to be, and when to be there. Without them I would have been utterly lost.

The Cranfield University Musicians' Society, and especially my various band-mates over the years have played no small part in keeping me sane over the years. *Rock on!*

I would also like to thank John Farley, and the Schools Aerospace Challenge/University Aerospace Challenge organisation for the opportunities they have given me over the years, as well as all those in the Industry, and especially Rolls-Royce, who have encouraged me over the years, in particular Tony Hewitt and John Whurr. Another early source of inspiration was the opportunity to fly during my school days as a member of the CCF(RAF); as Leonardo da Vinci is reported to have said:

When once you have tasted flight, you will forever walk the earth with your eyes turned skyward, for there you have been, and there you will always long to return.

It would be remiss of me not to acknowledge the Weeding family for their extraordinary generosity in donating the late Reg Weeding's library to me after his untimely death.

This thesis is dedicated to the memory of the late Reg Weeding, whose patient hours spent answering my endless questions regarding all aspects of aeronautical engineering provided both the inspiration for, and the foundation of, my studies.

List of Contents

Abstract	ii
Acknowledgements	iii
List of Contents.....	v
List of Figures	viii
Notation.....	x
Introduction.....	12
A Brief History of <i>practical</i> thermodynamics.....	12
A Brief History of <i>theoretical</i> thermodynamics.....	14
The purpose & applications of this work.....	15
An overview of Thermodynamics	16
Classical Thermodynamics	16
Historical context	16
The 1 st Law of Thermodynamics.....	18
Carnot and the Heat Engine.....	18
The Thermodynamic Cycle	19
The 2 nd Law of Thermodynamics and the Carnot Cycle.....	20
Thermodynamic processes	21
Standard expressions for the performance of selected thermodynamic cycles.....	26
The simplifying assumptions of classical thermodynamics.....	33
Problems associated with the simplifying assumptions of classical thermodynamics	37
Explanations for the use of unrealistic assumptions in the real world.....	46
Wheels within Wheels – lessons from the Orrery	47
Equilibrium Thermodynamics	48
A brief history of equilibrium chemistry	48
The NASA Chemical Equilibrium with Applications (CEA) Code	49

Limitations of Equilibrium assumptions.....	52
An overview of the Brayton Cycle gas turbine.....	54
Introduction	54
General arrangement.....	54
Intake	57
Compressor	58
Casey and Compressor efficiency.....	59
Casey's states	60
Combustor	60
Turbine	62
Turbine cooling	62
Casey and turbine efficiency	64
Nozzle.....	65
Turbine Analogy	65
Froude Efficiency.....	65
Casey and power turbine efficiency	66
Shaft Power Cycles	66
Thermodynamic modelling of the Brayton cycle gas turbine.....	66
Historical background.....	66
Methods in current use.....	67
TURBOMATCH	67
GASTURB	67
A note on the limitations of the open literature	68
The “ExcelCEA” model.....	69
The name “ExcelCEA”	69
Overview	69
Technological context.....	72
CEA Output.....	74

Calculation method	75
Background.....	75
Known parameters – the input file	78
Unknown parameters – building the model.....	79
A sample cycle calculation.....	86
Ambient conditions	86
Freestream conditions	87
Intake Delivery	88
Compressor Delivery	88
Combustor Front Face.....	92
Combustor delivery	92
Cooling Bleed Extraction.....	93
Mix NGV Cooling	95
Gas Generator Turbine.....	95
Mix Rotor cooling	98
Power turbine, Nozzle and Propulsor.....	98
Power turbine	102
Nozzle	104
Performance calculation	105
Results	108
Validation	110
Procedure	111
Predictive modelling.....	114
Mach 0.80, 11000 m altitude	114
Mach 2.0, 18000 m altitude	125
Stationary power	133
Thermodynamic surfaces	138
A note on Maxwell and the origin of thermodynamic surfaces.....	138

Discussion	138
Comparison with Kurzke's conclusions	139
Possibilities for further investigation	139
Modelling of additional processes	139
Capacity to handle additional phases	139
Extension of the <i>thermo.lib</i> database	140
Additional thermodynamic cycles	140
Rational automated searches for novel thermodynamic cycles	140
Extension of the ExcelCEA code to off-design-point cases	140
Publication	142
References	142
Bibliography	145
Appendices	146
Appendix A – CEA input and output files illustrating the extreme reversibility associated with equilibrium chemistry assumptions	146
A four species model of air evaluated at 2000 K, 10^5 Pa	146
Output file demonstrating equilibrium cooling of the products of the above reactions	149
Appendix B – the author's Patent	155

LIST OF FIGURES

Figure 1 – Google Ngram of selected thermodynamic cycles, English one million corpus, smoothing = 5.	13
Figure 2 - A relatively simple orrery modelling Mercury, Venus, Earth and the Moon (image credit: Kaptain Kobold, 2006, Flickr <i>via</i> Wikipedia).....	47
Figure 3 - Energy flows within a generalised Brayton-cycle gas-turbine.	54
Figure 4 - Stations and processes within a propulsive Brayton-cycle gas- turbine.....	56
Figure 5 - Compressor efficiency definitions after Casey (2007)	59

Figure 6 - Turbine efficiency definitions after Casey (2007).....	64
Figure 7 - ExcelCEA workflow.....	70
Figure 8 - CPU transistor counts 1971-2011, data from Wikipedia, 2011C	72
Figure 9 - Processor transistor counts per unit area, 1971-2011, data from Wikipedia (2011C).....	73
Figure 10 - Casey diagram for the compressor.....	89
Figure 11 - Casey diagram for gas generator turbine	96
Figure 12 - Casey diagram for power turbine	103
Figure 13 - Olympus 593 performance data, M2dude (2010)	113
Figure 14 – Brayton cycle performances with respect to fuel consumption; Mach 0.80, 11 km.	118
Figure 15 – Brayton cycle performances with respect to core air consumption; Mach 0.80, 11 km.	119
Figure 16 - Brayton cycle TSFC performances, Mach 0.80, 11 km.....	120
Figure 17 - Brayton cycle tPSFC performances, Mach 0.80, 11 km.....	121
Figure 18 - Brayton cycle overall thermal efficiency performances, Mach 0.80, 11 km.....	122
Figure 19 - Brayton cycle optimum bypass ratio, Mach 0.80, 11 km.....	123
Figure 20 - Brayton cycle overall specific thrust, Mach 0.80, 11 km.....	124
Figure 21 - Brayton cycle performances Imperial TSFC, Mach 2.0, 18 km..	127
Figure 22 - Brayton cycle specific thrust, Mach 2.0, 18 km	128
Figure 23 - Brayton cycle overall efficiency, Mach 2.0, 18 km.....	129
Figure 24 - Brayton cycle performances with respect to core air consumption, Mach 2.0, 18 km.....	130
Figure 25 - Brayton cycle performances with respect to fuel consumption, Mach 2.0, 18 km.....	131
Figure 26 - Brayton cycle optimum bypass ratio, Mach 2.0, 18 km.....	132
Figure 27 - Stationary Brayton cycle PSFC	134
Figure 28 - Stationary Brayton cycle performances with respect to air consumption.....	135
Figure 29 - Stationary Brayton cycle performances with respect to fuel consumption.....	136
Figure 30 - Stationary Brayton cycle overall efficiency.....	137

NOTATION

A = Helmholtz free specific energy, Jkg^{-1}

α = cutoff ratio for diesel engines, **dimensionless**

C = specific heat capacity, $\text{Jkg}^{-1}\text{K}^{-1}$

δ = infinitesimal difference

∂ = partial difference

Δ = finite difference

η = efficiency, **dimensionless**

F = Specific Force, usually specific thrust, Nkgs^{-1}

\mathbb{F} = Force, usually thrust, **N**

$\text{FAR} \equiv \frac{W_{\text{Fuel}}}{W_{\text{Air}}}$, **dimensionless**

G = Gibbs free specific enthalpy, Jkg^{-1}

JPLF = Jetpipe Pressure Loss Factor, **dimensionless**

$\gamma \equiv \frac{C_P}{C_V}$, **dimensionless**

\mathbb{H} = enthalpy, **J**

H = specific enthalpy, Jkg^{-1}

k = constant

M = mean molar mass, kgmol^{-1}

n = polytropic index, **dimensionless**, or some number

n.f. = non-flow

$\text{NER} = \text{nozzle expansion ratio} \equiv \frac{P_7}{P_{9\text{Static}}}$, **dimensionless**

P = pressure, **Pa**

Q = specific heat energy, Jkg^{-1}

\mathbb{Q} = heat energy, **J**

R = specific gas constant, $\text{Jkg}^{-1}\text{K}^{-1}$

\mathbb{R} = universal gas constant, JK^{-1}

ρ = density, $\text{kgm}^{-3} \equiv V^{-1}$

S = specific entropy, Jkg^{-1}

\mathbb{S} = absolute entropy, J

s.f. = steady-flow

T = Temperature, K

U = specific internal energy, Jkg^{-1}

v = velocity, ms^{-1}

v_{Sonic} = local speed of sound $\cong \sqrt{\gamma RT}$, ms^{-1}

V = specific volume, $\text{m}^3\text{kg}^{-1} \equiv \rho^{-1}$

\mathbb{W} = mass flow rate, kgs^{-1}

INTRODUCTION

The importance of heat engines has perhaps been best summed up by Matthew Boulton:

I sell here, sir, what all the world desires to have – POWER.

Many things have changed since those words were recorded in March of 1776¹; the desire for power remains.

Boulton & Watt's successful steam-engine business was not founded upon the invention of the steam engine itself, but rather upon its improvement. Their business model appears surprisingly modern – they licensed their patents to customers for a fee of one-third the calculated value of the coal saved by their machine when compared with a baseline Newcomen engine, paid annually for 25 years.

The success of this business model serves to demonstrate that the desire to minimise cost is at least as enduring as that to maximise power.

It is with the minimisation of cost that this thesis is primarily concerned; it is hoped that this will be achieved *via* reductions in both the development costs and fuel consumptions of future engines.

A Brief History of *practical* thermodynamics

The fact that Newcomen's engine worked was perhaps somewhat miraculous in itself; its invention (1712) predated Joule's assertion of the equivalence between heat and mechanical work (1845) by more than a century.

Carnot's (eventually) influential work also predated Joule and the Caloric theory upon which it was based was giving way to a unified concept of Energy by the time Clausius used it as a foundation stone on the path towards his statement of what became the 2nd law of thermodynamics in the 1850s and 1860s.

The early development of heat engines thus proceeded somewhat in advance of the theoretical techniques necessary to predict their performance from first

¹ March 22nd 1776 entry Boswell's Life of Johnson.

principles. Innovation in the field was therefore largely devoted to the circumvention of patents (and the patenting of those circumventions), and the empirical improvement of existing machines rather than to improved understanding of thermodynamics.

Interest in the underlying thermodynamics of heat engines began to grow in the late 19th century, as the theory caught up with the engineering reality. From this point onwards, it is possible to approximately correlate the frequency with which various thermodynamic cycles are mentioned in the literature and the importance attached to their development:

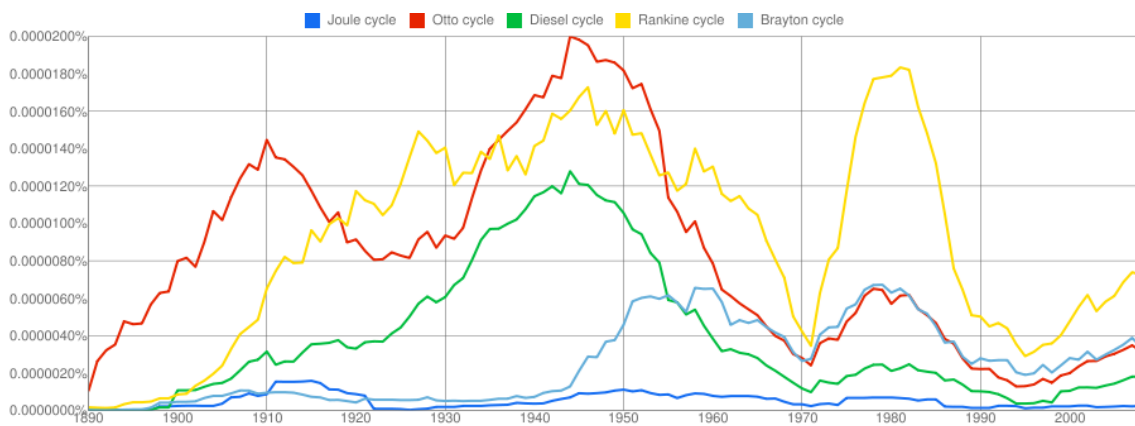


Figure 1 – Google Ngram of selected thermodynamic cycles, English one million corpus, smoothing = 5.

The thermodynamic cycles selected are, or have been, used in improving our understanding for achieving a variety of purposes ranging from cutting hedges to propelling aeroplanes and generating electricity.

The Ngram appears to naturally divide into two phases. Prior to about 1970, interest appears to broadly be in the achievement and then improvement of performance.

- Interest in the Otto cycle correlates well with the two World Wars and the arms races which preceded them.
- The Diesel cycle was approximately 20 years more recent than the Otto cycle, and was insufficiently mature to have a decisive influence upon the First World War. Approximately 20 years later, leading up to and during the Second World War, interest in the Diesel cycle closely

resembles to that displayed in the Otto cycle during the First World War.

- The Rankine cycle is a steam cycle primarily associated with stationary power-generation. Prior to 1970, interest appears to correlate with the construction and extension of electricity grids.
- The Joule and Brayton cycles are identical; interest prior to 1970 appears almost entirely driven by aerospace applications which arose from approximately 1940 onwards.

After approximately 1970, interest in the thermodynamic cycles considered appears to correlate with variations in the inflation-corrected price of oil. This suggests that having achieved various new industrial capabilities in the first two-thirds of the 20th century, human ingenuity is now primarily focussed upon reducing the cost of those capabilities, just as Boulton & Watt did over 230 years ago.

A Brief History of *theoretical* thermodynamics

When looking back from the vantage point of the early 21st century, the sheer ubiquity and extremely low cost of computational power can make it difficult to appreciate the difficulties faced by previous generations to whom this means was not available.

In the absence of cheap computational power, the analysis of complicated problems required judicious use of simplifying assumptions in order to create models which would yield closed-form analytical solutions.

The concept of a “thermodynamic cycle” derives from these simplifying assumptions:

- Cycling the working fluid obviates the need to model intake and exhaust processes.
- Maintaining a fixed mass of working fluid within the cycle, implies that one heat is added to the cycle; the consideration of combustion chemistry is unnecessary.
- Because no combustion chemistry is considered, the reduction in accuracy associated with assuming that the working fluid has constant specific-heat capacities is usually reduced.

- Because pure heat is added to and rejected from the cycle, and because the mechanical equivalence between heat and mechanical work is axiomatic, it is inherently simple to calculate the efficiency of the conversion of heat into mechanical work.

The analysis may be further simplified by assuming that the compression and expansion processes are isentropic and adiabatic.

With these drastic simplifying assumptions, it was possible for conclusions to be then drawn about the performances of many of the earlier thermodynamic cycles relatively easily.

Unfortunately, despite its complexities, practical engines must be built in the real world;

Nature cannot be fooled.

Feynman (1986).

As a result of this, the availability of increasing computational resources has led to the periodic re-investigation of thermodynamic cycles with progressively fewer simplifying assumptions in the hope of achieving better agreement between theoretical predictions and the experiences of reality.

The present investigation represents another step along this road.

The purpose & applications of this work

The development of highly complex thermodynamic models is difficult. It would therefore be most surprising if it were not undertaken with some purpose in mind.

There are in fact several purposes for this work:

- It is expected that more realistic thermodynamic models will enable the performances of future engines to be predicted with greater confidence; thereby reducing the cost of risk.
- Comparison between the performances of existing engines *potentially* allows the underlying component performance-assumptions to be improved.

- More general thermodynamic models allow new concepts, such as the use of alternative fuels or novel thermodynamic cycles to have certain of their risks assessed at far lower cost than would be incurred by experimenting upon a physical prototype.
 - The use of a single, generalised thermodynamic model is expected to facilitate genuine “like with like” comparison of engine concepts.
- More detailed modelling of the precise conditions under which engine components operate may allow them to be better optimised, more easily.

AN OVERVIEW OF THERMODYNAMICS

Classical Thermodynamics

Historical context

From the perspective of the early 21st Century, it is difficult to appreciate fully the challenges which faced the likes of Carnot, Joule, Clausius and Kelvin as they conducted their early investigations in thermodynamics.

Incredibly cheap computational technology has become so ubiquitous that it requires no small feat of imagination to conceive the reality of the world as it was prior to the advent of the digital computer².

It is important to attempt to understand this world without digital computers because if *politics is the art of the possible* then *engineering is the science of the possible*.

In the absence of digital computers, numerical calculations were considerably more laborious and time-consuming than is the case today. There was also a significant difference in the cost of the various operations. For example, addition and subtraction were cheaper than multiplication and division, whilst raising numbers to powers, especially powers less than unity, was extremely expensive.

² Both the “experimental investigation” and the writing of this thesis have been performed electronically using various PCs, and it seems possible that a substantial proportion of those who read these words will do so electronically.

Napier's invention of the logarithm in the 17th century allowed multiplication and division to be transformed into addition and subtraction operations respectively, provided that the logarithms of both numbers were known, e.g.

$$\begin{aligned}\log_b x + \log_b y &= \log_b (xy) \\ \therefore b^{(\log_b x + \log_b y)} &= xy\end{aligned}\tag{1}$$

An analogous approach reduced the process of raising numbers to powers to one of multiplying logarithms.

Great effort was therefore devoted to the generation of tables of the logarithms of different numbers; indeed one of the first applications proposed for one of the first "modern" computers (Babbage's difference engine) was the rapid and accurate³ generation of tables of logarithms. Indeed, the magnitude of the efforts devoted over several centuries to the generation of ever more comprehensive and accurate tables of logarithms serves as an illustration of the difficulties associated with performing numerical calculations without them.

The logarithm is a specific example of the general fact that historically it was necessary to devote considerable effort to finding ways of representing problems in ways which were soluble given the then available computational techniques and technologies.

In the context of classical thermodynamics, many of the aggressive simplifications which shall be outlined below stem from the over-riding need to bring the problems under consideration within the reach of the computational architecture then available.

³ Human error in the generation of tables of logarithms inevitably resulted in corresponding errors in those calculations based upon those tables: detecting errors in large tables of numbers is not something which human beings are generally very good at, and so errors could persist within standard tables for an extended subsequent period.

The 1st Law of Thermodynamics

The first law of thermodynamics states the equivalence of heat and work and reaffirms the principle of conservation of energy.

(Oxford Dictionaries Online, 2011)

The first law of thermodynamics was originally put forward by James Prescott Joule in the 1840s, though it took some time before it was accepted because it contravened the prevailing orthodoxy, which maintained that *caloric* could neither be created nor destroyed.

Mathematically, using modern notation, it may be expressed as follows:

$$dU = dQ - d\text{Work} \quad (2)$$

Carnot and the Heat Engine

It follows naturally from the First Law of thermodynamics that it should be possible to convert heat into mechanical work and *vice versa*.

A *heat engine* is a machine which performs the former operation, whereas the *heat pump* is an analogous machine which performs the latter.

Heat engines were successfully constructed some centuries prior to Carnot, but there was then little intellectual understanding of the principles underlying their operation.

Carnot's view of heat as a *caloric* fluid allowed him to draw an analogy between the fall of heat from a high to a low temperature and the fall of water.

Just as the amount of power which may be extracted from a given mass-flow rate of water is a function of the height available, so Carnot reasoned that the amount of power which might be extracted from a given flow of heat should be a function of the temperature drop that occurs.

As Murrell observed in 2008,

He [Carnot] believed that heat was a fluid until close to his death in 1832, and perhaps he would not have arrived at his conclusions without it; if heat reflected mechanical motion of the atoms the analogy between a water wheel and a steam engine would be far from obvious.

The Thermodynamic Cycle

One of Carnot's great contributions to thermodynamics was the concept of the thermodynamic cycle. It has become almost ubiquitous in thermodynamic analyses, and thus it is worth examining the implications of the assumptions upon which it is based.

The idea of a thermodynamic cycle is that a working fluid contained within a closed system is subjected to various processes before being returned to its initial state. Because the working fluid is returned to its initial state at the end of the cycle, not only may the cycle be repeated *ad infinitum*, but also the mathematical analysis of its performance is greatly simplified.

The performance of any heat engine based upon a thermodynamic cycle may be thought of in terms of three quantities, namely

1. Heat input to the cycle
2. Heat rejected from the cycle
3. Work output from the cycle

It follows from (2) that the efficiency of any such cycle may be defined as:

$$\eta_{\text{Cycle}} = \frac{|\text{Work}_{\text{Output}}|}{|Q_{\text{Input}}|} \equiv \frac{|Q_{\text{Input}}| - |Q_{\text{Output}}|}{|Q_{\text{Input}}|} \equiv \frac{|\text{Work}_{\text{Output}}|}{|\text{Work}_{\text{Output}}| + |Q_{\text{Output}}|} \equiv \dots \quad (3)$$

(Absolute values are used to avoid concerns over sign conventions which might otherwise erode the simplicity of the underlying concept)

As a result of this generalisation, not only does the thermodynamic cycle greatly simplify the analysis of individual engine concepts, but it also facilitates comparison between them.

However, despite these attractive features, there is an obvious problem with the concept of the thermodynamic cycle – the majority of heat engines (and the overwhelming majority of internal combustion engines) do not recycle their working fluid.

In reality, internal combustion engines usually use air as their working fluid, and because combustion vitiates the air, it must be replaced for subsequent “cycles”. This means that, in reality, the final step (which is usually the rejection of heat at the “cold” temperature) of most thermodynamic cycles is a virtual or inferred step rather than an actual step which may be directly observed.

As a result of this, observations about the performance of theoretical thermodynamic cycles do not necessarily identically apply to real heat engines.

The 2nd Law of Thermodynamics and the Carnot Cycle

The second law states that heat does not of itself pass from a cooler to a hotter body. Another, equivalent, formulation of the second law is that the entropy of a closed system can only increase.

(Oxford Dictionaries Online, 2011)

The second law is attributed to Clausius; it is mathematically related to Carnot’s theorem that the maximum performance of a thermodynamic cycle between two temperatures was that of a reversible cycle with isothermal heat addition and rejection, because reversible processes are isentropic.

The Carnot cycle itself is only of academic interest in the sense that physical machines based directly upon it are not in operation. However, the insights drawn from its analysis have fostered the design of practical machines. The efficiency of a Carnot cycle is given by:

$$\eta_{\text{Carnot}} = \frac{T_{\text{Hot}} - T_{\text{Cold}}}{T_{\text{Hot}}} = 1 - \frac{T_{\text{Cold}}}{T_{\text{Hot}}} \quad (4)$$

This represents the limiting efficiency of any thermodynamic cycle operating between these two temperatures. Because the cold temperature is fixed by that of the ambient conditions⁴ (usually either of the atmosphere or the sea), attention was rapidly focussed upon maximising the hot temperature.

This emphasis upon cycle's peak temperature naturally made the internal combustion engine appear attractive, because it is unencumbered by heat exchangers and therefore capable of attaining higher peak-cycle temperatures. Although the early development of the internal combustion engine was driven primarily by the mass savings it offered, its potential to exceed the thermal efficiency of the external combustion steam engine encouraged perseverance with it in the face of its initially prodigious thirst for fuel.

Thermodynamic processes

Thermodynamic cycles can be constructed from defined processes, in a manner analogous to Lego[®] or Meccano[®] models. This modularity is one of the key advantages of the concept of the thermodynamic cycle, because the understanding of relatively few processes allows for the investigation of a practically limitless array of possible cycles.

Dr. Eric Goodger has compiled a comprehensive table of thermodynamic processes (found in his excellent book *Transport Fuels Technology*) which is reproduced below.

Not all of these processes have been modelled in the current work. The intention behind reproducing the entire table and listing various cycles other than that of Brayton is to illustrate the considerable “economy of scale” which results from modular nature of the cycle concept, and the structure of the model produced. The number of cycles which may be constructed varies as the number of permutations of the processes modelled (though of course only a relatively small proportion of cycles generated at random will be viable, let alone attractive).

⁴ It may be mathematically proven that no benefit in overall efficiency is derived from any attempt to refrigerate the working fluid, because for reversible machines the efficiency gained from refrigeration is precisely cancelled by the energy required to drive the refrigeration cycle; naturally therefore it follows that real machines will tend to lose overall efficiency due to irreversibilities in the refrigeration process.

Process, Constraints	$\Delta\text{Work},$ ΔQ	Energy Equation for pure substance	Equation of state for perfect gas
Non-flow Isobaric	n.f. $({}_1\text{Work}_2)_P$	$({}_1Q_2)_P - (U_2 - U_1)$	$\int_1^2 P dV = P(V_2 - V_1) = R(T_2 - T_1)$
$P = k$ $n = 0$	n.f. $({}_1Q_2)_P$	$\int_1^2 \delta U + \int_1^2 (\delta \text{Work})_P = \int_1^2 (\delta U + PdV + VdP)$ $= \int_1^2 d(U - PdV) = H_2 - H_1$	$C_P(T_2 - T_1)$

(5)

Process, Constraints	$\Delta\text{Work},$ ΔQ	Energy equation for pure substance	Equation of state for perfect gas
Non-flow Isochoric	n.f. $({}_1\text{Work}_2)_V$	$({}_1Q_2)_V - (U_2 - U_1) = 0$	$0 \because dV = 0$
$V = k$ $n = \infty$	n.f. $({}_1Q_2)_V$	$U_2 - U_1$	$C_V(T_2 - T_1)$

(6)

Process, Constraints	$\Delta\text{Work},$ ΔQ	Energy Equation for pure Substance	Equation of state for perfect gas
Non-flow Isothermal	n.f. $({}_1\text{Work}_2)_T$	$({}_1Q_2)_T$	$PV \int_1^2 V^{-1} dV = RT \ln \left(\frac{V_2}{V_1} \right) = RT \ln \left(\frac{P_1}{P_2} \right)$
$T = k$ $n = 1$	n.f. $({}_1Q_2)_T$	n.f. $({}_1\text{Work}_2)_T$	$RT \ln \left(\frac{V_2}{V_1} \right) = RT \ln \left(\frac{P_1}{P_2} \right)$

(7)

Process, Constraints	Δ Work, ΔQ	Energy Equation for pure Substance	Equation of state for perfect gas
Non-flow Polytropic	n.f. ${}_1\text{Work}_2$	${}_1Q_2 - (U_2 - U_1)$	$\frac{P_1V_1 - P_2V_2}{n-1} = \frac{R}{n-1}(T_1 - T_2)$
$PV^n = k$ $n = n$	n.f. ${}_1Q_2$	n.f. ${}_1\text{Work}_2 + (U_2 - U_1)$	$\left(\frac{R}{n-1} - C_v\right)(T_1 - T_2) = C_v \left(\frac{\gamma - n}{n-1}\right)(T_1 - T_2)$

(8)

Process, Constraints	Δ Work, ΔQ	Energy Equation for pure Substance	Equation of state for perfect gas
Non-flow Isentropic	n.f. $({}_1\text{Work}_2)_s$	$U_1 - U_2$	$\frac{R}{\gamma - 1}(T_1 - T_2) = C_v(T_1 - T_2)$
$PV^\gamma = k$ $n = \gamma$	n.f. $({}_1Q_2)_s$	0	0

(9)

Process, Constraints	Δ Work, ΔQ	Energy Equation for pure substance	Equation of state for perfect gas
Steady flow Isobaric	s.f. $({}_1\text{Work}_2)_p$	$({}_1Q_2)_p - (H_2 - H_1)$	$\int_1^2 VdP = 0 \because dP = 0$
$P = k$ $n = 0$	s.f. $({}_1Q_2)_p$	$H_2 - H_1$	$C_p(T_2 - T_1)$

(10)

Process, Constraints	$\Delta\text{Work},$ ΔQ	Energy equation for pure substance	Equation of state for perfect gas	(11)
Steady flow Isochoric	s.f. $({}_1\text{Work}_2)_V$	$({}_1Q_2)_V - (H_2 - H_1)$	$V(P_1 - P_2) = R(T_1 - T_2)$	
$V = k$ $n = \infty$	s.f. $({}_1Q_2)_V$	$H_2 - H_1 + \text{s.f. } ({}_1\text{Work}_2)_V$	$(U_2 + P_2V_2) - (U_1 + P_1V_1) + V_1P_1 - V_2P_2$ $= U_2 - U_1 = C_V(T_2 - T_1)$	

Process, Constraints	$\Delta\text{Work},$ ΔQ	Energy Equation for pure Substance	Equation of state for perfect gas	(12)
Steady flow Isothermal	s.f. $({}_1\text{Work}_2)_T$	$({}_1Q_2)_T$	$-PV \int_1^2 P^{-1} dP = RT \ln \left(\frac{P_1}{P_2} \right) = RT \ln \left(\frac{V_2}{V_1} \right)$	
$T = k$ $n = 1$	s.f. $({}_1Q_2)_T$	s.f. $({}_1\text{Work}_2)_T$	$RT \ln \left(\frac{P_1}{P_2} \right) = RT \ln \left(\frac{V_2}{V_1} \right)$	

Process, Constraints	$\Delta\text{Work},$ ΔQ	Energy Equation for pure Substance	Equation of state for perfect gas	(13)
Steady flow Polytropic	s.f. ${}_1\text{Work}_2$	${}_1Q_2 - (H_2 - H_1)$	$-(PV^n)^{\frac{1}{n}} \left(\frac{n}{n-1} P^{\frac{n-1}{n}} \right)$ $= \frac{n}{n-1} (P_1V_1 - P_2V_2) = \frac{nR}{n-1} (T_1 - T_2)$	
$PV^n = k$ $n = n$	s.f. ${}_1Q_2$	n.f. ${}_1\text{Work}_2 + (H_2 - H_1)$	$\left(\frac{nR}{n-1} - C_p \right) (T_1 - T_2) = C_v \left(-\frac{\gamma - n}{n-1} \right) (T_1 - T_2)$	

Process, Constraints	$\Delta\text{Work},$ ΔQ	Energy Equation for pure Substance	Equation of state for perfect gas	
Steady flow Isentropic	s.f. $({}_1\text{Work}_2)_s$	$H_1 - H_2$	$C_p(T_1 - T_2)$	(14)
$PV^\gamma = k$ $n = \gamma$	s.f. $({}_1Q_2)_s$	0	0	

Process, Constraints	$\Delta\text{Work},$ ΔQ	Energy Equation for pure Substance	Equation of state for perfect gas	
Steady flow Isentropic non-work (throttling)	s.f. $({}_1\text{Work}_2)_s$	0	0	(15)
$PV^\gamma = k$ $n = \gamma$	s.f. $({}_1Q_2)_s$	0	0	

Equations (5)-(15) after Goodger (2000).

Standard expressions for the performance of selected thermodynamic cycles

Given the source of the comprehensive table of thermodynamic processes reproduced above, it is perhaps unsurprising that, in the opinion of the author, the description of reversible thermodynamic cycles put forward by Goodger(2000) has not been bettered. It is used as the basis of this section, but extended where required.

Although not all of the processes outlined in (5)-(15) are used in these cycles, it is hoped that they serve to illustrate the fundamental idea.

The Brayton Cycle

The Brayton cycle is sometimes also called the Joule cycle, though the reason for this is mysterious to the author. Success having many fathers, it has also been attributed to Ericsson.

Although today it is used to approximate the thermodynamic cycle of the internal-combustion gas-turbine, Brayton's original machine was in fact a "two-stroke"⁵ piston engine with discrete compression and expansion cylinders separated by a steady-flow combustion chamber. It was popular for a relatively brief period in the late 19th century.

Cycle	Process	ΔQ	ΔWork
Brayton	(1–2) s.f. Isentropic Compression	0	$-C_p(T_1 - T_2)$
	(2–3) s.f. Isobaric Heating	$C_p(T_3 - T_2)$	0
	(3–4) s.f. Isentropic Expansion	0	$C_p(T_3 - T_4)$
	(4–1) s.f. Isobaric Cooling	$-C_p(T_1 - T_4)$	0

$$\eta_{\text{Brayton}} = 1 - \left[\frac{-C_p(T_1 - T_4)}{C_p(T_3 - T_2)} \right]$$

Taking C_p to be constant and cancelling it,

$$\eta_{\text{Brayton}} = 1 - \frac{T_4 - T_1}{T_3 - T_2}$$

From isentropes 1-2 and 3-4,

$$\frac{T_4}{T_3} = \left(\frac{P_4}{P_3} \right)^{\frac{\gamma-1}{\gamma}} = \left(\frac{P_1}{P_2} \right)^{\frac{\gamma-1}{\gamma}} = \frac{T_1}{T_2}$$

Hence,

$$\eta_{\text{Brayton}} = 1 - \left(\frac{P_1}{P_2} \right)^{\frac{\gamma-1}{\gamma}}$$

(after Goodger, 2000)

⁵ Of course it may be argued that a pair of two-stroke pistons are equivalent to a single four-stroke piston so far as the power per unit engine size is concerned.

The Carnot Cycle

The Carnot cycle was first proposed by Nicolas Léonard Sadi Carnot in 1824, and is, as such, the oldest thermodynamic cycle of them all. It is also the most efficient cycle possible in classical thermodynamics.

Cycle	Process	ΔQ	$\Delta Work$
Carnot	(1–2) n.f. Isentropic Compression	0	$-C_V (T_1 - T_2)$
	(2–3) n.f. Isothermal Expansion	$RT_2 \ln(V_3/V_2)$	$RT_2 \ln(V_3/V_2)$
	(3–4) n.f. Isentropic Expansion	0	$C_V (T_3 - T_4)$
	(4–1) n.f. Isothermal Compression	$-RT_2 \ln(V_1/V_4)$	$-RT_2 \ln(V_1/V_4)$

(18)

$$\eta_{\text{Carnot}} = 1 - \frac{Q_{\text{Out}}}{Q_{\text{In}}}$$

$$\eta_{\text{Carnot}} = 1 - \left[\frac{-RT_1 \ln\left(\frac{V_1}{V_4}\right)}{RT_2 \ln\left(\frac{V_3}{V_2}\right)} \right]$$

Where R is constant,

$$\eta_{\text{Carnot}} = 1 - \frac{T_1 \ln\left(\frac{V_4}{V_1}\right)}{T_2 \ln\left(\frac{V_3}{V_2}\right)}$$

From isentropes 1-2 and 3-4,

$$\frac{v_1}{v_2} = \left(\frac{T_1}{T_2}\right)^{\frac{1}{(\gamma-1)}} = \left(\frac{T_4}{T_3}\right)^{\frac{1}{(\gamma-1)}} = \frac{V_4}{V_3}$$

Hence,

$$\frac{V_4}{V_1} = \frac{V_3}{V_2}, \text{ and}$$

$$\eta_{\text{Carnot}} = 1 - \frac{T_1}{T_2} \quad (19)$$

(after Goodger, 2000)

It may be seen that the efficiency of the Brayton cycle tends towards that of the Carnot cycle when $(T_3 - T_2) \rightarrow 0$. Unfortunately, under this condition of maximum notional efficiency, the useful work produced even by an ideal Brayton cycle would be zero.

The Diesel Cycle

The Diesel Cycle⁶ was devised by Rudolph Diesel; it is effectively a non-flow version of the Brayton Cycle, and involves the following processes:-

Cycle	Process	ΔQ	ΔWork
Diesel	(1–2) n.f. Isentropic Compression	0	$-C_v (T_1 - T_2)$
	(2–3) n.f. Isobaric Heating	$C_p (T_3 - T_2)$	$R(T_3 - T_2)$
	(3–4) n.f. Isentropic Expansion	0	$C_v (T_3 - T_4)$
	(4–1) n.f. Isochoric Cooling	$-C_v (T_1 - T_4)$	0

(20)

$$\eta_{\text{Diesel}} = 1 - \left[\frac{-C_v (T_1 - T_4)}{C_p (T_3 - T_2)} \right] = 1 - \frac{1}{\gamma} \frac{(T_4 - T_1)}{(T_3 - T_2)}$$

Let $r_v = \left(\frac{V_1}{V_2} \right)$, then, from isentrope 1-2,

$$T_2 = T_1 (r_v)^{\gamma-1}$$

From isobar 2-3,

$$\frac{T_3}{T_2} = \frac{V_3}{V_2} = \alpha, \text{ the cutoff ratio.}$$

Hence

$$T_3 = T_1 \alpha r_v^{\gamma-1}, \text{ and } (T_3 - T_2) = T_1 (\alpha - 1) r_v^{\gamma-1}$$

From isentrope 4-1,

$$\frac{T_4}{T_3} = \left(\frac{V_4}{V_3} \right)^{\gamma-1} = \left(\frac{V_3 V_2}{V_2 V_4} \right)^{\gamma-1} = \left(\frac{\alpha}{r_v} \right)^{\gamma-1}$$

Hence

$$T_4 = T_3 \left(\frac{\alpha}{r_v} \right)^{\gamma-1} = T_1 (\alpha - 1) r_v^{\gamma-1} \left(\frac{\alpha}{r_v} \right)^{\gamma-1} = T_1 \alpha^\gamma, \text{ and } (T_4 - T_1) = T_1 (\alpha^\gamma - 1)$$

(21)

Thus

$$\eta_{\text{Diesel}} = 1 - \frac{\alpha^\gamma - 1}{\alpha (\gamma - 1)} \left(\frac{1}{r_v} \right)^{\gamma-1}$$

(Goodger, 2000)

⁶ It is an accident of history that the majority of small compression-ignition internal-combustion engines in use today, commonly referred to as “diesel engines”, more closely approximate an Otto cycle, with the complication that most are now turbocharged.

The Ericsson Cycle

Ericsson was a prolific inventor of thermodynamic cycles; the cycle for which he is generally remembered was in fact his second, dating from 1853.

Interestingly, his first cycle, of 1833 was essentially identical to that now bearing Brayton's name.

The second Ericsson cycle incorporates isothermal compression and expansion processes, and therefore may be used to represent the limit of the application of intercooling and reheating to the Brayton-cycle gas-turbine.

Cycle	Process	ΔQ	$\Delta Work$
Ericsson	(1–2) s.f. Isothermal Compression	0	$-RT \ln\left(\frac{P_1}{P_2}\right)$
	(2–3) s.f. Isobaric Heating	$C_p(T_3 - T_2)$	0
	(3–4) s.f. Isothermal Expansion	0	$RT \ln\left(\frac{P_3}{P_4}\right)$
	(4–1) s.f. Isobaric Cooling	$-C_p(T_1 - T_4)$	0

(22)

The thermal efficiency of this cycle is identical to that of a Carnot cycle operating over the same temperature range.

(Krase, 1979)

The Humphrey Cycle

The Humphrey cycle is used to describe constant volume combustion gas-turbines or Pulsed Detonation Wave Engines.

Cycle	Process	ΔQ	$\Delta Work$
Humphrey	(1–2) s.f. Isentropic Compression	0	$-C_p(T_1 - T_2)$
	(2–3) n.f. Isochoric Heating	$C_v(T_3 - T_2)$	0
	(3–4) s.f. Isentropic Expansion	0	$C_p(T_3 - T_4)$
	(4–1) s.f. Isobaric Cooling	$-C_p(T_1 - T_4)$	0

(23)

(Kuentzmann & Falempin, 2002, modified to the form given in Goodger, 2000)

The cycle efficiency is given by equation (24), a monstrosity for which the author does not propose to provide a derivation.

$$\eta_{\text{Humphrey}} = 1 - \gamma \frac{T_1 \left(\frac{T_3}{T_2} \right)^{\frac{1}{\gamma}} - 1}{\frac{T_3}{T_2} - 1} \quad (24)$$

(ibid)

A more complex analysis of Pulsed Detonation Wave Engines (allowing for the irreversibility inherent in the detonation process) was conducted by Wintenberger & Jacobs in 2005.

The Lenoir Cycle

“The Lenoire cycle is an idealised thermodynamic cycle often used to model a pulse-jet engine. It is based upon the operation of an engine patented by Jean Joseph Etienne Lenoire in 1860”

(Wikipedia, 2011A).

Cycle	Process	ΔQ	ΔWork
Lenoir	(1–2) n.f. Isochoric Heating	$C_v (T_2 - T_1)$	0
	(2–3) n.f. Isentropic Expansion	0	$C_v (T_2 - T_1)$
	(3–1) n.f. Isobaric Cooling	$-C_p (T_1 - T_3)$	$P_1 (V_1 - V_3)$

(25)

(Wikipedia, 2011A, modified to the form given in Goodger, 2000).

The Otto Cycle

The Otto-cycle is probably the most commonly used thermodynamic cycle in the world, having found application in many piston engines across an extremely wide range of outputs.

Cycle	Process	ΔQ	ΔWork
Otto	(1–2) n.f. Isentropic Compression	0	$-C_v (T_1 - T_2)$
	(2–3) n.f. Isochoric Heating	$C_v (T_3 - T_2)$	0
	(3–4) n.f. Isentropic Expansion	0	$C_v (T_3 - T_4)$
	(4–1) n.f. Isochoric Cooling	$-C_v (T_1 - T_4)$	0

(26)

$$\eta_{\text{Otto}} = 1 - \frac{-C_v (T_1 - T_4)}{C_v (T_3 - T_2)} = 1 - \frac{(T_4 - T_1)}{(T_3 - T_2)}$$

from isentropes 1-2 and 3-4,

$$\text{Let } r_v = \left(\frac{V_1}{V_2} \right)$$

$$\frac{T_2}{T_1} = \left(\frac{V_1}{V_2} \right)^{\gamma-1} = \left(\frac{V_4}{V_3} \right)^{\gamma-1} = r_v^{\gamma-1} = \frac{T_3}{T_4} \quad (27)$$

Hence,

$$T_2 = T_1 r_v^{\gamma-1}, \text{ and } T_3 = T_4 r_v^{\gamma-1}$$

Thus,

$$\eta_{\text{Otto}} = 1 - \frac{(T_4 - T_1)}{(T_4 - T_1)} \left(\frac{1}{r_v} \right)^{\gamma-1} = 1 - \left(\frac{1}{r_v} \right)^{\gamma-1}$$

(Goodger, 2000).

It may be seen that the efficiency of the Otto cycle is identical to that of a

Diesel cycle with a cutoff ratio set such that $\frac{\alpha^\gamma - 1}{\alpha(\gamma - 1)} = 1$.

The Rankine Cycle

The Rankine cycle is that used to approximate a steam-turbine plant. It is similar to a Brayton cycle apart from the fact that heat is rejected isothermally *via* condensation of the steam.

Cycle	Process	ΔQ	ΔWork
Rankine	(1-2) s.f. Isentropic Compression	0	$-C_p (T_1 - T_2)$
	(2-3) s.f. Isobaric Heating	$C_p (T_3 - T_2)$	0
	(3-4) s.f. Isentropic Expansion	0	$C_p (T_3 - T_4)$
	(4-1) s.f. Isothermal Cooling	$RT \ln \left(\frac{V_1}{V_4} \right)$	0

(28)

(Moran & Shapiro, 2006, modified to the form given in Goodger, 2000)

Because this is a vapour power cycle, the analytical approach used to develop an expression for the thermal efficiency of the cycle, as employed with other cycles above is not especially useful for the Rankine cycle; it is clearly unreasonable to use a single value of C_p for both liquid water and steam.

The efficiency of the Rankine cycle is therefore generally expressed in terms of the specific enthalpy of its working fluid at each point in the cycle.

$$\eta_{\text{Rankine}} = 1 - \frac{H_4 - H_1}{H_3 - H_2} \quad (29)$$

(Goodger, 2000)

Historically, these specific enthalpy figures were extracted from Steam Tables; today some form of computer code would almost certainly be used. This approach of evaluating specific enthalpies for each defined state in the cycle forms the intellectual basis of many “higher fidelity” approaches to thermodynamic analysis, including that which forms the subject of this thesis.

The Stirling Cycle

The Stirling cycle is the non-flow equivalent of the second Ericsson cycle, *i.e.*

Cycle	Process	ΔQ	ΔWork
Stirling	(1–2) n.f. Isothermal Compression	0	$-RT \ln \left(\frac{P_1}{P_2} \right)$
	(2–3) n.f. Isochoric Heating	$C_v (T_3 - T_2)$	0
	(3–4) n.f. Isothermal Expansion	0	$RT \ln \left(\frac{P_3}{P_4} \right)$
	(4–1) n.f. Isochoric Cooling	$-C_v (T_1 - T_4)$	0

(30)

As with the second Ericsson cycle, its efficiency is identical to that of a Carnot cycle operating over the same temperature range.

(WolframAlpha, 2011, equation (30) modified to the form given in Goodger, 2000)

The simplifying assumptions of classical thermodynamics

The classical thermodynamic cycle models presented above all lead to relatively simple analytical expressions of cycle performance.

In many cases, these expressions have been constructed so that the influences of physical engine-design parameters, such as pressure ratios and peak cycle temperatures, may be investigated.

The majority of the investigations associated with producing such models are algebraic. Closed-form analytical solutions are produced which would be susceptible to attack with relatively simple computational tools such as slide-rules or tables of logarithms. Using such means, it would be possible to rapidly produce a parametric analysis for any of these cycles. The number of data points required could be reduced by graphical interpolation.

However, this analytical simplicity is only achieved by adopting several assumptions.

Process Assumptions

These relate to the physical processes such as compression, expansion, heat addition and so on.

Isentropic

Isentropic processes cause no entropy change. The second law of thermodynamics implies that isentropy is an abstraction for a closed system. In reality, this limit may only be approached rather than attained, and in most cases is not approached closely.

It is sometimes quite surprising how dramatic is the impact of relatively small increases in specific entropy upon the decrease in the overall efficiency of a thermodynamic cycle.

Adiabatic

An adiabatic process is one which takes place without heat transfers. It may be quite closely approached by a steady-flow system because, an individual unit of fluid in steady flow does not spend an appreciable length of time in close contact with the walls of the machine and therefore cannot experience a very large amount of specific enthalpy-transfer.

On the other hand, heat transfers may be quite significant for non-flow machines such as piston engines.

Isobaric

Isobaric processes are those which are intended to take place at constant pressure. In reality this is quite difficult to achieve. Gas-turbine combustion chambers suffer from both cold pressure losses due to their aerodynamic design, and also “hot losses” associated with the heat-addition process.

Piston engines intended to operate on a Diesel cycle will only attain constant-pressure combustion if the rate of heat addition due to combustion precisely balances the rate of combustion-chamber volume increase due to the progress of the piston along its power stroke. This is difficult to achieve in practice other than at a precisely defined design-point, because the rate of change of combustion chamber volume is a function of the crank angle and engine speed, whilst the rate of heat addition due to combustion is a function of the precise parameters of the working fluid and fuel.

In general, processes without heat or work transfer will only be isobaric if they are simultaneously isentropic.

Isochoric

Constant volume processes may be reasonably approximated by piston engines close to top-dead-centre because the rate of displacement of the piston is small with respect to changes in crank angle. Therefore there is generally sufficient time for combustion to proceed at close to the constant-volume condition for most reasonable combinations of stroke and mean piston speed (because the inertial loads imposed upon the reciprocating components and the crank shaft tend to limit practical engine developments).

Indicator diagrams for piston engines often still appear rounded when compared with theory, but it is quite difficult to untangle the effects of combustion-chamber volume variation, heat transfer, and leakage flows. It is the author’s suspicion that heat transfer may often be predominantly responsible for rounding of the indicator diagram.

Working Fluid Assumptions

These are related to the working fluid itself. As may be seen from the process equations quoted earlier, it was common in classical thermodynamics to assume that the working fluid was a “Perfect Gas”.

The Perfect Gas is quite unique in its properties, as may be realised from the following.

Constant Specific Heat Capacity

It is assumed that the specific heat-capacities at constant pressure and at constant volume are constants. This simplifies the associated equations, but it also allows extensive use to be made of the identity $\gamma \equiv \frac{C_P}{C_V}$.

In reality, the specific heat-capacity of a working fluid is a variable with respect to temperature.

Continuity of Mass Flow & the Cycle concept

It is inherent in the concept of a thermodynamic cycle that the working fluid is returned in all respects to its initial macrostate at the end of the cycle, such that the end of one cycle is identical to the start of the next.

This is in fact the basis underlying Clausius' concept of entropy, namely:

$$\oint \frac{dQ}{T} \leq 0 \quad (31)$$

In this inequality, the use of the \oint symbol indicates “*that the integral is to be performed over all parts of the system boundary and over the entire cycle*” (Moran and Shapiro, 2006).

The d symbol indicates that the differential is inexact; this is because heat, like work, is a path function and therefore,

...in general, the following integral cannot be evaluated without specifying the details of the process

$$\int_1^2 dQ = Q \quad (32)$$

(ibid⁷)

⁷ Though in the original the example chosen is $\int_1^2 d\text{Work} = \text{Work}$.

The use of the path integral \oint overcomes the inexact nature of dQ .

Philosophically, work described in this thesis may be thought of as a numerical approach to path integration around the Brayton-cycle, though the nature of the method is sufficiently general that it may be extended to the general case of any arbitrary thermodynamic cycle (see *Possibilities for further investigation* on page 139).

The Specific Gas Constant

Whilst the universal gas constant is fixed, the specific gas constant is a function of the mean molecular mass of the working fluid, which may vary continuously due to chemical reactions.

$$R = \frac{\mathbb{R}}{\mathbb{M}} \quad (33)$$

Problems associated with the simplifying assumptions of classical thermodynamics

Imperfect Processes

Increases in Entropy

In general, it will be found that processes which are modelled as being isentropic will in fact be those processes which, in reality, could only approach isentropy under extremely idealised circumstances.

For example, steady-flow compression and expansion processes are often modelled under the assumption of isentropic flow, when it is intuitively obvious that isentropy cannot be achieved due to friction.

Heat transfer

It is conventional to model many steady-flow processes as adiabatic. In reality, whenever a temperature gradient exists, it is an axiom of thermodynamics that *heat will flow from a hot body to a colder body*.

The degree to which the adiabatic assumption falls short of reality is a strong function of the observer's point of view. For example, if the intention is to calculate the heat flow from an engine's casing into the engine compartment of

a vehicle, the adiabatic assumption would imply zero heat flow, which is obviously grossly in error in most practical cases. On the other hand, if the objective of the modelling exercise was to calculate the temperature of the air delivered by a steady-flow compressor, then because such compressors deliver a relatively large mass flow in relation to their physical size, it is possible that the quantity of heat transferred per unit mass flow may be quite small, despite a large overall quantity of heat being transferred out of the compressor casing.

Pressure losses

In general, it is found that the total temperature of flows is conserved, and that entropy rises are thus realised in the form of pressure losses, either to the static or dynamic pressure of the flow. Physically, a loss in dynamic pressure at the constant total temperature means that the flow velocity has been reduced.

Because the temperature of a gas is primarily a function of the kinetic energy of its constituent molecules (though e.g. vibration of atomic bonds may assume importance at higher temperatures), it follows that the root mean square speed of the molecules within the gas remains constant, but that the bias in the population of vector directions of the gas molecules has been reduced (zero bias implying zero overall velocity of the bulk fluid). It is intuitively obvious that zero bias in velocity vector directions is the most probable macrostate, and thus the maximum entropy state of the overall bulk velocity of any fluid must be zero. This is, of course, exactly what one would expect from experience.

Leakage

It is generally assumed in classical thermodynamics that all of the working fluid completes the entire cycle being investigated.

In reality, fluid tends to leak from areas of high pressure to those of low pressure. Such leaks damage the performance of the cycle, because the pressure difference responsible for driving the leak in the first place must have previously been produced by the cycle itself at some thermodynamic expense.

In certain cases, leaks may be encouraged, despite their thermodynamic cost, for practical reasons. The most common such reasons are cooling, and the supply of compressed air for other purposes.

For various reasons, the efficiency of compressors tends to increase as some power of their Reynolds number (albeit a power less than unity). This means that it is generally cheaper to draw compressed air from the main compressor than to use some portion of the mechanical work produced by the cycle to drive an auxiliary compressor for this purpose (although this was generally the approach adopted until the 1950s, with for example certain marks of Rolls-Royce Merlin having provision for "cabin blower drive", and many early centrifugal flow turbojets, most famously the Nene family, using a small centrifugal compressor on the main shaft to provide cooling air).

Such auxiliary compressors may return, at least for cabin pressurisation, if the contamination of cabin air by engine lubrication oil (or the products of their combustion/pyrolysis) cannot be completely excluded by other means.

An imperfect working fluid

Various simplifying assumptions as to the behaviour of working fluids are habitually made by thermodynamicists in order to reduce their calculations to manageable proportions.

Rather than attempt to “re-invent the wheel”, a section of Anderson’s 2006 book *Hypersonic and High-Temperature Gas Dynamics* is reproduced below:

Classification of gases

For the analysis of gas dynamic problems, we can identify four categories of gases, as follows.

Calorically Perfect Gas

By definition, a calorically perfect gas is one with constant specific heats C_p and C_v . In turn, the ratio of specific heats $\gamma = C_p/C_v$ is constant. For this gas, the enthalpy and internal energy are functions of temperature, given explicitly by

$$H = C_p T \quad (34)$$

And

$$U = C_v T \quad (35)$$

The perfect-gas equation of state holds, for example,

$$PV = RT \quad (36)$$

where R is a constant. In the introductory study of compressible flow, the assumption of a calorically perfect gas is almost always made [...]

Thermally Perfect Gas

By definition, a thermally perfect gas is one where C_p and C_v are functions of temperature only.

$$\begin{aligned} C_p &= f_1(T) \\ C_v &= f_2(T) \end{aligned} \quad (37)$$

Differential changes in H and U are related to differential changes in T via

$$\begin{aligned}dH &= C_p dT \\dU &= C_p dT\end{aligned}\tag{38}$$

Hence, H and U are functions of T only, that is

$$\begin{aligned}H &= H(T) \\U &= U(T)\end{aligned}\tag{39}$$

The perfect gas equation of state holds [equation (36)] where R is a constant. [...]

Chemically Reacting Mixture of Perfect Gases

Here we are dealing with a multispecies, chemically reacting gas where intermolecular forces are neglected; hence, each individual species obeys the perfect-gas equation of state [...]. At this stage, we need to make a distinction between equilibrium and non-equilibrium chemically reacting gases. [...] For the time being, imagine that you take the air in the room around you, and instantly increase the temperature to 5000 K, holding the pressure constant at 1 atmosphere. We know [...] that dissociation will occur. Indeed, let us allow some time (maybe several hundred milliseconds) for the gas properties to “settle out,” and come to some steady state at 5000 K and 1 atmosphere. The chemical composition that finally evolves in the limit of “large” times (milliseconds) is the *equilibrium* composition at 5000 K and 1 atmosphere. In contrast, during the first few milliseconds immediately after we instantly increase the temperature to 5000 K, the dissociation reactions are just beginning to take place, and the variation of the amount of O_2, O, N_2, N , etc. in the gas is changing as a function of time. This is a non-equilibrium system. After the lapse of sufficient time, the amounts of O_2, O, N_2 , etc. will approach some steady values, and those values are the equilibrium values. It is inferred from the preceding that, once the system is in equilibrium, then the

equilibrium values of $\frac{\rho_{O_2}}{\rho}, \frac{\rho_{N_2}}{\rho}, \frac{\rho_O}{\rho}, \frac{\rho_N}{\rho}$, etc. will depend only upon the

pressure and temperature, that is, at 5000 K and 1 atmosphere, the equilibrium chemical composition is uniquely defined. [...]

In contrast, for the non-equilibrium system, $\frac{\rho_{\text{O}_2}}{\rho}$, $\frac{\rho_{\text{N}_2}}{\rho}$, etc. depend not only on P and T , but also on *time*. If the non-equilibrium system were a fluid element rapidly expanding through a shock-tunnel nozzle, another way of stating this effect is to say that $\frac{\rho_{\text{O}_2}}{\rho}$, $\frac{\rho_{\text{N}_2}}{\rho}$, etc. depend on the “history” of the flow.

With these thoughts in mind, we can define a chemically reacting mixture of perfect gases as follows. Consider a system at pressure P and temperature T . For convenience, assume a unit mass for the system. The number of particles of each different chemical species per unit mass of mixture are given by N_1, N_2, \dots, N_n . For each *individual* chemical species present in the mixture (assuming a perfect gas), the enthalpy and internal energy per unit mass of i , H_i , and U_i respectively will be functions of T (i.e., each individual species, by itself, behaves as a thermally perfect gas). However, H and U for the chemically reacting mixture depend not only on H_i , and U_i , but also on how much of each species is present. Therefore, for a chemically reacting mixture of perfect gases, in the general non-equilibrium case, we write

$$\begin{aligned}
 H &= H(T, N_1, N_2, N_3, \dots, N_n) \\
 U &= U(T, N_1, N_2, N_3, \dots, N_n) \\
 C_P &= f_1(T, N_1, N_2, N_3, \dots, N_n) \\
 C_V &= f_2(T, N_1, N_2, N_3, \dots, N_n)
 \end{aligned}
 \tag{40}$$

Where, in general, $N_1, N_2, N_3, \dots, N_n$ depend on P , T , and the “history of the gas flow”. The perfect-gas equation of state [equation (36)] still holds.

However, here R is a variable because in a chemically reacting gas, the molecular weight of the mixture $R = \frac{\mathbb{R}}{\mathbb{M}}$.

For the special case of an equilibrium gas, the chemical composition is a unique function of P and T ; hence $N_1 = f_1(P, T), N_2 = f_2(P, T)$, etc..

Therefore, the preceding results for H, U, C_p , and C_v become

$$\begin{aligned} H &= H(T, P) \\ U &= U_1(T, P) = U_2(T, V) \\ C_p &= f_1(T, P) \\ C_v &= f_2(T, P) = f_3(T, V) \end{aligned} \quad (41)$$

In the preceding, it is frequently convenient to think of U and C_v as functions of T and V rather than T and P . It does not make any difference, however, because for a thermodynamic system in equilibrium (including an equilibrium chemically reacting system) the state of the system is uniquely defined by any two state variables. The choice of T and P , or T and V in the preceding, is somewhat arbitrary in this sense.

Real gas

Here, we must take into account the effect of intermolecular forces. We could formally consider a chemically reacting gas as well as a non-reacting real gas. However, in practice, a gas behaves as a real gas under conditions of very high pressure and low temperature – conditions that accentuate the influence of inter-molecular forces on the gas. For these conditions, the gas is rarely chemically reacting. Therefore, for simplicity, we will consider a non-reacting gas here. Recall that for both the cases of a calorically perfect gas and a thermally perfect gas, H and U were functions of T only. For a real gas, with intermolecular forces, H and U depend on P (or V) as well:

$$\begin{aligned} H &= H(T, P) \\ U &= U(T, V) \\ C_p &= f_1(T, P) \\ C_v &= f_2(T, V) \end{aligned} \quad (42)$$

Moreover, the perfect-gas equation of state is no longer valid here. Instead, we must use a real-gas equation of state, of which there are many versions.

Perhaps the most familiar is the Van der Waals equation, given by

$$\left(P = \frac{k_1}{V^2} \right) (v - k_2) = RT \quad (43)$$

Where k_1 and k_2 are constants that depend on the type of gas. Note that (43) reduces to a perfect-gas equation of state when $k_1 = k_2 = 0$. In equation (43) the terms k_1/V^2 take into account the intermolecular force effects, and k_2 takes into account the actual volume of the system occupied by the volume of the gas particles themselves.

In summary, the preceding discussion has presented four different categories of gases. Any existing analyses of thermodynamic and gas dynamic problems will fall into one of these categories; they are presented here so that you can establish an inventory of such gases in your mind. It is extremely helpful to keep these categories in mind when performing any study of gas dynamics.

Also, to equate these different categories to a practical situation, let us once again take the case of air. Imagine that you take the air in the room around you and begin to increase its temperature. At room temperature, the air is essentially a calorically perfect gas, and it continues to act as a calorically perfect gas until the temperature reaches approximately 800 K. Then, as the temperature increases further we see [...] that vibrational excitation becomes important. When this happens, air acts as a thermally perfect gas. Finally, above 2500 K, chemical reactions occur, and air becomes a chemically reacting mixture of perfect gases. If we were to go in the opposite direction, that is, reduce the air temperature considerably below room temperature, and/or increase the pressure to a very high value, say, 1000 atmospheres, then the air would behave as a real gas.

Finally, it is important to note a matter of nomenclature. We have followed classical physical chemistry in defining a gas where intermolecular forces are important as a real gas. Unfortunately, an ambiguous term has evolved in the aerodynamic literature that means something quite different. In the 1950s, aerodynamicists were suddenly confronted with hypersonic entry vehicles at velocities as high as 26,000 ft/s (8 km/s). [...] The shock layers around such vehicles were hot enough to cause vibrational excitation, dissociation and even ionization. These were “real” effects that happened in air in “real life”. Hence, it became fashionable in the aerodynamic literature to denote such conditions as real-gas effects. For example, the categories just itemized as a thermally perfect gas, and as a chemically reacting mixture of perfect gases, would come under the classification of real-gas effects in some of the aerodynamic literature. But in light of classical physical chemistry, this is truly a *misnomer*. A real gas is truly one in which intermolecular forces are important, and this has nothing to do with vibrational excitation or chemical reactions.

(The above boxes are quotations from Anderson, 2006, modified to use the nomenclature of this thesis, with some internal references, e.g. to chapters or figures not reproduced here, removed.)

Violation of the Cycle concept

As is explained on page 36 above, the concept of entropy as put forward in Clausius' inequality is only truly valid for completed thermodynamic cycles.

Because internal combustion engines rely upon the conversion of chemical potential energy within fuel and oxidiser to provide the heat which it is their *raison d'être* to convert into mechanical work, they cannot recycle their working fluid. For this reason they tend not to operate on a complete thermodynamic cycle, instead discarding old working fluid & drawing in fresh air from the atmosphere.

This means that the process between the exhaust and intake of a classical thermodynamic cycle is only notional in most practical engines. Although it may at first appear that this is a distinction of trifling importance, and indeed may be such if the other simplifying assumptions of classical thermodynamics

are assumed to hold, it is not obvious to the author that this remains the case when the fact that returning the working fluid to its initial state to permit the operation of a genuine cycle would require the products of combustion to be converted back to air and fuel, a process of rather greater complexity than the changes of temperature and pressure assumed in classical thermodynamics.

Explanations for the use of unrealistic assumptions in the real world

Difficulties in posing the problem

It is relatively simple to imagine idealised forms of real processes, such as isentropic compression, or isochoric combustion. Such idealised processes are inherently simpler to analyse than more generalised processes, because the idealised process will usually hold constant the value of a parameter which might ordinarily be a variable.

For this reason, two difficulties immediately present themselves to the thermodynamicist who wishes to make more realistic modelling assumptions:

1. Modelling of generalised processes
2. Justification of the new model of the behaviour of the previously idealised parameter

The first problem is really two-fold, because the mere fact that a model of a process may be derived does not guarantee that it shall be soluble⁸.

The second problem is one with which large portions of this thesis are concerned; it is hoped that the validation of the code presented on page 110 is considered satisfactory by the reader.

⁸ The most obvious example of a model which is both accurate and insoluble is perhaps the Navier-Stokes equations, which theoretically provide a perfect description of fluid flow, but have yet to be solved analytically.

Wheels within Wheels – lessons from the Orrery

In the 1713, after Newton had put forward the inverse square law of gravitation in *Philosophiæ Naturalis Principia Mathematica* (1687)⁹, and the concept of a heliocentric solar system had gained general acceptance, George Graham, under the patronage of Charles Boyle, the 4th Earl of Orrery, created a mechanical model of the solar system.

This model was named “the Orrery” in the Earl’s honour, and many similar models were subsequently built.

An orrery uses gear wheels to regulate the movement of the various planets and moons within the solar system. It may be seen from visual inspection that the complexity of such a model increases rapidly as additional planets and moons are added to the model:



Figure 2 - A relatively simple orrery modelling Mercury, Venus, Earth and the Moon (image credit: Kaptain Kobold, 2006, Flickr via Wikipedia)

⁹ In fact, the 2nd edition was published in 1713; it does not seem unreasonable to suppose some connection between this publication and the creation of the original orrery, since the 4th Earl was also a Fellow of the Royal Society.

It may also be seen that this model is capable only of approximating a simplified model of the solar system which is composed of a series of independent two-body problems. That is to say that, for example, the motion of the Earth around the Sun in this model is entirely independent of the positions of Mercury and Venus.

In reality, the motion of the every single body within the solar system depends to some greater or lesser extent on the position of every other body within the system. Such a complex system is not susceptible to analytical solution other than in special cases; it must instead be attacked numerically¹⁰.

An analogous problem applies to classical thermodynamics. Whilst it is possible to increase the fidelity of a classical thermodynamic model by adding additional “computational gear wheels”, this approach begins to encounter serious difficulty when attempting to account for interactions between factors (such as for example the second-order interaction between γ and the isentropic efficiency of a component assumed to have a known polytropic efficiency, or that between the pressure of a gas and its C_p).

Just as it is easy to see that attempting to produce an orrery capable of modelling the motion of the bodies within the solar system to match the level of fidelity made possible by the great advances in both theoretical physics and practical astronomy since the early 18th century, it would be quite impractical despite the corresponding advances in gear manufacturing technology over that period. So it also seems apparent to the author that an alternative approach to thermodynamic modelling is now appropriate.

Equilibrium Thermodynamics

A brief history of equilibrium chemistry

Le Châtelier’s principle

Le Châtelier’s principle is in effect a consequence of the concept of equilibrium, in that it states that a system disturbed from chemical equilibrium

¹⁰ Although there are several methods by which this may be done, Feynman made an excellent case for The Principle of Least Action in the second of his lectures *On the Character of Physical Law*: <http://www.youtube.com/watch?v=kd0xTfdt6qw>

will tend to behave so as to return to equilibrium. It is perhaps obvious from a modern perspective that if this were not the case then the system would necessarily be unstable, and therefore would have to be far from equilibrium.

Le Châtelier's principle is often used in schools as the first introduction to equilibrium chemistry in the context of reversible reactions, because it is far easier to understand than the idea that the Gibbs free enthalpy or Helmholtz free energy will tend towards a minimum.

The Helmholtz free energy

The Helmholtz free energy is defined as:

$$A \equiv U - TS \quad (44)$$

Given that the entropy group has a negative sign, minimisation of the Helmholtz energy is directly compatible with the statement of the second law that *the entropy of a system will tend towards a maximum*.

The Helmholtz free-energy is a concept applicable to non-flow processes.

The Gibbs free-enthalpy

It is defined as:

$$G \equiv H - TS \quad (45)$$

This might also be thought of as:

$$G \equiv A + PV \quad (46)$$

It is applicable to steady-flow processes.

The NASA Chemical Equilibrium with Applications (CEA) Code

CEA is a program which calculates chemical equilibrium product concentrations from any set of reactants and determines thermodynamic and transport properties for the product mixture.

(Zehe 2010 A)

This is the culmination of extended investigations in this field at NASA; indeed its roots are in analyses conducted under the auspices of the NACA. A detailed history has been produced by Zehe (2010 B).

The original purpose of these chemical equilibrium investigations at NACA was to assist in rocket development in the 1940s. At this time, relatively few fuel-oxidiser combinations had been used (Ethanol or Gasoline and Liquid Oxygen being favoured in the USA), and given the vast array of possibilities available, the case for a theoretical selection approach was obvious, even given the relatively large budget available for rocketry research in this period and the computational challenges involved, both of which would tend to favour practical experimentation.

The CEA code itself dates from 1994, though it has been updated since then. It is written in FORTRAN. CEA reads an input text file, processes it, and produces an output text file. When using a modern PC, the time taken to manually type an input file is several orders of magnitude longer than the time required to process it. In fact, even the time taken to manually command CEA to read an input file is orders of magnitude longer than the time taken for CEA to run.

Theoretical basis

A detailed explanation of the theoretical basis of the CEA code was provided by Gordon & McBride when they released the code (Gordon & McBride 1994); the following is a brief summary of that document.

CEA attempts to find the equilibrium composition of mixtures by the minimisation of free energy¹¹ (Gibbs or Helmholtz as appropriate).

Various assumptions are made:

- Gases are assumed to be ideal.
- Interactions between phases (solid, liquid and gas) are neglected.
 - $PV = nRT$ is assumed to hold even in the presence of small amounts of condensed species.

¹¹ The alternative approach would be to use equilibrium constants, but Gordon & McBride discarded this approach as it would require the reactions under consideration to be specified explicitly, which would have been difficult given the general nature of the code.

- Condensed species are assumed to be pure
- Ions are considered optionally.
 - However, when ions are considered, coulombic interactions are not modelled, which limits the validity of the results to those situations in which ions are only present in small concentrations.

The Bridgman differentials

In 1914, Bridgman published a paper setting out a method for expressing the first and second derivatives of a wide variety of thermodynamic properties in terms of any three independent derivatives.

This is extremely useful when attempting to converge upon a solution with constraints, since in general a partial derivative may be found of the form:

$$\left(\frac{\partial \text{Input}}{\partial \text{Output}} \right)_{\text{Constraint}} \quad (47)$$

Then, trivially,

$$(\text{Target} - \text{Output}) \left(\frac{\partial \text{Input}}{\partial \text{Output}} \right)_{\text{Constraint}} = \delta \text{Input} \quad (48)$$

The following list of Bridgman partial differentials has been used in this work:

$$(\partial H)_P = -(\partial P)_H = C_P \quad (49)$$

$$(\partial H)_S = -(\partial S)_H = \frac{-VC_P}{T} \quad (50)$$

$$(\partial S)_P = -(\partial P)_S = \frac{C_P}{T} \quad (51)$$

$$(\partial S)_T = -(\partial T)_S = \left(\frac{\partial V}{\partial T} \right)_P \quad (52)$$

$$(\partial T)_P = -(\partial P)_T = 1 \quad (53)$$

Practical application to thermodynamic modelling

The original intention of behind codes such as CEA was that they would be selectively used to investigate specific problems in equilibrium thermodynamics.

Although CEA is built around the proposition that one might evaluate several cases of an individual problem using a single instance of the executable file, the intention behind this appears to have been to allow several data points to be used for subsequent interpolations in order to reduce the need for iteration.

CEA allows various different classes of problem to be investigated:

- Fixed temperature and pressure (“tp” or “pt”)
- Fixed specific enthalpy and pressure (“hp” or “ph”)
- Fixed specific entropy and pressure (“sp” or “ps”)
- Fixed temperature and volume (“tv” or “vt”)
- Fixed internal energy and volume (“uv” or “vu”)
- Fixed specific entropy and volume (“sv” or “vs”)
- Rocket combustion (“ro” or “rkt”)
- Shockwave problems (“sh”)
- Chapmen-Jouget detonation (“det”)

(McBride & Gordon, 1996)

There have been considerable advances in computational technology since CEA was released (see Figure 8 on page 72) and therefore the computational cost of running CEA is considerably less important than would have been the case when it was first released.

Limitations of Equilibrium assumptions

Equilibrium chemistry represents one of two extreme cases, the other being the so-called “frozen” case where no chemical changes are considered.

Any real system will lie somewhere between these two extremes.

The fundamental implication of equilibrium assumptions is that the mixture under consideration has an infinite amount of time in which to arrive at its final state.

This should be intuitively obvious from the fact that the driving force behind chemical change must tend towards zero as equilibrium is approached (because at equilibrium the overall force must be zero) and therefore equilibrium may only be asymptotically approached within a finite time.

Problems of scale

For any given set of flow parameters, it follows that the residence time available for the attainment of equilibrium is a function of the size of the system. Smaller systems will tend to be further from equilibrium than larger systems. In this sense, equilibrium implies an infinite physical scale.

Meta-stable chemical mixtures

Due to the infinite-time assumption implicit within the wider assumptions of equilibrium chemistry, it is not obvious that meta-stable mixtures will be treated reasonably. For example, if CEA is given a 4-species model of air and told to evaluate it under ISA sea level conditions, it will produce a small amount of NO_x .

In reality, the formation of NO_x is generally held to occur only at high temperatures, because an activation energy is required to break up diatomic Oxygen and Nitrogen molecules before NO_x may form.

Taking this example further, if the air is heated to some high temperature at which large quantities of NO_x are generally expected to form, and then cooled back to room temperature, it would be expected in reality that a large amount of the NO_x would remain, because the cooling process would almost certainly be far faster than the rate at which the NO_x would be expected to break up and re-combine as diatomic Oxygen and Nitrogen.

However, because CEA assumes that the mixture of reactants is always at equilibrium, any reaction which would be reversible given infinite time is effectively treated as being genuinely reversible (see *Appendix A – CEA input and output files illustrating the extreme reversibility associated with equilibrium chemistry assumptions* on page 146).

AN OVERVIEW OF THE BRAYTON CYCLE GAS TURBINE

Introduction

This section is intended to describe the Brayton-cycle gas-turbine configuration, as modelled in the ExcelCEA code outlined below: it is therefore both a generalisation and a compromise.

General arrangement

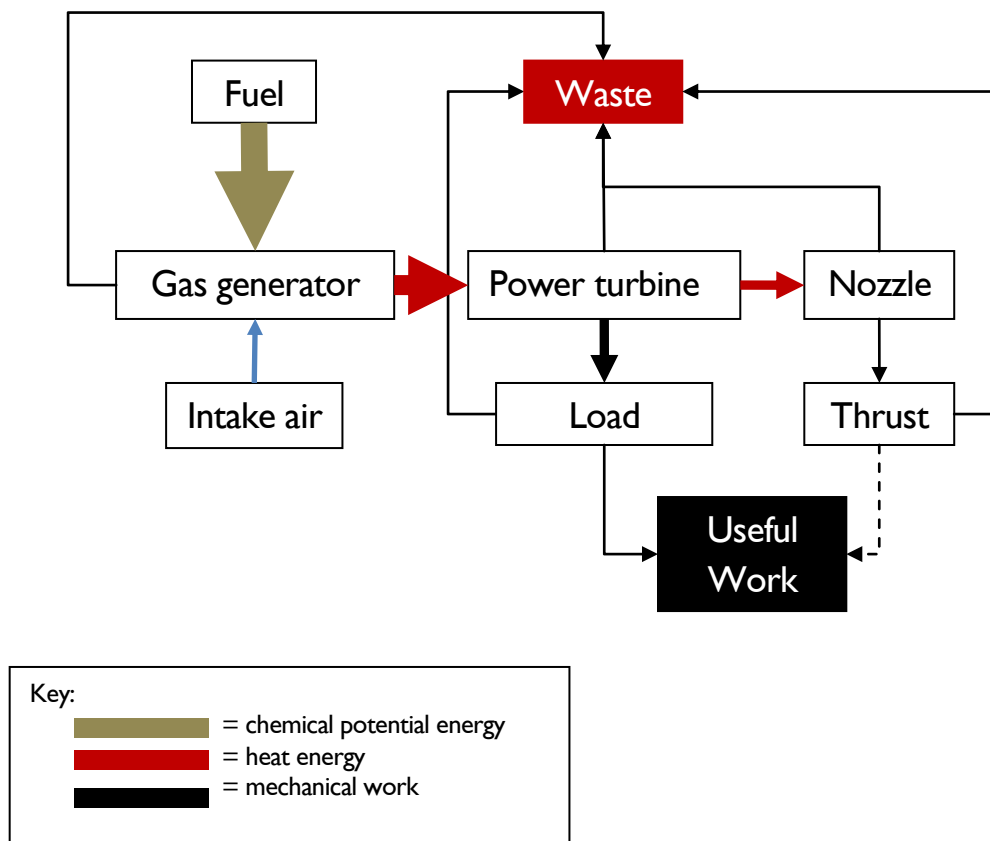


Figure 3 - Energy flows within a generalised Brayton-cycle gas-turbine.

The weight of the arrows in Figure 3 approximately indicates the magnitude of the energy flows. Because arrows can only be drawn in a single colour, losses are considered to be mechanical, although in reality there would also be heat-transfer losses.

N.B. - Figure 3 is a generalisation, and therefore it is not known whether jet thrust produced by the nozzle is able to perform useful work or not. As such this link is represented with a dashed line. Although a similar argument might be advanced regarding the power turbine, in that a turbojet might not extract useful mechanical work, such engines are becoming increasingly rare due to the inherent inefficiency and noise of direct jet propulsion, whereas stationary power engines are common.

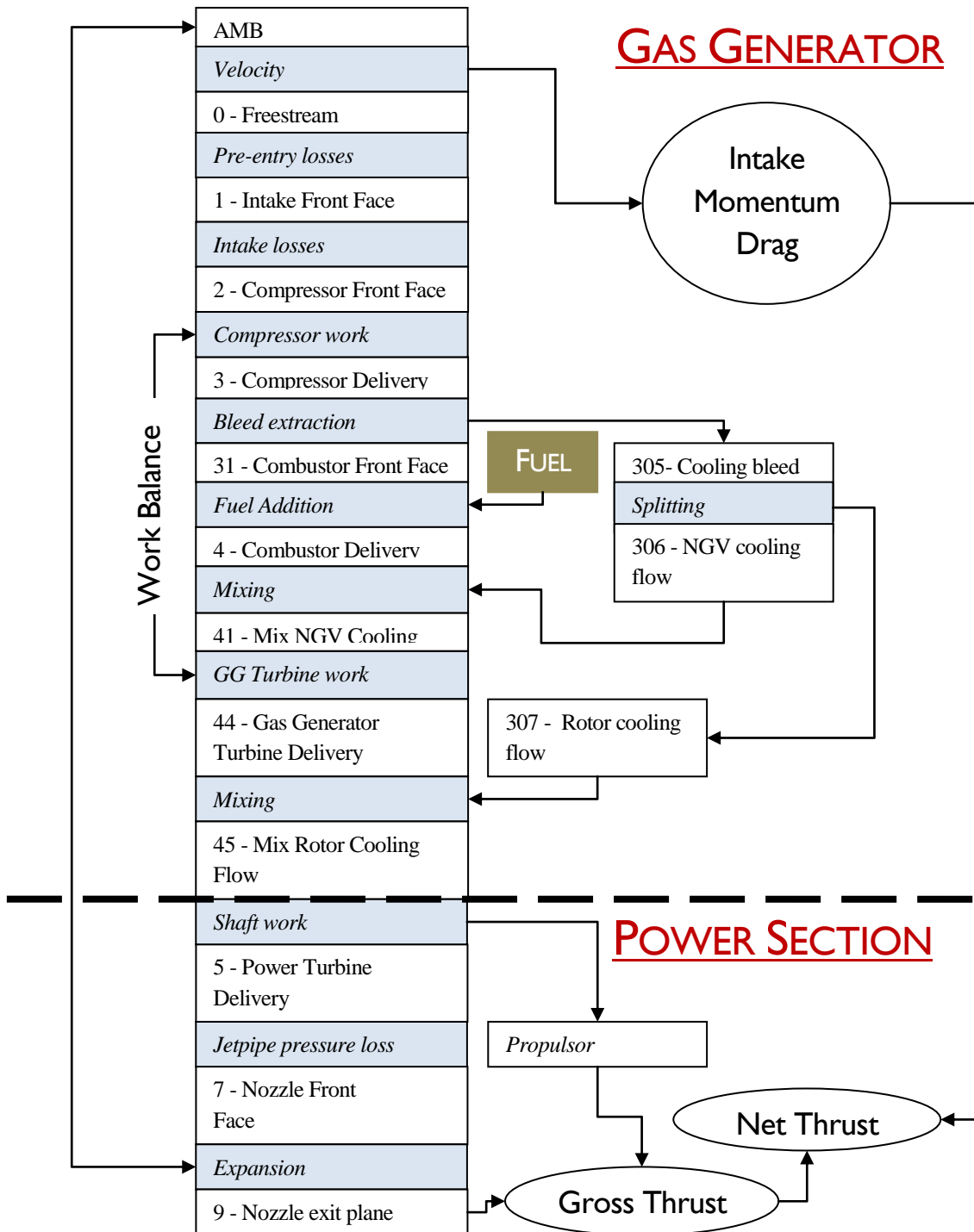


Figure 4 - Stations and processes within a propulsive Brayton-cycle gas-turbine

Flow (both physical and numerical) proceeds vertically from top to bottom except where otherwise indicated by arrows.

Intake

The purpose of the intake is to provide the compressor with a smooth and stable flow of air which it is able to handle efficiently.

From a practical engineering standpoint, the even quality of the air (i.e. freedom from total temperature and total pressure distortions) is more important than the exact fraction of the total pressure and temperature retained by the air upon its arrival at the compressor face.

However, because this thesis is concerned with a one-dimensional thermodynamic performance model of the engine, rather than with the prediction of the performances of installed engines, the flow is isotropic by definition and therefore intake-flow distortion is not of interest.

Having assumed the flow to be isotropic, the intake is simply treated as an adiabatic duct whose cross section is such as to deliver air to the compressor front face at a defined velocity.

In reality, gas turbines operate such that the flow is almost invariably choked somewhere along its path through the engine (usually at the first stage of turbine nozzle guide vanes if nowhere else). The flow velocity upstream of the choking point is effectively set by the amount of flow which may pass through the choked passage. This means that subsonic intakes do not really control the one-dimensional flow parameters that they deliver.

However, from a modelling perspective, it is far simpler to assign an intake delivery velocity and assume that the rest of the machine has been designed so as to achieve this velocity than it would be to define the geometry of the machine, work out which section chokes first and then calculate the upstream flow-parameters accordingly. Such expended effort is the province of Computational Fluid Dynamics rather than thermodynamic performance modelling.

Because the intake is a physical duct, it inevitably suffers from friction, which imposes a loss upon the flow. It is generally held that intakes are adiabatic, and that losses are therefore manifested as reductions in the total pressure of the flow.

Subsonic intakes in commercial transport aircraft are often assumed to achieve 99% total pressure recovery when operating under cruising conditions. This impressive figure is achievable because in subsonic flow, it is possible to achieve substantial pre-entry diffusion, which is held in the literature to be isentropic (e.g. Seddon & Goldsmith, 1999). This means that the intake is short and of almost constant area, and therefore essentially aerodynamically-benign.

The main source of loss associated with the intake system of a subsonic transport aircraft is therefore the cowl drag associated with the flow rejected by the engine itself.

Compressor

The compressor converts mechanical work into an increase in the total pressure of the working fluid. All but the smallest modern engines use axial-flow compressors, but the design of the compressor is only of secondary importance in the context of one-dimensional modelling¹².

The most important thermodynamic parameter associated with the compressor is its efficiency.

This may be described either in terms of the isentropic efficiency, which is the ratio of the work required for isentropic compression to the desired pressure to that actually required, or the polytropic efficiency, which is the isentropic efficiency of an infinitesimal part of the compression process.

¹² The second-order difference arises because centrifugal flow compressors impose large velocity changes upon the flow: this means that they operate with a larger split between total and static temperature.

This is important because the chemical and transport properties of the flow are associated with the static temperature. Therefore a compression process based upon extremely large velocity changes could potentially operate far from equilibrium, meaning that its performance (and indeed the isentropic performance standard against which its efficiency might be measured) would be different from that of a machine designed to keep its working fluid close to equilibrium.

It is worth observing in passing that it would not be impossible to achieve quite large differences between the total and static temperature for axial flow compressors, though this would require a somewhat different design methodology than that adopted in current practice.

The latter measure of efficiency is useful when performing design studies, because the polytropic efficiency is approximately constant between different designs executed at the same technology level.

Casey and Compressor efficiency

This thesis is constructed around the entropy-based definition of both isentropic and polytropic efficiency put forward by Casey in his 2007 paper *Accounting for losses and definitions of efficiency in turbomachinery stages*.

The key advantage of this methodology is that it greatly reduces the amount of iteration required, because it does not require knowledge of the value of γ , which is, of course, itself a function of the compressor efficiency.

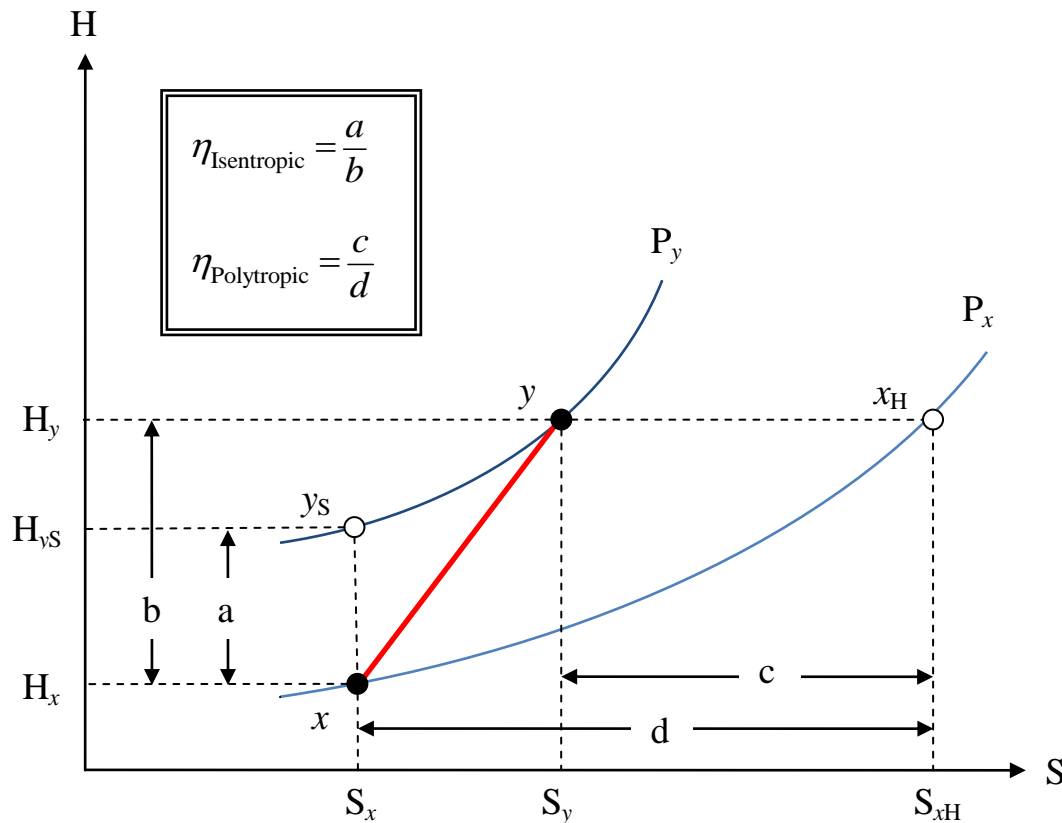


Figure 5 - Compressor efficiency definitions after Casey (2007)

All of the points in the diagram above are described by H,P,S coordinates. Note that the path between x and y need not be known.

Casey's states

x = Initial State

x_H = Dissipated state; initial pressure, final specific enthalpy

y = Final State

y_S = Isentropic State; final pressure, initial specific entropy

States x_H and y_S are virtual states, denoted by open circles in Figure 5 on page 59 and Figure 6 on page 64, the real states being denoted by solid circles.

Given one of the fractions $\frac{a}{b}$ or $\frac{c}{d}$, and either the specific enthalpy change, b , or the final pressure, P_y , it is possible to calculate all thermodynamic properties of the final state, y .

This also applies to turbines.

Combustor

The purpose of the combustor is to mix and combust the air and fuel in order to increase the temperature of the working fluid.

Because the laminar-flame speed for mixtures of air and kerosene is relatively slow when compared with the velocity at which most compressors deliver air, a diffuser is required; this inevitably incurs some pressure loss. Additionally, some degree of turbulence is required to mix the air and fuel.

All of these aerodynamic losses, which may be measured directly in the absence of combustion, are termed the “cold pressure loss”.

In addition to the cold pressure loss, there is also a fundamental hot pressure loss associated with the addition of heat to the flow, as predicted under the Rayleigh flow model¹³. This loss is generally small in most modern combustors because the Mach number of the flow is low.

¹³ It is not immediately obvious that this hot loss is indeed fundamental because the flow cannot “know” what its Mach number is relative to some external reference. Ignoring legal technicalities, one would not expect to see any great difference in the flame of a cigarette lighter ignited in the cabin of an airliner at Mach 0.80 and that of one ignited on a mountain under ambient conditions equivalent to those within the cabin. [*Continued overleaf...*]

It is conventional to take account of the flow losses as a single fixed percentage of total pressure, usually around 4%.

Much current development effort is focussed upon the control of the engine's exhaust emissions. These emissions are produced within the combustor. They may be conceptually separated into products of incomplete combustion, such as soot and carbon monoxide, and products of dissociation, such as Ozone and Oxides of Nitrogen.

Assuming that the peak combustion temperature is less than approximately 1800 K, then the quantity of NO_x and Ozone produced may be reduced by improving the homogeneity of the fuel-air mixture in order to reduce local temperature overshoots.

If higher delivery total temperatures are required, then alternative strategies are likely to be required.

In any case, the one-dimensional equilibrium chemistry model implicitly assumes a perfectly homogeneous mixture of fuel and air.

[Footnote 13 Continued] It is the author's opinion that any pressure loss associated with the addition of heat to flow must stem from some initial velocity gradient, such as that due to turbulence, and therefore is not fundamental in the same sense as for example the exchange between pressure and velocity implied in the Bernoulli equation.

It is also worth observing that hot losses may be explained without necessarily making recourse to a Rayleigh flow model because the kinematic viscosity and density of the working fluid are functions of both its composition and temperature. Because the Reynolds number of a flow depends upon kinematic viscosity and density, it follows intuitively that the nature of any turbulence in that flow will be different under "hot" conditions than under cold-flow testing. This change in turbulence scale will subsequently change the velocity of the flow at any given point, imposing a second-order change in the Reynolds number.

Because this second-order effect must necessarily lag behind the first-order change in turbulence scale, it is easy to see how a time dependent behaviour can emerge, which the author surmises to be partially responsible for the flickering of candle flames and the production of "combustion noise".

Turbine

Intellectually, a turbine is just a compressor operating in reverse, reducing the pressure of its working fluid in order to extract mechanical work.

Turbines are generally able to achieve higher stage pressure-ratios than compressors because they operate with a favourable pressure-gradient: this means that they are able to produce considerably more work per stage than a compressor is able to add, because a pressure ratio corresponds to a temperature ratio, and the temperature of the gas with which the turbine operates is much higher than that with which the compressor performs.

Turbines are used both to supply mechanical work to the compressor and also sometimes to extract mechanical work for other purposes.

Conceptually the engine modelled, as described within this thesis, uses separate turbine stages for this purpose, but this is simply done for mathematical convenience rather than because there is any particular thermodynamic¹⁴ requirement to do so.

Turbine cooling

Turbines are highly stressed components. The turbine is subject to aerodynamic loads from the gas impacting upon it, and to centrifugal loads associated with the turbine's rotation. It is also subject to considerable oxidative stress because current gas-turbines operate lean of stoichiometric conditions.

Because the strength of materials decreases as their temperatures increases, the turbine therefore poses considerable mechanical design challenges.

¹⁴ There are physical arguments for doing so in cases where the mechanical work is not desired at the same rotational speed as that of the compressor, because this allows the compressor and its turbine to be matched independently of the useful mechanical load, so permitting greater operational flexibility. It may also permit the omission of a gearbox, depending upon the precise requirements the engine is designed to meet.

These challenges were amongst the main arguments¹⁵ used by sceptics of Whittle's work to support their contention that an internal-combustion gas-turbine of flight weight was impractical.

Towards the end of the Second World War, the Germans, faced with a massive shortage of high-temperature materials, attempted to innovate their way out of trouble by actively cooling their turbine blades.

This technology has since become universal in advanced engines.

Most modern engines attempt to envelop their turbine blades in a blanket of (relatively) cool air. The cooling air must therefore be at a higher pressure than the local static pressure of the gas flow: this means that at least the initial turbine cooling air must be drawn from the compressor delivery.

This air is extremely thermodynamically expensive because of the large amount of compressor work required to get it up to the full compressor delivery pressure.

The amount of cooling air required is a function of various factors. For the purposes of this thesis, a correlation put forward by Kurzke in 2003 is used:

$$\eta_{\text{Cooling}} = \frac{T_{\text{Gas}} - T_{\text{Metal}}}{T_{\text{Gas}} - T_{\text{Coolant}}} \quad (54)$$

$$\frac{W_{\text{Coolant}}}{W_{\text{Gas}}} = k \frac{\eta_{\text{Coolant}}}{\eta_{\text{Coolant}} - 1} \quad (55)$$

Kurzke suggests that setting $k = 0.05$ produces sensible results over a wide range of pressure ratios and therefore this value is adopted in the present work, although the value of k is a user-input within the ExcelCEA code.

¹⁵ The others being that the combustion intensity required was orders of magnitude higher than that previously demonstrated industrially and that Whittle's target of 80% isentropic efficiency for his single stage centrifugal compressor of pressure ratio 4.0:1 was optimistic – in this regard at least they were partially justified since his design *only* achieved approximately 79% (Hooker, 1984).

Casey and turbine efficiency

The efficiency calculations for the turbine under Casey's scheme are similar to, but slightly different from, those used in the compressor¹⁶.

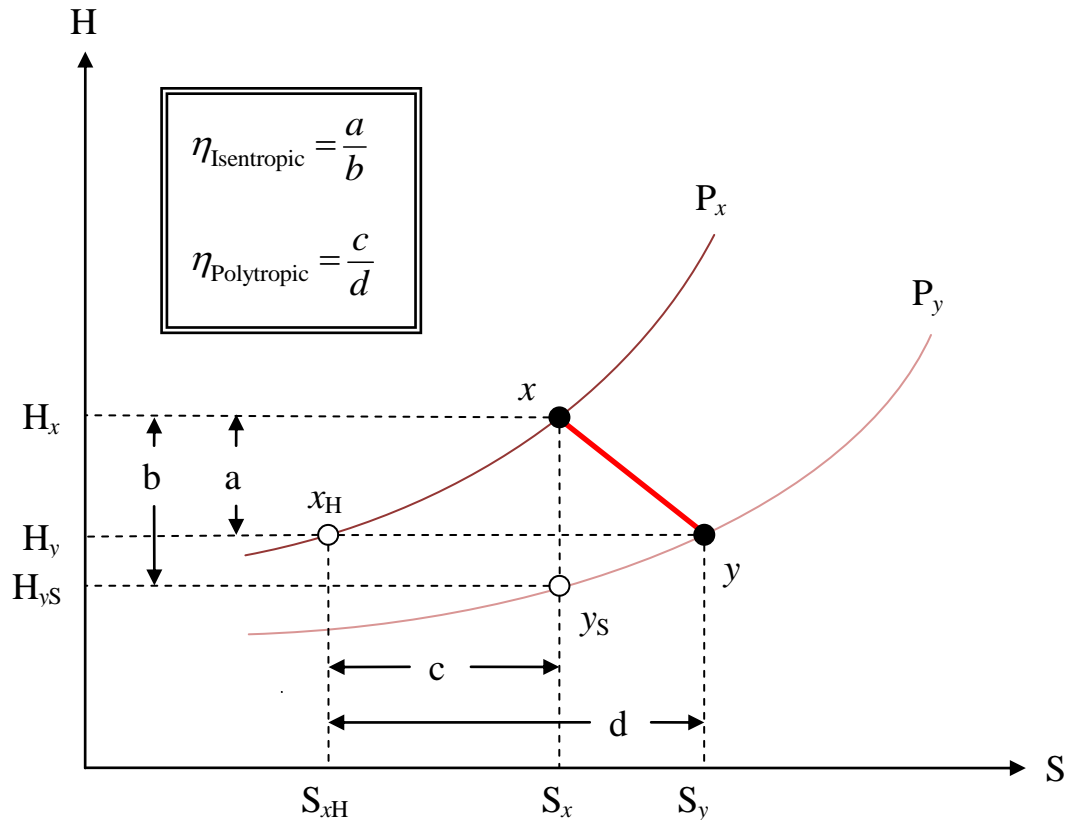


Figure 6 - Turbine efficiency definitions after Casey (2007)

The meaning of the states is identical to that for compressors, as given on page 60. Note, however, that state x_H is now more obviously virtual, given that its entropy is less than that of state x itself, which is implausible for an adiabatic process.

¹⁶ Unfortunately, Casey only makes passing reference to them, and as with many things claimed to be “trivial”, the author has found them anything but...

Nozzle

Turbine Analogy

Nozzles and free power turbines are mathematically equivalent (e.g. Saravanamutto 2001¹⁷). The purpose of the nozzle is to expand the flow such that its static pressure is equal to that of the ambient environment; the work extracted from the gas is used to increase its kinetic energy, and the momentum flux across the nozzle provides the gross thrust.

Froude Efficiency

The fundamental efficiency with which mechanical power may be converted into propulsive work by a jet was first seriously investigated by Froude in connection with the screw propulsion of ships in the late 19th century. This fundamental efficiency is:

$$\eta_{\text{Froude}} = \frac{2}{1 + \frac{v_{\text{Jet}}}{v_{\text{Freestream}}}} \quad (56)$$

In any propulsive cycle whose primary thrust is produced by a mechanical load driven by the turbine rather than directly by the propulsive jet formed by the main cycle flow, it follows that there must be an optimal way in which to split the enthalpy drop between the power turbine and the nozzle.

Because the efficiency with which a propulsive jet converts its kinetic energy into propulsive work has long since been defined by Froude, and declines with increasing jet velocity for any given vehicle speed, it appears intuitively obvious that the optimal split may be achieved via the following procedure:

1. Start by assuming that the nozzle extracts just enough work to produce zero net thrust; this thrust is produced with 100% Froude efficiency.
2. It therefore follows that the enthalpy used to develop this thrust was used more efficiently than that used to produce mechanical work in the turbine.

¹⁷ p.339

3. Hence, increasing the enthalpy drop across the nozzle at the expense of that across the power turbine is sensible.
4. At some point the efficiency with which the nozzle and power turbine produce propulsive work will become equal; at this point it is reasonable to assume that the optimal work split has been achieved.

Since the isentropic efficiency of the turbine is known either exactly (if the design procedure assumes it to be fixed) or to a close approximation (if constant polytropic efficiency is used as in the design procedure), convergence may be accelerated by calculating a Froude efficiency target and hence a Nozzle velocity target.

Casey and power turbine efficiency

The Power Turbine uses the same diagram as the gas generator turbine (Figure 6, page 64); however, whereas the gas generator turbine extracts a known quantity of work from an unknown expansion ratio, the power turbine extracts an unknown quantity of work from a known expansion ratio. This means that a different sequence of calculations is required.

Shaft Power Cycles

It is of course possible to use a gas turbine for non-propulsive purposes, such as the generation of stationary shaft-power either for satisfying a base load or contingency utilisation.

In such cases, the efficiency of enthalpy expended across the nozzle is zero. However, it is still necessary to leave some excess total-pressure in reserve across the nozzle in order that the engine will continue to run in the event that the prevailing wind blows into its exhaust.

THERMODYNAMIC MODELLING OF THE BRAYTON CYCLE GAS TURBINE

Historical background

The Brayton-cycle gas-turbine is perhaps unique amongst the commonly used internal-combustion engines in that it may definitely be stated that

thermodynamic modelling of its performance predates its first successful application. Whittle undertook pertinent calculations in support of his solicitations for funds in the 1930s.

Early work was based upon the sort of approach outlined in Equation (17) above, but with the addition of isentropic efficiency factors to account for losses in the compressor and turbine.

Methods in current use

Today there are a variety of gas-turbine analysis tools available, based upon various different technologies.

TURBOMATCH

TURBOMATCH is a computer code used at Cranfield University for the design-point and off-design-point analysis of gas turbine engines and ramjets.

The author has not seen the source code.

It appears to be written in FORTRAN77 and to use Imperial units internally; SI units must be selected with a switch.

Text input files are generated manually; this process must be carried out with great care as the code does not fail gracefully!

Output is delivered in the form of a second text file. The most impressive aspect of the code is its ability to model the off-design-point case by using a selection of component maps which are scaled to approximate¹⁸ to the performance of engines of varying efficiency.

GASTURB

GASTURB is a commercially available code developed by Kurzke.

¹⁸ It is the author's contention that a compressor or turbine map ceases to be a map once scaled and becomes a pseudo-map because scaling is not constrained by physical reality; therefore it is quite possible for scaled maps to produce off-design-point isentropic-efficiencies in excess of 100%!

A note on the limitations of the open literature

Due to the commercially sensitive nature of gas-turbine development, it would not be at all surprising if a large proportion of the computer modelling codes used industrially were treated as trade secrets.

A list of gas turbine performance codes was published by NATO in 2007 as part of *RTO-TR-AVT-036 Performance Prediction and Simulation of Gas Turbine Engine Operation for Aircraft, Marine, Vehicular, and Power Generation*:

- SOAPP (P&W)
- CWS/ICS (GE)
- GECAT/NEPP (SRS Technologies)
- TERMAP (Allison/USAF)
- RRAP (Rolls-Royce)
- JANUS (Snecma)
- ON-X/OFF-X (Jack Mattingly)
- PYTHIA (Cranfield)
- TURBOMATCH (Cranfield)
- FAST (Honeywell Allied Signal)
- TESS (University of Toledo)
- ATEST (AEDC)
- MOPS/MOPEDS (MTU)
- GasTurb (Kurzke)

Unfortunately, only MOPS/MOPEDS and GasTurb are discussed in any detail in the NATO document, and it is therefore impossible, within this thesis, to make any definitive claims about the novelty of the intellectual knowledge contained therein.

Indeed, it would be somewhat surprising if no previous attempt has been made to integrate CEA with a gas-turbine performance code, because the advantages appear obvious to the author.

However, in the absence of definitive information on this subject, it is the author's judgement that even if similar work has been undertaken previously in secret, this thesis still contains a contribution to *public* knowledge.

THE “EXCELCEA” MODEL

The name “ExcelCEA”

Excelsior is a Latin word meaning “ever higher”.

It is also the title of a poem by Henry Wadsworth Longfellow, first published in 1841, which has at times seemed to the author rather an apt allegory for the risks and sacrifices inherent in the pursuit of a PhD.

ExcelCEA /ɛk'sɛlsɪə¹⁹/ is the name chosen by the author to describe a thermodynamic modelling-tool, which attempts to combine the best features of the CEA code already described with those of the Microsoft Excel programme, i.e. its user-friendly interface and its ability to effectively and rapidly produce charts.

Overview

Thermodynamic analyses may be split into two parts:

- 1) Process calculations
- 2) Working fluid calculations

The ExcelCEA code uses CEA to perform working fluid calculations, and a thermodynamic process code developed by the author to perform process calculations.

Excel is used for data input and output.

¹⁹ International Phonetic Alphabet, *via* the Oxford English Dictionary online, constructed using the majority of the pronunciation of “excelsior”, /ɛk'sɛlsɪɔː/, combined with the first “a” sound from “attack”, /ə'tak/; the author makes no claim to expertise in the field of phonetic transcription!

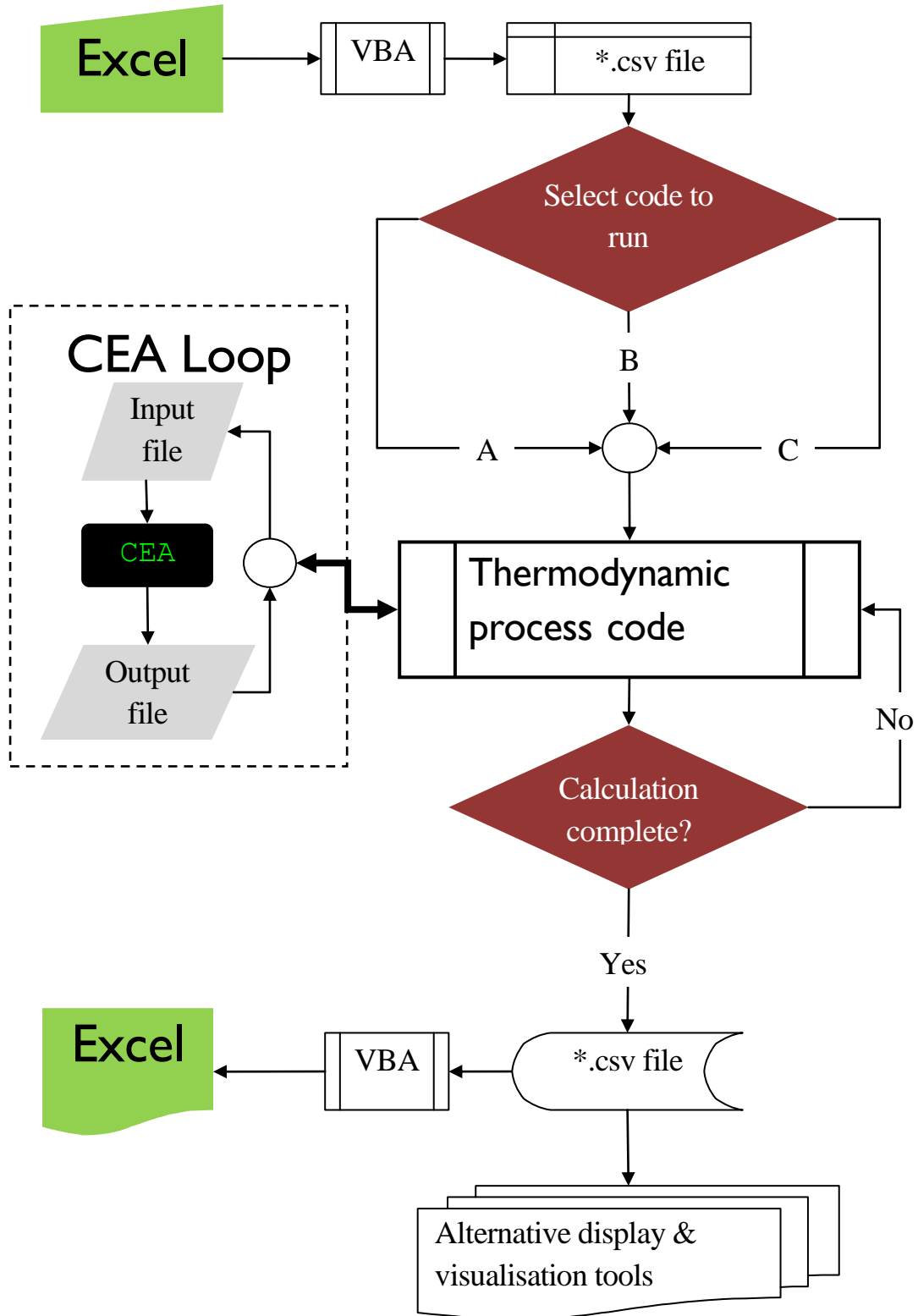


Figure 7 - ExcelCEA workflow

The central idea behind ExcelCEA is that the operation of CEA itself is automated. The CEA loop will typically be called upon anything from hundreds up to millions of times when ExcelCEA is run.

The storage of the output data both within Excel and as a *.csv file simultaneously provides a primitive backup, and also facilitates the use of alternative display and visualisation software if desired.

Although Excel is used to build the input *.csv file for the thermodynamic process code, given such an input file, the thermodynamic process code is independent of Excel. This means that calculation tasks may be split across multiple independent PCs if desired. It also means that the output file size is not constrained by Excel's limitations.

Technological context

When CEA was released in 1994, the standard desktop PC was based upon the Intel 486 CPU. There has been a dramatic improvement in computer technology since then!

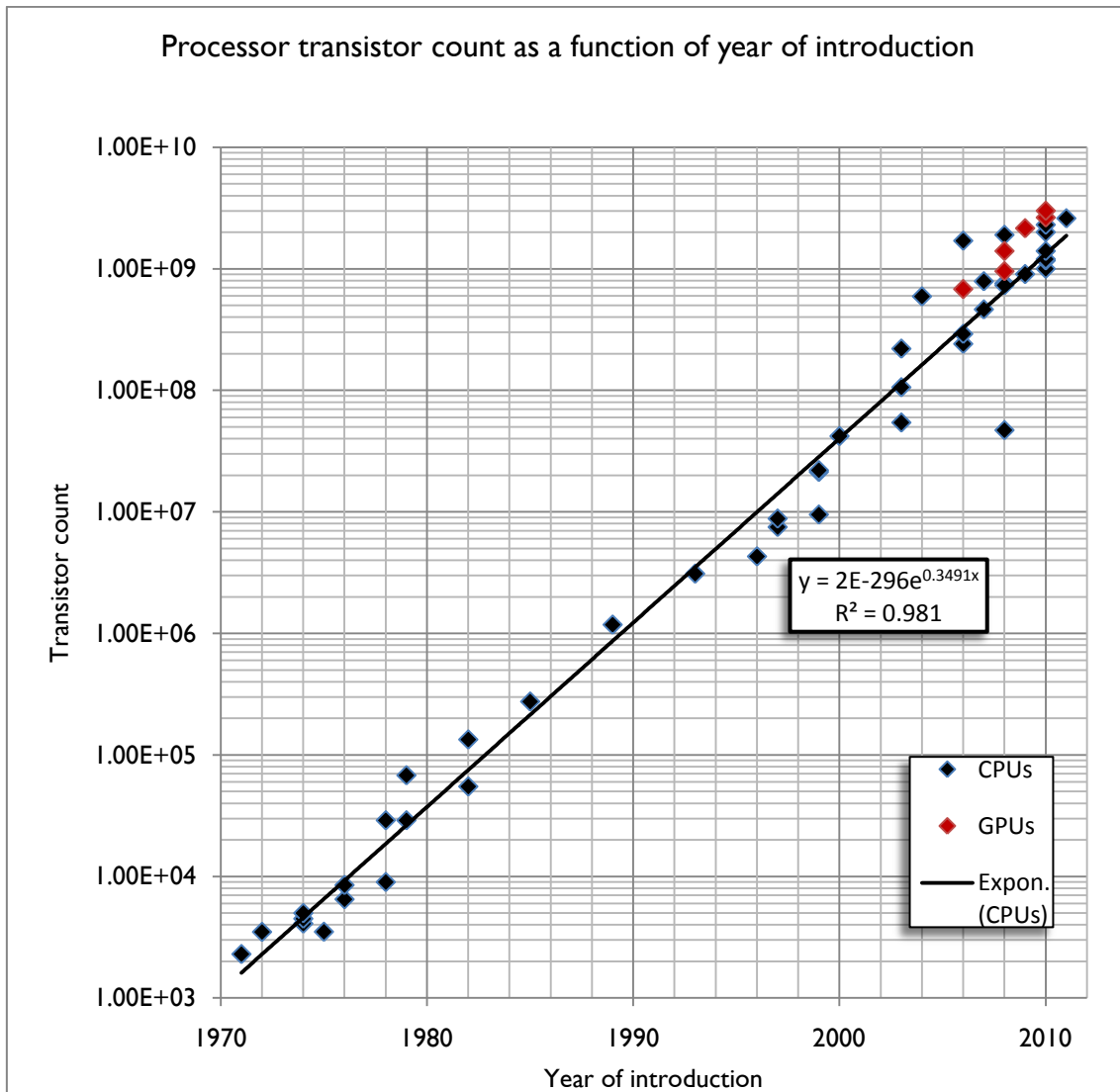


Figure 8 - CPU transistor counts 1971-2011, data from Wikipedia, 2011C

As a first-order approximation, the calculation speed of a CPU varies in proportion to its transistor count, whilst its production cost varies approximately in proportion to its area. Thus, the approximate cost of calculation will vary as the inverse of the transistor count per unit area.

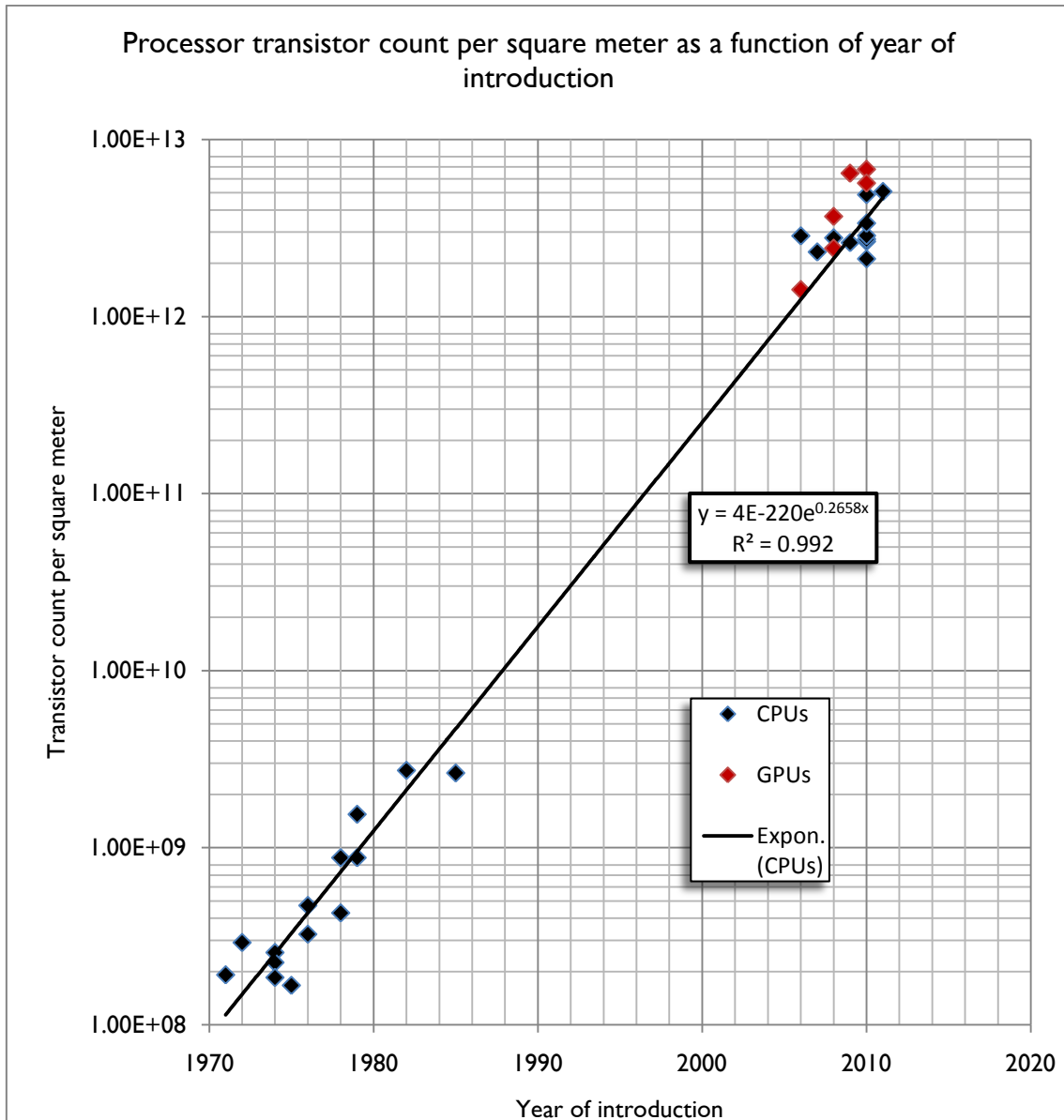


Figure 9 - Processor transistor counts per unit area, 1971-2011, data from Wikipedia (2011C)

It is worth observing that, especially prior to approximately 1995, CPU releases were relatively infrequent, which means that Moore's law applied in discrete steps rather than in a continuous fashion. The amount of processing power available when CEA was developed was therefore somewhat less than would be suggested by a naïve application of Moore's law (Moore, 1965)

based upon its release date, as it slightly preceded the general availability of the Pentium[®] CPU²⁰.

This means that a modern PC is somewhat in excess of 1000 times as fast as the machines for which CEA was originally written, which means that it is practical to consider using CEA in a manner which would have been quite impractical when it was first released.

CEA Output

The CEA code, when run in “tp”, “hp”, or “sp” mode, produces the following output data:

- a. Input file**
- b. Restatement of input chemical composition:**
 1. Mass fraction keys & values
- c. Measures of Equivalence ratio:**
 1. $\frac{W_{\text{Oxidizer}}}{W_{\text{Fuel}}}$
 2. % Fuel in overall reactants
 3. Chemical equivalence ratio, $r_{\text{Equivalence}}$
 4. Chemical equivalence ratio, ϕ
- d. Thermodynamic Properties:**
 1. Pressure, P
 2. Temperature, T
 3. Density, ρ
 4. Specific Enthalpy, H
 5. Specific Internal Energy, U
 6. Specific Gibbs Enthalpy, G
 7. Specific Entropy, S
 8. Mean Molecular Mass, M

²⁰ Although the first Pentiums were introduced in March 1993, the author remembers that his first PC was based on a 100 MHz 486DX4 in 1995; progress was somewhat more leisurely in those days, partly because prices were so high; 4 MB of RAM then cost approximately £200; one could actually buy an entry level PC for approximately this sum of money at the time of writing if inflation is taken into account!

9. Bridgman Differentials:

- $\left(\frac{\partial \ln V}{\partial \ln P}\right)_T$
- $\left(\frac{\partial \ln V}{\partial \ln T}\right)_P$

10. Specific heat capacity at constant pressure, C_p

11. Ratio of specific heats at Mach 1, γ_{Sonic}

12. Local speed of sound, v_s

e. General Transport properties:

1. Viscosity

f. Equilibrium Transport properties:

1. C_p

2. Conductivity

3. Prandtl Number

g. Frozen Transport properties:

1. C_p

2. Conductivity

3. Prandtl Number

h. Output chemical composition:

1. Mass fraction keys & values

These data form the basis of the various calculations performed by the code.

Calculation method

Background

In 2008, the author was engaged in the investigation of novel aerospace propulsion concepts. One of these concepts was a turbo-compound piston engine design. Classical analytical methods resulted in estimations of cycle efficiency which were considerably higher than expected. It was concluded that the engine and its thermodynamic cycle were potentially interesting, but that considerable further work was required.

A patent was obtained for the engine, and simultaneously, work on a more comprehensive thermodynamic analysis was begun. (The patent has since been assigned to Rolls-Royce.)

The novel cycle under consideration, briefly, consists of a supercharged, compression-ignition piston-engine with variable valve timing. The exhaust valve timing is set so as to achieve work balance, such that the supercharged piston engine acts as self-contained gas-generator. Useful shaft work is then extracted via an independent power turbine, with the possibility of further jet thrust being extracted via a propulsive nozzle.

This cycle would appear to have the potential to achieve high peak cycle efficiencies for several reasons:

- The peak cycle temperatures are reached intermittently, and therefore inherently exceed the metal temperature without recourse to active cooling.
- Combustion may proceed at approximately constant volume, raising peak cycle pressure.
- As much compression as practical is conducted as a non-flow process, whilst as much expansion as possible is conducted as a steady-flow process; therefore the difference between the specific heat capacities at constant pressure and constant volume appears to be available for exploitation, although the author would not wish to claim this appearance to be reality without recourse to practical experiment.

The merit of any novel cycle is relative rather than absolute. That is to say that the justification for departure from the *status quo* is the superiority of the alternative, rather than the absolute value of any performance parameter.

This means that in order to justify work on a novel cycle it is necessary to produce a fair comparison between it and the currently incumbent cycle, such that the superiority of the novel cycle may be demonstrated beyond doubt.

Because the novel cycle put forward involved both higher peak temperatures and higher peak pressures than a Brayton cycle of equivalent technology level, the thermodynamics of dissociation might potentially assume considerably greater importance.

Irrespective of the reality of dissociation under the actual peak cycle conditions envisaged, the fact that such an argument might be made requires that the modelling methodology used must be capable of rendering such effects within its results.

Meanwhile, in order to produce a fair comparison, it is necessary that both the incumbent and novel cycles be modelled using the same methodology and assumptions.

Given the wide range of cycle parameters, and the variety of thermodynamic processes involved, this required the creation of an extremely general modelling methodology.

A review of the literature suggested that the NASA CEA code was suitable as a basis for the thermodynamic analysis of reacting chemical mixtures under a wide range of conditions. However, reading the documentation which accompanies the code (Gordon & McBride/McBride & Gordon) suggested that considerable work would be required to produce a working design-point performance code in this way.

Therefore, initial work attempted to limit the use of CEA to the analysis of the combustion process, the intention being to use the polynomial approach put forward by Walsh & Fletcher (2004) for the less thermodynamically extreme parts of the cycle.

Unfortunately, it was quickly found that such a hybrid approach was fundamentally impractical due to the limitations inherent in the conversion between 2-d polynomials (H or S as a function of T) and the full-chemical equilibrium calculations performed by CEA.

It was therefore reluctantly decided to proceed with the altogether more ambitious process of modelling entire cycles using CEA.

This has proven even more challenging than expected, which perhaps goes some way towards further validating Hofstadter's Law:

It always takes longer than you expect, even when you take into account Hofstadter's Law.

(Hofstadter, 1979)

The process of calculating the performance of a thermodynamic cycle is analogous to that of solving a number puzzle such as Sudoku, in the sense that a limited amount of initial information is gradually used to fill in gaps in knowledge until eventually a complete solution emerges.

The key differences lie in the scale of the problem and the complexity of the rules which must be applied to calculate the unknown values, such that it is very unlikely that an incomplete calculation of the performance of a Brayton-cycle gas turbine under equilibrium chemistry assumptions shall find its way to the puzzle pages of a national newspaper, to be completed for the amusement of its readers²¹.

Known parameters – the input file

Whereas a Sudoku player is furnished with a partially completed square, from which a unique solution may be inferred, the thermodynamicist must provide his own starting point in the form of an input file which uniquely defines a thermodynamic cycle design-point. For the Brayton-cycle gas-turbine, the variables specified are:

- Atmosphere model
- Altitude
- ISA temperature deviation
- Cruise Mach number
- Intake Pressure recovery factor
- Intake delivery velocity
- Compressor pressure ratio
- Compressor efficiency
- Compressor efficiency type (isentropic or polytropic)
- Compressor delivery pseudo Mach number
- Combustor total pressure loss factor
- Combustor mean velocity
- Fuel
- T_4
- Cooling constant

²¹ Though if it did, the author would feel considerably less useless than when expected by friends or relatives to furnish answers to a cryptic crossword...

- Fraction of cooling air to NGV, $\frac{W_{306}}{W_{307}}$
- Maximum metal temperature
- Gas generator turbine efficiency
- Gas generator turbine efficiency type (isentropic or polytropic)
- Gas generator turbine delivery pseudo Mach number
- Power turbine efficiency
- Power turbine efficiency type (isentropic or polytropic)
- Power turbine delivery pseudo Mach number
- Jet pipe pressure loss factor
- Core nozzle velocity coefficient
- Propulsor overall efficiency

In order to produce a broad picture of the possibilities offered by the Brayton-cycle, the ExcelCEA code permits each of these inputs to be varied. This is controlled by allocating to each variable a smallest value, a largest value, and a number of steps to be taken from one to the other. This arrangement has been chosen in order to allow the total number of calculations undertaken to be easily calculated as the product of the number of steps at each stage.

The rapid growth of the number of calculations with the number of steps in each variable means that considerable circumspection is required when selecting the number of steps and the number of variables to be stepped.

Unknown parameters – building the model

The model has evolved gradually over the course of the author's PhD. It may be traced back to an Excel spreadsheet constructed to perform simple gas turbine performance calculations in order to get a better feel for the content of the Gas Turbine Performance MSc lectures which the author was attending in the autumn of 2007.

This extremely simple model assumed $\gamma = 1.4$ for compressors, and $\gamma = 1.33$ for turbines. It rapidly became apparent that considerably more realistic results could be obtained by using polynomial approximations of γ extracted from chapter 3 of Walsh & Fletcher. Unbeknownst to the author, this was the first step along the path which would lead to the current ExcelCEA model.

Initial versions of the model were based entirely upon Excel, with the calculations performed within cells. This approach was selected in order to allow progress to be made rapidly without recourse to “real programming”.

The ability to cut & paste formulae around the spreadsheet allowed initial progress to be quite fast, and simple logic could be incorporated using nested IF formulae, which enabled the use of a standard atmosphere.

The downside of this approach was the formulae became quite large (indeed, the maximum character limit was a factor, especially in early versions of the model based upon Excel 2003).

There was also no obvious method of incorporating automatic control of iteration. This meant that the only practical matching strategy was to simply hard-code a fixed number of iterations into each stage of the calculation. This inevitably had to be based upon the worst case scenario, and therefore 10 steps were used.

The first generation of the model calculated the performance of a single engine at design-point, using individual worksheets for each component.

It was possible to optimise engine performance by using the built-in solver package in Excel to find the optimal pressure ratio. However, convergence could not be guaranteed, and the optimisation was relatively computationally expensive.

Additionally, it was impossible to guarantee that the solver had converged upon a global rather than a local optimum, and the fact that only a single engine was considered meant that the considerable effort would be required to investigate trends.

The next generation of models used a sequential approach.

The entire engine was modelled within a single worksheet, with the pressure ratio increasing gradually from row to row.

This approach allowed each row to use the previous row as the first guess in its iteration, because of the gradual variation of flow parameters with increasing pressure ratio.

Despite the reduction in the number of calculations made possible by this approach, the resulting worksheet was still extremely large (of the order of thousands of columns and hundreds of rows, the latter being driven by the requirement that the pressure ratio increments be small in order to limit error).

It was found by experience that beyond approximately 800 columns of data, it was *extremely* difficult to maintain and debug the model.

Work was therefore undertaken to simplify the Excel spreadsheet by using custom functions.

These functions were written in the VBA language supplied with Excel. The use of a “proper” programming language allowed the use of controlled iterative loops for matching purposes. This allowed a fixed level of error in matching the temperature-enthalpy polynomials to be maintained. Although this would theoretically speed up the execution of the model by reducing the number of calculations to the minimum required for any given level of error, the reality was more complex.

By this time, Excel 2007 was in use. This version of excel incorporates multi-threading technology, but only for its default functions. This meant that, on a PC with four processors, the default functions would execute almost four times as fast as custom functions written in VBA. Because controlling the iterative loops reduced the number of calculations required by less than a factor of 2, the overall execution time was not actually reduced by the switch to custom functions.

However, the reduction in the size of the spreadsheet, and subsequent improvement in the maintainability of the code was well worth the relatively small increase in execution time, especially given that the total time to calculate 100 engines was of the order of seconds.

Unfortunately, this approach ran into several difficulties. The entire code was, at this stage, based upon formulae taken from Walsh & Fletcher²². The first difficulty was that the limits of the polynomials were not explicitly

²² The intention at this stage was to produce an extremely reliable model of the Brayton-cycle gas-turbine to serve as a basis for comparison with the novel engine concept set out in the author’s patent, and therefore a conscious decision had been taken to avoid novelty in this part of the code.

documented, leading to some uncertainty as to how far the model could be trusted, especially at high temperatures and pressures.

The second difficulty was that there appeared to be some typographical errors in certain formulae dealing with the enthalpy of air and products of combustion²³.

In order to settle the question of this potential typographical error, it was decided to consult the references cited by Walsh & Fletcher. This led the author to Gordon & McBride (1994), and its companion work, McBride & Gordon (1996).

²³ e.g. F3.29, page 117 of Walsh & Fletcher (2004), which reads:

$$\int_{T_1}^{T_2} \frac{C_p}{T} dT = f(T_2) - f(T_1),$$

$$f(T) = A_0 \ln T + A_1 \frac{T}{10^3} + \frac{A_2}{2} \left(\frac{T}{10^3} \right)^2 + \frac{A_3}{3} \left(\frac{T}{10^3} \right)^3 + \frac{A_4}{4} \left(\frac{T}{10^3} \right)^4 + \frac{A_5}{5} \left(\frac{T}{10^3} \right)^5 + \frac{A_6}{6} \left(\frac{T}{10^3} \right)^6 + \frac{A_7}{7} \left(\frac{T}{10^3} \right)^7 + \frac{A_8}{8} \left(\frac{T}{10^3} \right)^8 + A_{10} + \frac{\text{FAR}}{1 + \text{FAR}} \left(B_0 \ln T + B_1 \frac{T}{10^3} + \frac{B_2}{2} \left(\frac{T}{10^3} \right)^2 + \frac{B_3}{3} \left(\frac{T}{10^3} \right)^3 + \frac{B_4}{4} \left(\frac{T}{10^3} \right)^4 + \frac{B_5}{5} \left(\frac{T}{10^3} \right)^5 + \frac{B_6}{6} \left(\frac{T}{10^3} \right)^6 + \frac{B_7}{7} \left(\frac{T}{10^3} \right)^7 + B_9 \right)$$

It would appear to the author that, by symmetry, and comparison with F.3.28 on the previous page, this should read:

$$\int_{T_1}^{T_2} \frac{C_p}{T} dT = f(T_2) - f(T_1),$$

$$f(T) = \frac{1}{1 + \text{FAR}} \left(A_0 \ln T + A_1 \frac{T}{10^3} + \frac{A_2}{2} \left(\frac{T}{10^3} \right)^2 + \frac{A_3}{3} \left(\frac{T}{10^3} \right)^3 + \frac{A_4}{4} \left(\frac{T}{10^3} \right)^4 + \frac{A_5}{5} \left(\frac{T}{10^3} \right)^5 + \frac{A_6}{6} \left(\frac{T}{10^3} \right)^6 + \frac{A_7}{7} \left(\frac{T}{10^3} \right)^7 + \frac{A_8}{8} \left(\frac{T}{10^3} \right)^8 + A_{10} \right) + \frac{\text{FAR}}{1 + \text{FAR}} \left(B_0 \ln T + B_1 \frac{T}{10^3} + \frac{B_2}{2} \left(\frac{T}{10^3} \right)^2 + \frac{B_3}{3} \left(\frac{T}{10^3} \right)^3 + \frac{B_4}{4} \left(\frac{T}{10^3} \right)^4 + \frac{B_5}{5} \left(\frac{T}{10^3} \right)^5 + \frac{B_6}{6} \left(\frac{T}{10^3} \right)^6 + \frac{B_7}{7} \left(\frac{T}{10^3} \right)^7 + B_9 \right)$$

(Proposed correction highlighted in red).

It was decided to compare the results produced by the CEA code with those given by Walsh & Fletcher's formulae.

Unfortunately, careful reading of the Gordon & McBride/McBride & Gordon papers revealed that there were important differences between the assumptions underlying CEA and those underlying the Walsh & Fletcher formulae, and it rapidly became apparent that it would not be possible to convincingly combine these two approaches.

It was felt that, due to the higher pressures and temperatures expected to be produced within the novel engine concept described in the author's patent, it would be prudent to base the intended thermodynamic comparison upon the output of the CEA code, which was clearly better able to handle these more extreme conditions.

It was also clear that the attributes which made the CEA code attractive for use in producing a comparison between the author's proposed novel engine concept and the Brayton-cycle gas-turbine conferred upon it the ability to form the basis for a new approach to thermodynamic modelling.

In order for this to happen, the first requirement was to modify the CEA source code to produce output at the full precision level of its internal calculations (namely 10^{-16} rather than 10^{-4}). Other than this change, achieved by the modification of formatting statements within the FORTRAN77 source code of CEA, and the implementation of a bug fix to catch a silent error in cases when the number of species specified in the input file exceeded the maximum number of species the code was set to handle, the source code was left untouched in order that its fidelity would remain intact, the author having neither the intention, desire, or resources required to repeat the work of Gordon & McBride.

It was decided to continue to use Excel for basic input & output, as this avoided both the difficulties of a console interface and the complexities of producing a bespoke graphical user interface.

However, due to the anticipated complexity of the code required, it was decided that a more powerful development environment than that associated with the Excel/VBA combination was required. It was therefore decided to

produce the vast majority of the code in VB.net, developed using Visual Studio 2010[®].

In order to achieve this, VBA code was written to convert the Excel spreadsheet into a comma separated variable file (*.csv), which would be passed to the VB.net code. The VB.net code would then run, producing results in another *.csv file, which would then be read back into Excel by the VBA code (see Figure 7 on page 70).

Development was then effectively split into two tasks:

- Creation of the Excel GUI
- Creation of the VB.net code

The Excel GUI was relatively simple to create; the main source of error being the author's tendency to forget to add the necessary companion VBA code required to write the user's input to the *.csv file.

The vast majority of the work was therefore associated with the VB.net code.

The first task was to enable communication between this code and CEA. This required code to write input files for CEA, run CEA, and parse CEA's output files.

This having been achieved, it was then necessary to use this capability to perform thermodynamic process calculations.

This was developed on a modular basis, following the Station Numbering Scheme through the engine. Each module added had its own direct output to the Excel spreadsheet.

The data structure underlying all of the stations is called CeaData. The data entries correspond to the output from CEA, i.e. the values detailed in *CEA Output* on page 74 (sections c to h).

StationData, the next higher level structure, typically contains two sets of CeaData (for Static and Total flow parameters), plus some further parameters. Stations such as the compressor and turbine stages contain one StationData set for each of the three states put forward by Casey in his 2007 paper (Dissipated, Isentropic and Real), plus efficiency information.

As the modelling work progressed through to the Combustor, it became clear that it was essential to maximise the speed of calculation, so a new multithreading loop structure was devised, and direct output to a *.csv file was substituted for writing data to the spreadsheet line by line.

Additionally, given the considerable computational cost associated with producing output data, it was decided that all intermediate results (i.e., the datasets described above) should be output by the program²⁴, and these can optionally be loaded into a new spreadsheet after the main routine finishes execution.

Once the current strategy was established, it became clear that the program could only be realistically tested by a process of trial and error. It rapidly became apparent that results which looked realistic for one stage of the engine in isolation could be rendered totally void when used as input to later stages. Development thus took the form of increasingly large loops through the cycle, starting with the establishment of correct initial logic for CEA calls in the current code segment & examination of convergence in iterative loops, followed by analysis of the effect of inputs from earlier stages, with revision of detail in these earlier stages... and so on to the end of the code. There were particular problems with sign conventions – positive for enthalpy added, negative for work done – and with values of H which vary from highly negative to highly positive within a single set of mass fractions and from one Station to another.

One of the major programming problems was, and shall undoubtedly remain, the selection of the correct CEA call for a particular situation and of correct input parameters for it. In many situations, it was not possible to obtain the expected performance from what initially appeared to be the “obvious” CEA call & parameters because of the unexpected behaviour of CEA (e.g. holding H constant when variation was expected). In these circumstances, the only recourse was to try all possible alternatives until a viable solution was found.

²⁴ Many of these data might be thought of as “a solution waiting for a problem”, but data storage is cheap and getting cheaper, and it was therefore felt pragmatic to output all the results produced rather than to discard results which might potentially be of interest for as-yet un-thought-of applications.

The results of interim calculations have been assessed throughout on a trial and error basis: “it looks good” being reinforced wherever possible by “real” data obtained from the very meagre resources which are publicly available. Some parameters have been tested by comparing results from Kurzke’s GasTurb code, although this approach poses some difficulties in interpretation due to the considerable differences between its underlying assumptions and those of ExcelCEA.

A source of reliable, comprehensive performance data for real engines would have greatly simplified proceedings.

A sample cycle calculation

Ambient conditions

At the time of writing, only one atmosphere model has been implemented. This is the ISO standard atmosphere, which has been extracted from Walsh & Fletcher (2004). It would be relatively simple to expand the code to incorporate a number of atmosphere models for selection by the user,

The first input used is the altitude, which allows the ambient static temperature to be calculated.

Altitude < 11000 m,

$$T_{\text{Standard, K}} = 288.15 - 0.0065 \text{Altitude}$$

11000 m ≤ Altitude < 24994 m,

$$T_{\text{Standard, K}} = 216.65 \tag{57}$$

24994 m ≤ Altitude < 30000 m,

$$T_{\text{Standard, K}} = 216.65 + 0.0029892(\text{Altitude} - 24994)$$

The temperature deviation is then accounted for:

$$T_{\text{Ambient}} = T_{\text{Standard}} + T_{\text{Deviation}} \tag{58}$$

The ambient temperature is then used to calculate the ambient pressure:

Altitude < 11000 m,

$$P_{\text{Ambient}}, \text{Pa} = 101325 \left(\frac{288.15}{T_{\text{Ambient}}} \right)^{-5.25588}$$

11000 m ≤ Altitude < 24994 m,

$$P_{\text{Ambient}}, \text{Pa} = \frac{22632.53}{e^{0.000157689(\text{Altitude}-10998.1)}} \quad (59)$$

24994 m ≤ Altitude < 30000 m,

$$P_{\text{Ambient}}, \text{Pa} = 2523.7 \left(\frac{216.65}{T_{\text{Ambient}}} \right)^{11.8}$$

An error message is generated if the input altitude exceeds 30 km because the atmosphere is not defined above this altitude.

Since temperature and pressure have now been fixed, it is possible to run CEA in “tp” mode to derive the other ambient properties.

Freestream conditions

The freestream static conditions are the ambient conditions. The freestream flow velocity is:

$$v_{\text{Freestream}} = A_{\text{Ambient}} M_{\text{Cruise}} \quad (60)$$

Total and Static flow parameters

Since the total flow parameters are those derived from the isentropic stagnation of the flow, it follows that:

$$H_{\text{Total}} = H_{\text{Static}} + \frac{V^2}{2} \quad (61)$$

And trivially,

$$S_{\text{Total}} = S_{\text{Static}} \quad (62)$$

The total pressure is unknown. Because CEA does not have an “hs” mode, it is necessary to use the “hp” mode, iterating the total pressure until the specific entropy target is matched.

This is done using a Bridgman equation.

$$\left(\frac{\partial P}{\partial S}\right)_H = \frac{(-C_p)}{\left(\frac{VC_p}{T}\right)} \quad (63)$$

$$= -\frac{T}{V}$$

Both the temperature and specific volume are output from CEA, and it is therefore possible to rapidly correct the pressure guess:

$$P_{\text{Total?n+1}} = \frac{S_{\text{Guessed}} - S_{\text{Target}}}{\left(\frac{\partial P}{\partial S}\right)_H} \quad (64)$$

Intake Delivery

The intake is treated as a simple duct with no work or heat transfer. Total temperature is therefore constant.

A pressure loss is modelled by arbitrarily stating

$$P_2 = P_0 (\text{Intake Pressure Recovery Factor}) \quad (65)$$

A single “tp” mode CEA run can therefore be used to derive the total flow parameters at intake delivery.

Compressor Delivery

Compressor performance may be referenced to either isentropic or polytropic efficiency standards, entailing different calculation procedures discussed separately below.

Isentropic Compressor Efficiency

At this point, if the compressor performance is being calculated relative to an isentropic efficiency standard, given that this fixes the value of $\frac{a}{b}$, and a is already known, it follows that

$$\begin{aligned} H_3 &= H_2 + \frac{\Delta H_{\text{Isentropic}}}{\eta_{\text{Isentropic}}} \\ &= H_2 + \frac{H_{3S} - H_2}{\frac{a}{b}} \end{aligned} \quad (67)$$

Given that the specific enthalpy at station 3 is now known, it is possible to run CEA in "hp" mode to derive the other flow parameters.

It is useful to know what polytropic efficiency is implied by a given isentropic efficiency. The code therefore calls CEA again in "hp" mode to calculate the flow properties at station 2_H. The polytropic efficiency may then be calculated:

$$\begin{aligned} \eta_{\text{Polytropic}} &= \frac{c}{d} \\ &= \frac{S_{2H} - S_3}{S_{2H} - S_2} \end{aligned} \quad (68)$$

This completes the compressor calculation in the isentropic efficiency mode.

Polytropic Compressor efficiency

Were the specific gas constant truly constant, the polytropic efficiency of the compressor would be given by the following equation, after Casey(2007):

$$\eta_{\text{Polytropic}} = \frac{R \ln \frac{P_3}{P_2}}{R \ln \frac{P_3}{P_2} + S_3 - S_2} \quad (69)$$

The only unknown in equation (69) is S_3 . Rearrangement yields

$$S_3 = S_2 - \frac{R(\eta_{\text{Polytropic}} - 1) \ln \frac{P_3}{P_2}}{\eta_{\text{Polytropic}}} \quad (70)$$

This is very nearly correct. However, in reality, the specific gas constant is not truly constant if equilibrium chemistry is assumed, because chemical changes to the working fluid may alter its mean molecular mass.

This means that Equation (70) may only serve as a first guess for use within an iterative procedure. By reference to the Bridgman equations and the Casey diagram, it is possible to derive a correction scheme:

$$\left(\frac{\partial \eta_{\text{Polytropic}}}{\partial H_3} \right) = \frac{\left(\frac{C_P^2}{T} \right)_{2_H} - \left(\frac{C_P^2}{T} \right)_3}{\left(\frac{C_P^2}{T} \right)_{2_H} - \left(\frac{C_P^2}{T} \right)_2} \quad (71)$$

$$\begin{aligned} \Delta \eta_{\text{Polytropic}} &= \eta_{\text{Polytropic-Target}} - \eta_{\text{Polytropic-Guessed}} \\ H_{3_{\text{Correction}}} &= \Delta \eta_{\text{Polytropic}} \frac{\left(\frac{C_P^2}{T} \right)_{2_H} - \left(\frac{C_P^2}{T} \right)_2}{\left(\frac{C_P^2}{T} \right)_{2_H} - \left(\frac{C_P^2}{T} \right)_3} \end{aligned} \quad (72)$$

Then

$$H_{3_{?n+1}} = H_{3_{?n}} + H_{3_{\text{Correction}}} \quad (73)$$

The solution is considered to have converged when $H_{3_{\text{Correction}}} < 10^{-3}$ J/kg. This may appear to be an excessively strict criterion, given that typical compressors may easily increase the specific enthalpy of their working fluid by hundreds of kJ/kg; however it has been found that convergence to this standard is computationally inexpensive due to the efficiency of the iterative scheme, and so it is easier to produce results which are obviously excessively accurate than to calculate what level of accuracy is appropriate or acceptable.

Combustor Front Face

All flow properties are conserved between compressor delivery and combustor front face, *i.e.*

$$\begin{aligned} P_{305} &= P_3, \\ T_{305} &= T_3 \\ &etc. \end{aligned} \tag{74}$$

with the sole exception of mass flow, which is reduced due to the extraction of cooling bleed.

$$\mathbb{W}_{31} = \mathbb{W}_3 - \mathbb{W}_{305} \tag{75}$$

However, the quantity of cooling bleed actually required by the cycle cannot be calculated at this stage because knowledge of all thermodynamic properties at combustor delivery is required.

This does not impede the combustion calculations because all the parameters used for these are *specific*, and thus entirely independent of the absolute mass flow rate.

Combustor delivery

The combustor delivery temperature, T_4 , is an input to the model, as are the combustor pressure loss factor and the mean flow velocity; the key unknown is the fuel:air ratio, FAR , required to deliver this temperature. The $[FAR]$ is unknown.

$$P_4 = P_{305} (1 - \text{Combustor Pressure Loss Factor}) \tag{76}$$

The combustion code uses the chemical equivalence ratio, φ , as the control variable, because its behaviour is independent of the fuel used; the maximum temperature obtainable from combustion will always be reached at approximately $\varphi = 1$. This means that a standardised matching scheme may be used for any fuel.

Initially,

$$\varphi_{\gamma 1} = 0.5 \tag{77}$$

Then

$$\varphi_{\gamma_{n+1}} = \varphi_{\gamma_n} \frac{T_4 - T_{305}}{T_{\text{Actual}} - T_{305}} \quad (78)$$

However, this scheme does not converge for small combustor temperature rises, and an alternative, considerably more gentle scheme is therefore employed:

$$\begin{aligned} &\text{If } (T_4 - T_{305}) < 75 \text{ K:} \\ &\varphi_{\gamma_{n+1}} = \frac{9\varphi_{\gamma_n} + \varphi_{\gamma_n} \frac{T_4 - T_{305}}{T_{\text{Actual}} - T_{305}}}{10} \end{aligned} \quad (79)$$

Cooling Bleed Extraction

The combustor delivery flow parameters now being known, it is possible to calculate the quantity of cooling bleed required based upon the cooling equations put forward by Kurzke in 2003:

$$\eta_{\text{Cooling}} = \frac{T_{\text{Gas}} - T_{\text{Metal}}}{T_{\text{Gas}} - T_{\text{Coolant}}} \quad (80)$$

$$\frac{W_{\text{Coolant}}}{W_{\text{Gas}}} = k \frac{\eta_{\text{Cooling}}}{1 - \eta_{\text{Cooling}}} \quad (81)$$

Kurzke suggests $C = 0.05$ will give sensible results; this is a user input.

Obviously,

$$\begin{aligned} &\text{If } T_4 \leq T_{\text{Metal}}, \\ &W_{\text{Coolant}} = 0 \end{aligned} \quad (82)$$

This condition is tested for in the code in order to both slightly increase execution speed and remove a potential source of floating point errors in the mass flow calculations.

If cooling is required, the relationship outlined in equations (80) and (81) is somewhat more complex than it initially appears, because the mass of gas and coolant are intimately related.

$$\begin{aligned}\mathbb{W}_{\text{Gas}} &= (1 + \text{FAR}) \mathbb{W}_{31} \\ &= (1 + \text{FAR})(\mathbb{W}_3 - \mathbb{W}_{\text{Coolant}})\end{aligned}\quad (83)$$

The cooling mass flow may be found analytically, as follows:

Let

$$x = k \frac{\eta_{\text{Cooling}}}{1 - \eta_{\text{Cooling}}}\quad (84)$$

Then

$$\mathbb{W}_{\text{Coolant}} = \frac{x(1 + \text{FAR}) \mathbb{W}_3}{x\text{FAR} + x + 1}$$

It is assumed that the cooling bleed is passed to its injection point within the hot section of the engine adiabatically, and therefore

$$T_{\text{Coolant}} \equiv T_3\quad (85)$$

This imposes a fundamental limit upon the cycle:

$$T_3 < T_{\text{Metal}}\quad (86)$$

This inequality is strictly less than, rather than less than or equal to, because if $T_3 = T_{\text{Metal}}$ then the cycle could not produce useful work because either $T_4 \leq T_3$ or else $\mathbb{W}_{\text{Coolant}} = \mathbb{W}_3$, *i.e.* $\mathbb{W}_{\text{Fuel}} = 0$.

This means that the inequality presented in (86) may be used with confidence to capture illegal cycles at the end of the compressor calculations. When this inequality is violated, the code throws an exception, which means that computational effort is not wasted in carrying the cycle calculation further. This can produce considerable savings when large numbers of cycles are calculated, especially if a wide range of Mach numbers are considered, because of the considerable increase in T_0 due to ram at high Mach number.

Of course, the specific power output of a cycle will tend towards zero as the limiting T_3 is approached, and therefore practical cycles will be constrained to lower pressure ratios by considerations of physical size and cost.

Mix NGV Cooling

The cooling bleed is split into that used to cool the Nozzle Guide Vanes and that used to cool the rotor. The former is accounted as doing useful work in the gas generator turbine, whilst the latter is not.

The split is a user input; Eames's 2006 paper implies that a sensible split would send around 40% of the total cooling flow to the NGV, with the remainder going to the rotor.

The mixing code calculates a weighted mean value of the mass fractions within, and specific enthalpies of, the combustor delivery and NGV cooling bleed flows, and adds together their mass flows. The resultant flow is passed to the Gas Generator Turbine.

Gas Generator Turbine

The gas generator turbine must supply sufficient mechanical work to drive the compressor. Because of the addition of fuel and the subtraction of cooling bleeds, the mass flow through the gas generator turbine does not necessarily equal that through the compressor, and therefore the specific enthalpy drop across the turbine required to match the absolute enthalpy rise across the compressor does not necessarily equate to the specific enthalpy rise across the same.

Therefore, the specific enthalpy drop required across the gas generator turbine must be calculated:

$$\mathbb{W}_{41}(H_{41} - H_{44}) = \mathbb{W}_3(H_3 - H_2) \quad (87)$$

Thus

$$H_{41} - H_{44} = \frac{\mathbb{W}_3}{\mathbb{W}_{41}}(H_3 - H_2) \quad (88)$$

Having calculated the specific enthalpy drop required, the next stage is to calculate the flow parameters at the virtual station 41_H.

$$H_{41_H} \equiv H_{44} \quad (89)$$

We may therefore use an "hp" call to fully evaluate the thermodynamic parameters at this virtual station.

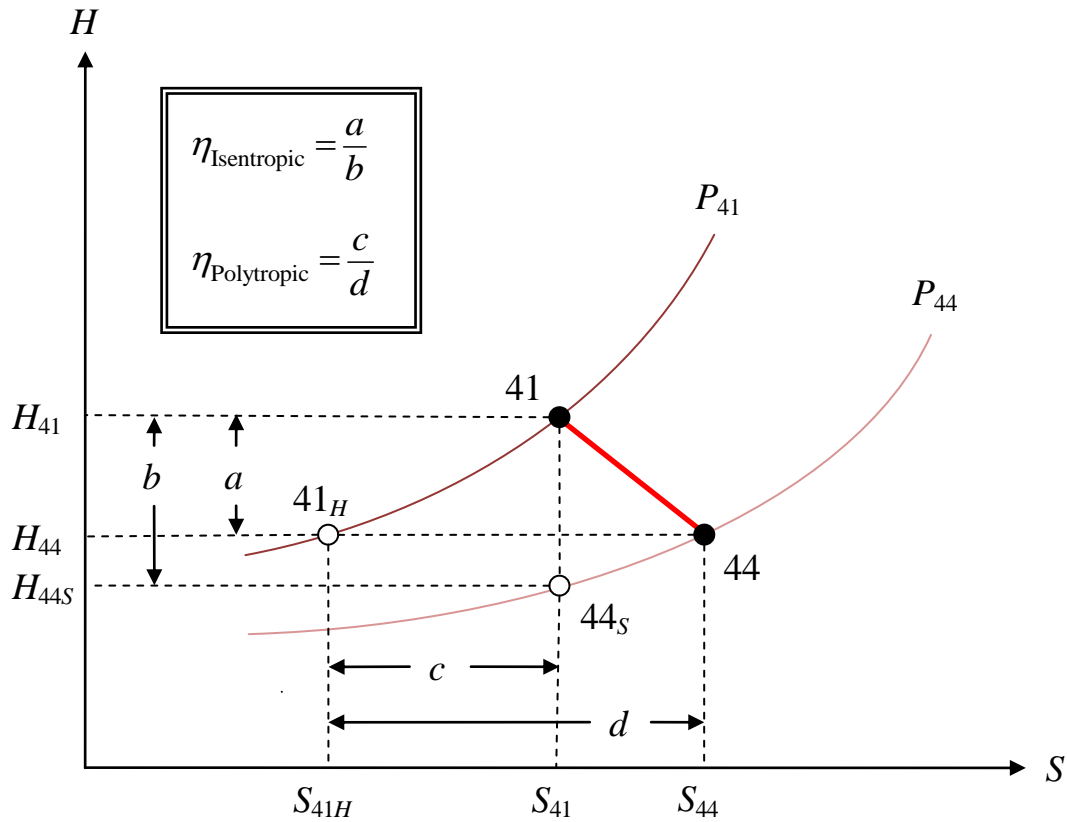


Figure 11 - Casey diagram for gas generator turbine

At this point, the calculation branches depending upon the efficiency standard employed.

Isentropic gas generator turbine efficiency

Trivially,

$$S_{44S} \equiv S_{41} \tag{90}$$

$$H_{41H} \equiv H_{44} = H_{41} - \text{Compressor Work} \frac{\mathbb{W}_{41}}{\mathbb{W}_3} \tag{91}$$

Perhaps less obviously, the specific enthalpy at station 44_S may also be calculated by using the definition of isentropic efficiency:

$$\eta_{\text{Isentropic}} = \frac{\Delta H_{\text{Actual}}}{\Delta H_{\text{Isentropic}}} \quad (92)$$

By trivial rearrangement,

$$\Delta H_{\text{Isentropic}} = \frac{\Delta H_{\text{Actual}}}{\eta_{\text{Isentropic}}} \quad (93)$$

$$\begin{aligned} \Delta H_{\text{Actual}} &= -\text{Compressor Work} \\ &= -(H_3 - H_2) \frac{\mathbb{W}_{41}}{\mathbb{W}_3} \end{aligned} \quad (94)$$

Therefore, the enthalpy at station 44S may be found:

$$H_{44S} = H_{41} + \frac{\Delta H_{\text{Actual}}}{\eta_{\text{Isentropic}}} \quad (95)$$

With both the enthalpy and entropy known, it is now possible to define the pressure at station 44_S by setting the enthalpy and iterating the pressure until the known entropy level is matched (see equations (63) and (64) above).

The thermodynamic parameters at Station 44 itself may now be found.

$$P_{44} \equiv P_{44S} \quad (96)$$

$$H_{44} = H_{41} + \Delta H_{\text{Actual}} \quad (97)$$

These data are sufficient to enable a single call to CEA in "hp" mode to find all other thermodynamic parameters.

Polytropic gas generator turbine efficiency

As in the isentropic efficiency case, it is possible to find the flow properties at station 41_H using equation (91). Then,

$$c = S_{41} - S_{41H} \quad (98)$$

By simple rearrangement,

$$\eta_{\text{Polytropic}} = \frac{c}{d} \quad (99)$$

$$\therefore d = \frac{c}{\eta_{\text{Polytropic}}}$$

It then follows that

$$S_{44} = S_{41H} + d \quad (100)$$

and

$$H_{44} = H_{41H} \quad (101)$$

With enthalpy and entropy known it is now possible to run CEA in "hp" mode and iterate the pressure to match the entropy target.

Mix Rotor cooling

The methodology for this process is essentially identical to that used in mixing the NGV cooling flow, as described on page 95 above.

Power turbine, Nozzle and Propulsor

The power turbine and nozzle are considered to form a single unit, because the objective of the cycle is to produce the maximum possible quantity of useful work, irrespective of whether that work comes in the form of shaft work or direct jet thrust.

This considerably complicates analysis and, to the author's knowledge, it has not previously been attempted with this level of rigor.

At this stage, it is worthwhile to observe that the code only considers turbojets, and turboshaft/turbofan engines with separate exhaust flows. Mixed exhausts offer practical²⁵ thermodynamic advantages for a relatively narrow range of engines with low to medium bypass ratios; the benefits of mixing fall rapidly, whilst the difficulties thereof simultaneously rise rapidly at higher bypass ratios.

²⁵ Which is to say small, but both significant and achievable.

In order to benefit from mixed exhaust flow, the engine must be designed with exhaust mixing in mind; the nature of this code is such that both specific thrust and bypass ratio are emergent behaviours, and therefore the only practical way to decide whether or not mixing would be appropriate would be to run an unmixed cycle calculation, use the bypass ratio and specific thrust output to decide whether or not mixing might be beneficial, and then repeat the calculation for mixed exhausts.

It was decided that not only would the effort required for this be considerable, but that the step-change in the results brought about by the switch from unmixed to mixed exhausts (which would be based upon somewhat arbitrary rules) would risk obscuring more fundamental trends.

The intellectual basis of the optimisation is explained qualitatively on page 65 above. However, the actual method used in the code is somewhat more complex.

The total expansion ratio available to the power turbine and nozzle combination is set by the ambient static pressure and the gas generator delivery total pressure.

The code attempts to maximise the useful work produced by the cycle by optimising the trade between expansion across the power turbine and that across the nozzle.

The code achieves this *via* separate subroutines for the calculation of turbine and nozzle performance which are called and controlled by a higher level combined subroutine.

The combined subroutine attempts to set the nozzle expansion ratio to match a target Froude efficiency.

$$\eta_{\text{Froude-Target}} = \eta_{\text{Propulsor}} \eta_{\text{Turbine}} \quad (102)$$

The turbine efficiency in equation (102) is its isentropic efficiency. This somewhat complicates the calculation if the turbine efficiency input is the polytropic efficiency. In that case, the first iteration approximates the isentropic efficiency of the turbine to be equal to the polytropic efficiency

input, using the actual calculated isentropic efficiency of the turbine in subsequent steps.

Setting $\eta_{\text{Propulsor}} = 0$ will force the optimisation to ignore the power turbine entirely, producing a turbojet cycle.

The definition of Froude efficiency (see equation (56) above) implies a definite exhaust jet velocity.

$$v_{\text{Jet-Target}} = \left(\frac{2}{\eta_{\text{Froude-Target}}} - 1 \right) v_0 \quad (103)$$

This means that if $v_0 = 0$ the code will naturally set the target exhaust jet velocity to 0, producing a pure shaft power engine, as might be used for power generation.

In reality, stationary engines must have a non-zero exhaust gas velocity for two reasons:

1. $v_{\text{Jet}} = 0$ implies infinite nozzle area!
2. The engine must continue operating even if the prevailing wind blows into its exhaust; if the exhaust it is intuitively apparent that although the ability to do this comes fundamentally from the engine's surge margin, the sensitivity of the engine to adverse wind conditions will be reduced as its jet velocity increases.

It would be possible to impose a fixed nozzle pressure ratio upon the code to account for this (or to simply "pretend" that a stationary engine was moving at some non-zero velocity), but in this work it is assumed that the jet pipe pressure loss factor and nozzle velocity coefficient provide sufficient total pressure margin for a successful cycle.

The nozzle expansion ratio required to produce the target jet velocity is initially approximated as:

$$\text{NER} = \left(\frac{C_p T - \frac{v_{\text{JetTarget}}^2}{2}}{C_p T} \right)^{\frac{\gamma}{\gamma-1}} \quad (104)$$

The values of $C_p T$ and γ used in this approximation are those already calculated for station 45.

Having calculated the nozzle expansion ratio, it is possible to calculate the power turbine's pressure ratio.

$$P_5 = P_{AMB} \text{NER} \quad (105)$$

The turbine performance is then calculated on the basis of this turbine delivery total pressure as described on page 102.

This allows the velocity target to be recalculated based upon the thermodynamic data from station 5.

The nozzle performance is then calculated using the method described on page 104, and the resultant velocity is compared with the target.

$$v_{\text{Factor}} = \frac{v_{\text{Jet}}}{v_{\text{JetTarget}}} \quad (106)$$

The velocity factor is used to control subsequent iterations.

$$\text{If } \sqrt{v_{\text{Factor}}^2} > 0.1, \quad (107)$$

$$\text{NER} = \left(\frac{C_{p9} T_9 - \frac{v_{\text{JetTarget}}^2}{2}}{C_{p9} T_9} \right)^{\frac{\gamma_9}{\gamma_9-1}}$$

Alternatively,

$$\begin{aligned} \text{If } \sqrt{v_{\text{Factor}}}^2 &\leq 0.1 \\ \text{NER}_{\eta_{n+1}} &= \frac{\text{NER}_{\eta_n}}{\sqrt{v_{\text{Factor}}}} \end{aligned} \quad (108)$$

The routine then loops until either

$$\sqrt{(\text{NER}_{\eta_n} - \text{NER}_{\eta_{n-1}})^2} < 10^{-4} \quad (109)$$

or 20 iterations have been completed.

Power turbine

The matching scheme for the power turbine differs from that for the gas generator turbine in that whilst the latter delivers known work from an unknown pressure ratio, the former delivers unknown work from a known pressure ratio.

In this respect it is analogous to the compressor.

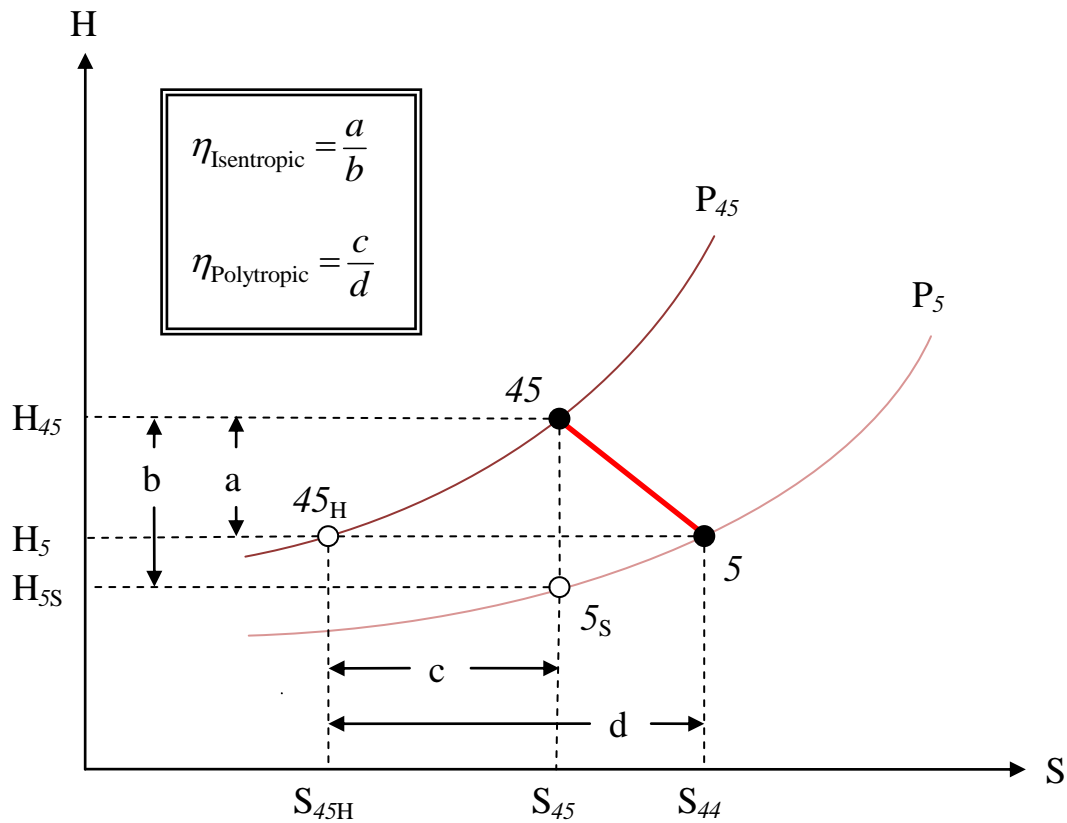


Figure 12 - Casey diagram for power turbine

Because the pressure ratio and input pressure are known, it is trivial to find P_5 .

The isentropic work may therefore be calculated by running CEA in "sp" mode.

Isentropic power turbine efficiency

From the definition of isentropic efficiency, the real work is then simply:

$$\Delta H_{\text{Actual}} = \Delta H_{\text{Isentropic}} \eta_{\text{Isentropic}} \quad (110)$$

The delivery pressure is already known, and therefore the real flow parameters may be calculated using a single "hp" call to CEA.

Another single "hp" call may be made to evaluate the dissipated state 45_H ; there is then sufficient data to calculate the polytropic efficiency implied by the isentropic efficiency input.

Polytropic power turbine efficiency

As a first guess, the isentropic efficiency of the turbine is assumed to be equal to the polytropic efficiency target. For small expansion ratios, it has been found that convergence with a genuine polytropic efficiency is extremely difficult to achieve. Because the actual isentropic efficiency of compressors and turbines tends towards the polytropic efficiency as the pressure ratio tends towards unity, the pragmatic solution is to simply use isentropic efficiency calculations for small expansion ratios, and accept the error inherent in this simplification.

$$\frac{P_{45}}{P_5} \leq 1.9, \eta_{\text{Isentropic}} \approx \eta_{\text{Polytropic}} \quad (111)$$

This particular expansion ratio has been chosen somewhat arbitrarily; it has been found from practical experience with the code that convergence rapidly deteriorates if lower expansion ratios are modelled polytropically. It is not trivial to calculate the error associated with the simplification, as this will vary as a function of the expansion ratio and the ratio of specific heat capacities, which will in turn depend upon cycle parameters which are evaluated upstream (*i.e.* the error cannot be immediately inferred from inspection of the input file).

No attempt has been made to quantify the size of the error, but it is anticipated that it will generally be less than 1% isentropic efficiency - see Kerrebrock (1992), page 77.

For larger expansion ratios, the first guess of the enthalpy at station 5 is used to calculate the thermodynamic properties at station 45. It is then possible to calculate the values of c & d.

It has been found that surprisingly good results are achieved without recourse to iteration.

Nozzle

The nozzle calculations are conceptually very similar to those for a turbine. However, there are differences in the methods by which losses are accounted for.

Firstly, there is a jet pipe pressure loss factor:

$$P_7 = P_5(1 - \text{JPLF}) \quad (112)$$

The flow is then expanded to ambient static pressure, and the enthalpy change noted. This enthalpy drop is converted into kinetic energy of the flow; nozzle losses are accounted for via a Velocity Coefficient.

$$v_{\text{Jet}} = \text{Velocity Coefficient} \sqrt{\frac{\Delta H}{2}} \quad (113)$$

Performance calculation

PSFC

The useful power output of the engine is dependent upon operational context. A stationary engine derives no benefit from core jet thrust, and therefore its useful power output is

$$[\text{PW}] = (\dot{W}_{45} H_{45} - \dot{W}_5 H_5) \eta_{\text{Propulsor}} \quad (114)$$

In this case, the "propulsor" efficiency represents the efficiency with which the shaft work from the power turbine is converted into whatever form of power is transmitted from the engine. If the desired output is shaft work, then this efficiency factor might, for example, represent the efficiency of the gearbox used to achieve some desired output shaft speed. The variable has not been renamed simply because this would introduce additional complexity to the code.

The fuel consumption may be calculated simply enough

$$\dot{W}_{\text{Fuel}} = \dot{W}_{31} \text{FAR} \quad (115)$$

It is then trivial to find the power specific fuel consumption:

$$\text{PSFC} = \frac{[\text{PW}]}{\dot{W}_{\text{Fuel}}} \quad (116)$$

If the engine is not stationary, the core jet thrust makes a contribution to the propulsion of the vehicle. The core jet thrust is given by the momentum flux through the engine, *i.e.*

$$F_{\text{Net}} = \dot{W}_9 v_9 - \dot{W}_1 v_0 \quad (117)$$

The useful propulsive power from the perspective of the vehicle is then simply

$$PW_{\text{CorePropulsive}} = F_{\text{Net}} v_0 \quad (118)$$

Thus

$$PW_{\text{Overall}} = PW_{\text{PropulsiveCore}} + PW_{\text{Propulsor}} \quad (119)$$

TSFC

The thrust specific fuel consumption is a commonly used metric in aerospace propulsion, because historically it was easier to measure thrust, and because early turbojet engines of low pressure ratio tended to exhibit roughly constant thrust specific fuel consumption in subsonic flight. This arose because although the useful power increased in proportion to true airspeed, the overall efficiency of early engines also increased in roughly the same proportion, due to the fact that jet velocities were high, and pressure ratios low, allowing both propulsive and thermal efficiencies to increase rapidly from a low base.

Today's engines start from a considerably higher level of efficiency, and therefore tend to exhibit increasing TSFC with increasing TAS, albeit in slightly less than direct proportionality.

PSFC arguably gives a better indication of the efficiency of the engine as it is independent of TAS, but TSFC calculations remain important because TSFC has become such a widely accepted metric.

The simplest way to calculate TSFC is to separately account the thrust of the core and propulsor, sum them to arrive at total thrust, and then divide by the fuel flow. Core thrust may be calculated via equation (117), fuel flow via equation (115). Propulsor thrust is given by

$$F_{\text{Propulsor}} = \frac{PW_{\text{Propulsor}}}{v_0} \quad (120)$$

Thus,

$$\text{TSFC} = \frac{\mathbb{F}_{\text{NetCore}} + \mathbb{F}_{\text{NetPropulsor}}}{\mathbb{W}_{\text{Fuel}}} \quad (121)$$

Bypass stream

The propulsor performance having been fixed by the input, it is possible to calculate the *maximum* allowable jet velocity:

$$v_{\text{Propulsor}} = v_{\text{Freestream}} \left(\frac{2}{\eta_{\text{Propulsor}}} - 1 \right) \quad (122)$$

This is the maximum velocity because a real propulsor would be expected to experience flow losses of some sort; the actual overall efficiency of the propulsor would be the product of its isentropic efficiency and its fundamental Froude efficiency.

The Propulsor specific thrust is then

$$F_{\text{NetPropulsor}} = \frac{\mathbb{F}_{\text{NetPropulsor}}}{\mathbb{W}_{\text{Propulsor}}} = v_{\text{Propulsor}} - v_{\text{Freestream}} \quad (123)$$

And the useful thrust power per unit propulsor mass flow

$$\frac{[\text{PW}]_{\text{NetPropulsor}}}{\mathbb{W}_{\text{Propulsor}}} = F_{\text{NetPropulsor}} v_{\text{Freestream}} \quad (124)$$

The propulsor thrust power per unit core intake mass flow has already been defined in equation (114); the ratio between these two figures is therefore the ratio between the bypass and core streams, ie the bypass ratio

$$\text{BPR} = \frac{(\mathbb{W}_{45} H_{45} - \mathbb{W}_5 H_5) \eta_{\text{Propulsor}}}{F_{\text{NetPropulsor}} v_{\text{Freestream}}} \quad (125)$$

Finally, the overall specific thrust is

$$\frac{\mathbb{F}_{\text{Net}}}{\mathbb{W}} = \frac{F_{\text{NetCore}} + \text{BPR} F_{\text{NetPropulsor}}}{1 + \text{BPR}} \quad (126)$$

This gives an idea of the physical size of the overall engine, because the thrust per unit intake capture streamtube area is

$$\frac{\mathbb{F}_{\text{Net}}}{\text{Intake Capture Streamtube Area}} = \frac{\mathbb{F}_{\text{Net}} \rho_{\text{Ambient}} v_{\text{Freestream}}}{\mathbb{W}} \quad (127)$$

N.B. – the intake capture streamtube area is measured infinitely far upstream of the engine; in the subsonic case there may be substantial pre-entry diffusion, which will tend to increase the actual intake area above and beyond that of the intake capture streamtube.

The actual thrust per unit maximum intake area will be more closely approximated by

$$\frac{\mathbb{F}_{\text{Net}}}{\text{Compressor frontal Area}} = \frac{\mathbb{F}_{\text{Net}} \rho_2 v_2}{\mathbb{W}} \quad (128)$$

In the supersonic case, the compressor frontal area may be smaller than the intake capture streamtube area; such are the joys of intake design. The interested reader is directed to Seddon & Goldsmith (1999) for a full treatment of this extremely interesting subject.

RESULTS

The code produces an extremely large amount of output data, approximately 1500 columns for each engine cycle, and when run on a desktop PC at the time of writing (June 2011) will calculate results for a single Brayton cycle in approximately one second.

This means that in approximately 2 weeks, a million engines may be analysed, resulting in approximately one billion data points, even when "illegal" cycles are discarded.

Such volumes of numerical data are not conducive to direct human analysis. Indeed, given that the output files can be hundreds or even thousands of megabytes, even desktop PCs cannot manipulate them with consummate ease.

It is therefore necessary to simplify the output as far as possible, and present it in a graphical form, such that important trends and design trades may be elucidated.

Data is generated under the following headings. Many of these represent Station Data, which contains a multiplicity of sub-entries:

Ambient	Static_GGT_Isentropic_Eta
Combustor_Delivery	Static_GGT_Polytropic_Eta
Combustor_Front_Face	Static_PT_Isentropic_Eta
Compressor_Front_Face	Static_PT_Polytropic_Eta
Cooling_Bleed_Offtake	Steady_Flow_Compressor
Core_Nozzle_Exit_Plane	Thermal_Efficiency
Core_Nozzle_Front_Face	THRUST_Specific_Fuel_Consumpt
Core_Specific_Power	
Freestream	Total_GGT_Isentropic_Eta
Fuel_Flow	Total_GGT_Polytropic_Eta
Gas_Generator_Turbine	Total_PT_Isentropic_Eta
Gas_Generator_Turbine_Deliver	Total_PT_Polytropic_Eta
y	Brayton_Cycle.Heat_Input_per_
Heat_Input_per_unit_fuel_flow	unit_fuel_flow
Heat_into_Combustor	Brayton_Cycle.POWER_Specific_
Heat_out_of_Combustor	Fuel_Consumption
Intake_Front_Face	Brayton_Cycle.Thermal_Efficie
Mix_NGV_Cooling	ncy
Mix_Rotor_Cooling	(GGT = Gas Generator Turbine)
NGV_Cooling_Flow	(PT= Power Turbine)
Overall_Specific_Thrust	
Overall_Specific_Thrust_Power	
POWER_Specific_Fuel_Consumpti	
on	
Power_Turbine	
Power_Turbine_Delivery	
Rotor_Cooling_Flow	
Specific_Core_Gross_Thrust	
Specific_Core_Intake_Momentum	
_Drag	
Specific_Core_Net_Thrust	
Specific_Core_Net_Thrust_Powe	
r	
Specific_Fuel_Flow	
Specific_Intake_Momentum_Drag	
Specific_Propulsor_Nett_Thrus	
Specific_Propulsor_Thrust_Pow	
er	

Station Data structure:	U
CalculatedAt	V
FlowVelocity	VS
HasStatics	StationNumber
HasTotals	Total
MassFlow	dLnV_by_dLnP_
SpecificArea	dLnV_by_dLnT_
SpecificPower	EquilibriumConductivity
StaticIsentropicEfficiency	EquilibriumCp
StaticPolytropicEfficiency	EquilibriumCv
Statik	EquilibriumPrandtlNumber
dLnV_by_dLnP_	FAR
dLnV_by_dLnT_	FuelPercent
EquilibriumConductivity	G
EquilibriumCp	Gamma
EquilibriumCv	GammaS
EquilibriumPrandtlNumber	H
FAR	MassFlowRate
FuelPercent	MassFractions
G	MeanMolecularMass
Gamma	OuponF
GammaS	P
H	PhiEquivalenceRatio
MassFlowRate	R_Specific
MassFractions	REquivalenceRatio
MeanMolecularMass	Rho
OuponF	S
P	T
PhiEquivalenceRatio	U
R_Specific	V
REquivalenceRatio	VS
Rho	TotalIsentropicEfficiency
S	TotalPolytropicEfficiency
T	

Validation

In order to demonstrate the validity of any gas-turbine performance code, it is desirable to compare its predictions with experimental data. It is usually extremely difficult to find such data in the public domain, because it is extremely expensive to conduct the necessary tests, and engine manufacturers are mostly disinclined to give away such valuable intellectual property for free.

The author was therefore pleasantly surprised to find unexpectedly detailed information published online by a user of the PPRuNe (Professional Pilots

Rumour Network, www.pprune.org) forum. These data are reproduced in Figure 13 on page 113.

Only the supersonic cruise case (which has been placed within a red box) has been used for validation, because additional work would be required to model reheat, for which sufficient time was not available.

Procedure

The first step in the validation procedure is to match the ambient conditions.

- Altitude = 58000 feet = 17678.4 m
- $T_{\text{Ambient}} = -52^{\circ}\text{C} = 221.15\text{ K} \cong \text{ISA}+5$

This crosschecks against the total temperature. It is assumed that temperatures are quoted to the nearest 1°C.

The quoted pressure (assumed to be the total pressure) at the intake front face was then compared with the ideal total pressure, and it was found that this represented an intake total pressure recovery of 94.1%.

The compressor was treated as a single unit, as this avoided the need for modification of the model; no great error is inherent in this procedure, as only this single engine operating point is under consideration. Indeed, because no data is supplied between the two turbines, it is arguable that no great increase in fidelity could be had from splitting the compressors.

The overall compressor total pressure ratio was found to be 11.52:1. With this figure being known, the compressor polytropic efficiency input was iterated until the compressor delivery total temperature matched that quoted in the diagram. This match was achieved for an overall compressor polytropic efficiency of 88.0%.

The fuel was assumed to be Jet-A, and the fuel temperature was assumed to be equal to the freestream total temperature. The combustor total pressure loss was found to be 5.32%

Turbine efficiency was iterated to match the turbine delivery total pressure, the implied polytropic efficiency being 82.65%. This relatively low polytropic efficiency may well be due to the spoiling effect of the turbine cooling flow.

The maximum metal temperature input was iterated until the turbine delivery total temperature was matched. This figure is entirely arbitrary in the sense that there is no way of disentangling it from Kurzke's cooling constant; a value of 1088 K was found to produce a good match when using a cooling constant of 0.05. This yielded a total cooling bleed equal to about 5.5% of the intake mass flow.

Turbojet operation of the ExcelCEA model was achieved by setting the propulsor overall efficiency to zero.

The jet pipe total pressure loss was found to be 5.88% (this relatively large figure presumably being due to the reheat system, although the diagram suggests that that this is the nozzle throat total pressure, implying that some nozzle losses may also have been accounted at this point).

The nozzle velocity coefficient for the remaining supersonic nozzle was assumed to be 99%.

The quoted thrust and fuel flow imply an Imperial TSFC of $1.205 \text{ lb}_f \text{ lb}_m^{-1} \text{ hr}^{-1}$; the ExcelCEA model outputs an Imperial TSFC of $1.215 \text{ lb}_f \text{ lb}_m^{-1} \text{ hr}^{-1}$, a difference of 0.8%.

The quoted intake mass flow rate implies an imperial specific thrust of $42.59 \text{ lb}_f \text{ lb}_m^{-1}$; the ExcelCEA model predicts $42.82 \text{ lb}_f \text{ lb}_m^{-1}$, a difference of 0.5%.

It is likely that most of this difference has been caused by rounding errors and unit conversion errors, and therefore the author feels reasonably confident in stating that the model is almost certainly accurate to within 1%.

It has also been possible to cross-check some of these performance data against that published in Sir Stanley Hooker's 1984 autobiography, wherein an Imperial TSFC of $1.20 \text{ lb}_f \text{ lb}_m^{-1} \text{ hr}^{-1}$ and a thermal efficiency of 42% are quoted (ExcelCEA calculates a thermal efficiency of 41.99%).

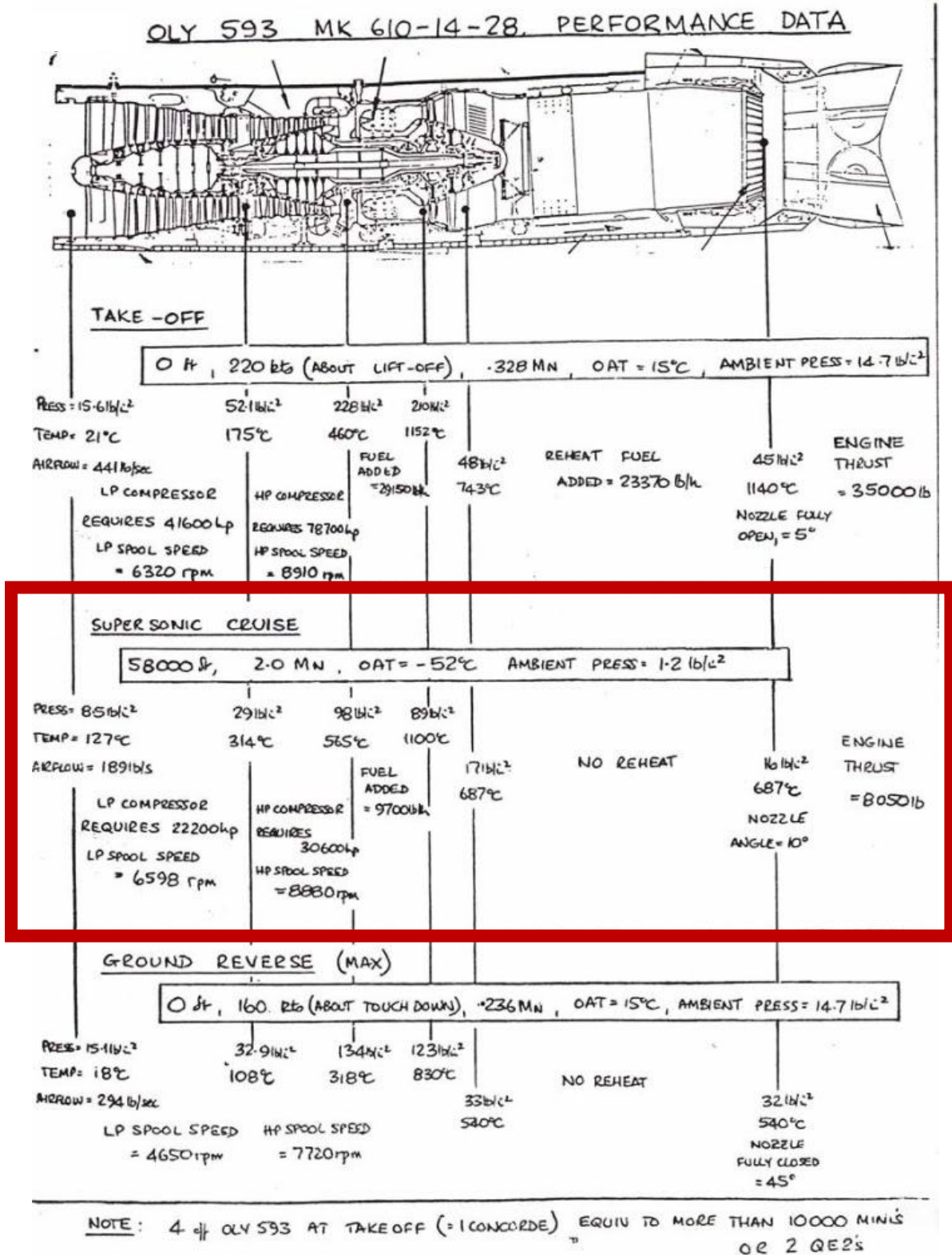


Figure 13 - Olympus 593 performance data, M2dude (2010)

Predictive modelling

In order to demonstrate the capabilities of the ExcelCEA, code three cases have been considered:

- A civil aero-engine cruising at Mach 0.80 at 11 km
- A civil aero-engine cruising at Mach 2.0 at 18 km
- A stationary industrial engine

Mach 0.80, 11000 m altitude

Figure 14 and Figure 15 on pages 118 and 119 respectively show the overall specific power

$$\text{overall specific power} = \frac{F_{\text{net}} v_0}{\dot{W}_2} \quad (129)$$

(which is a measure of physical size) and the work per unit fuel flow

$$\text{work per unit fuel flow} = \frac{F_{\text{net}} v_0}{\dot{W}_{\text{Fuel}}} = \text{PSFC}^{-1} \quad (130)$$

for engine cycles of various mechanical pressure ratios at four peak cycle temperatures and three levels of propulsor overall efficiency, *viz.* 70%, 80% and 90%.

The input file used to produce these data assumed:

- ISO Standard atmosphere
- 11 km
- Zero temperature deviation
- Mach 0.80
- Intake Pressure recovery factor = 0.99
- Intake delivery velocity = 200 m/s
- Compressor pressure ratio 1-200 in steps of 1
- Compressor efficiency = 90%
- Polytropic compressor efficiency standard

- Compressor delivery pseudo Mach number = 0²⁶
- Combustor total pressure loss factor = 0.04
- Combustor mean velocity = 50 m/s
- Fuel = Jet A
- $T_4 = 1600\text{-}2000$ K in steps of 200 K
- Cooling constant = 0.05
- Fraction of cooling air to NGV = 0.40
- Maximum metal temperature = 1375 K
- Gas generator turbine efficiency = 90%
- Polytropic Gas generator turbine efficiency standard
- Gas generator turbine delivery pseudo Mach number = 0²⁶
- Power turbine efficiency = 90%
- Polytropic Power turbine efficiency standard
- Power turbine delivery pseudo Mach number = 0²⁶
- Jet pipe pressure loss factor = 0.01
- Core nozzle velocity coefficient = 0.99
- Propulsor overall efficiency = 70%, 80%, 90%

Several important trends are in evidence:

- Overall specific power increases approximately linearly with T_4 .
- The mechanical pressure ratio which maximises overall specific power increases only gradually with T_4 .

²⁶ Due to the extreme chemical equilibrium assumptions inherent in CEA, there is no difference in engine performance (specific thrust, TSFC etc.) associated with the axial velocity through the engine. Before this was realised, the code was written so as to pass static flow parameters from station to station in the hope that this would allow higher fidelity.

Although there is in fact no difference in the result of performance calculations associated with the axial flow velocity, having written the code it was felt pointless to expend further effort to remove the velocity inputs.

Additionally, the flow velocity does have some value beyond performance calculation, because, in conjunction with the density and mass flow, it allows a first-order estimate of the flow area required to be calculated. It also allows the calculation of additional compressor and turbine efficiencies (Total to Static, Static to Static) to be calculated, which may be of interest in the detailed analysis of different cycles, especially in cases where kinetic energy downstream of a turbine is accounted as a loss.

- *PSFC* decreases only gradually with T_4 .
- The pressure ratio for minimum *PSFC* increases quite rapidly with T_4 .

A strong law of diminishing returns would appear to be in operation. Increasing T_4 from 1600 K to 2000 K (i.e. by 25%) would, at the optimum pressure ratio for minimum *PSFC*, reduce *PSFC* by approximately 10%; the majority of the improvement being obtained at 1800 K.

This would tend to strongly imply that the Brayton-cycle is approaching the limit of its development potential, at least as regards fuel consumption.

Increases in overall specific power would suggest opportunities for reduction in engine size, which would likely also reduce engine mass. However, as engines already represent quite a small proportion of aircraft zero-fuel mass, any resultant reductions in overall mission fuel are likely to be strictly limited, perhaps of the order of 1-2%.

Furthermore, any such reduction in physical size would imply a reduction in turbomachinery Reynolds number, which would tend to reduce the polytropic efficiency attainable.

At 2000 K, pressure ratios below 80 did not produce “legal” cycles because the enthalpy drop across the gas generator turbine was insufficient to reduce the gas temperature below the input maximum metal temperature limit of 1375 K, and so the power turbine could not have run un-cooled. This means that, under the freestream conditions considered, it would not be possible to construct a cycle at having the pressure ratio for maximum specific power output at values of $T_4 > 2000$ K.

This does not represent a “show-stopping” performance limitation, in as much as it is quite possible to produce cooled power turbines.

Figure 18 on page 122 shows the overall thermal efficiency of the cycle; this differs very slightly in shape from Figure 14 because the heating value of the fuel varies slightly with compressor delivery flow parameters and the value of T_4 .

Figure 19 on page 123 shows the optimum bypass ratio calculated by the code, which rapidly increases as increased propulsive efficiency is demanded. As

discussed on page 107, this is a minimum bypass ratio because it implicitly assumes that the propulsor changes the momentum of the bypass stream isentropically, with the only loss being that associated with the Froude efficiency.

In reality, irreversibility within the propulsor would need to be compensated by increases in Froude efficiency if constant propulsive efficiency were to be maintained; this would require an increase in the bypass ratio.

Finally, Figure 20 on page 124 shows the overall specific thrust of the engine. As one might expect, this is set by the overall propulsive efficiency standard.

The small increase in specific thrust at high pressure ratio is caused by the decreasing bypass ratio (the core specific thrust will always be somewhat higher than the bypass specific thrust – see equation (102)).

The change in specific thrust is greater at lower levels of propulsive efficiency because the bypass ratio changes by a larger factor.

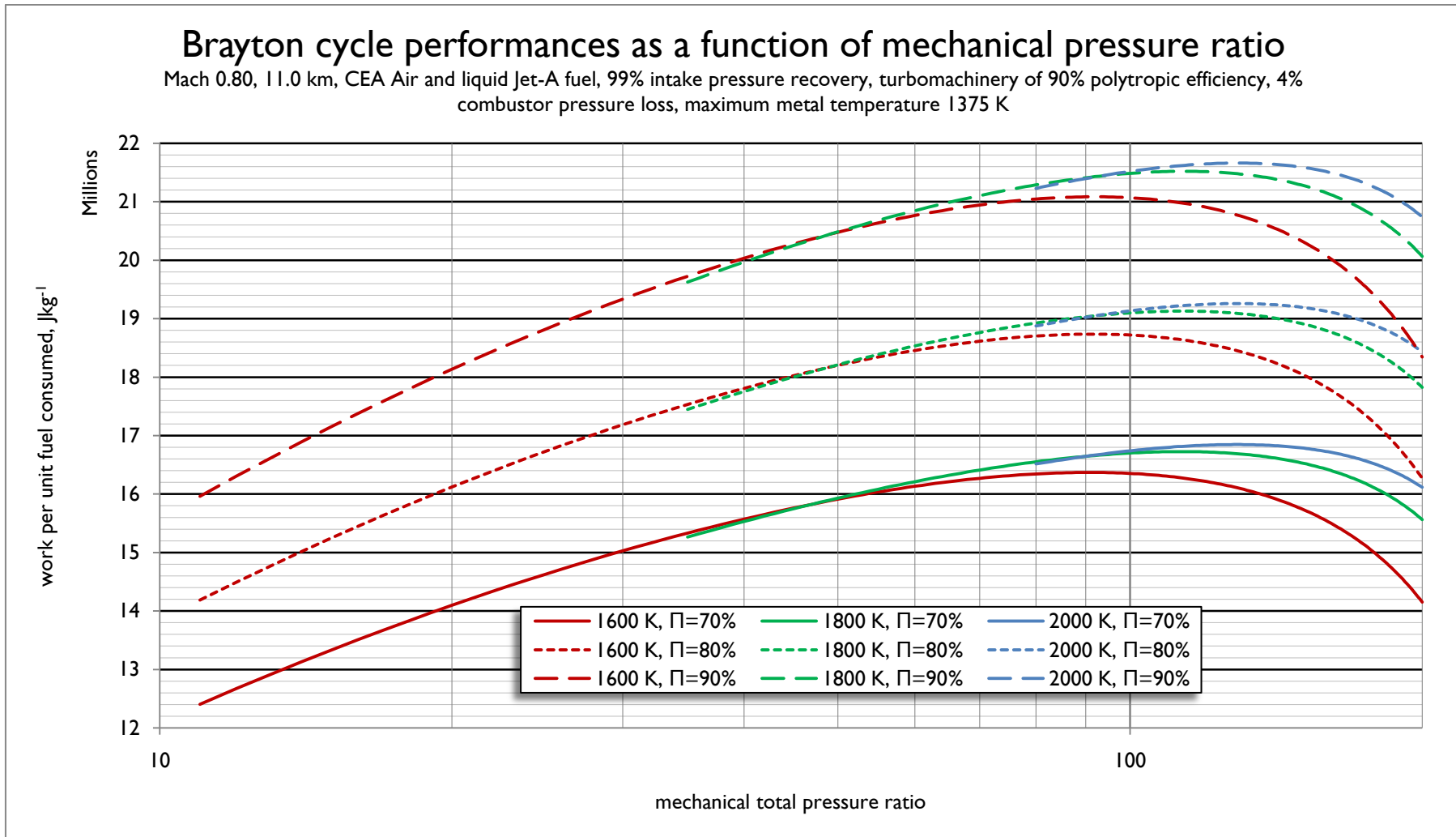


Figure 14 – Brayton cycle performances with respect to fuel consumption; Mach 0.80, 11 km.

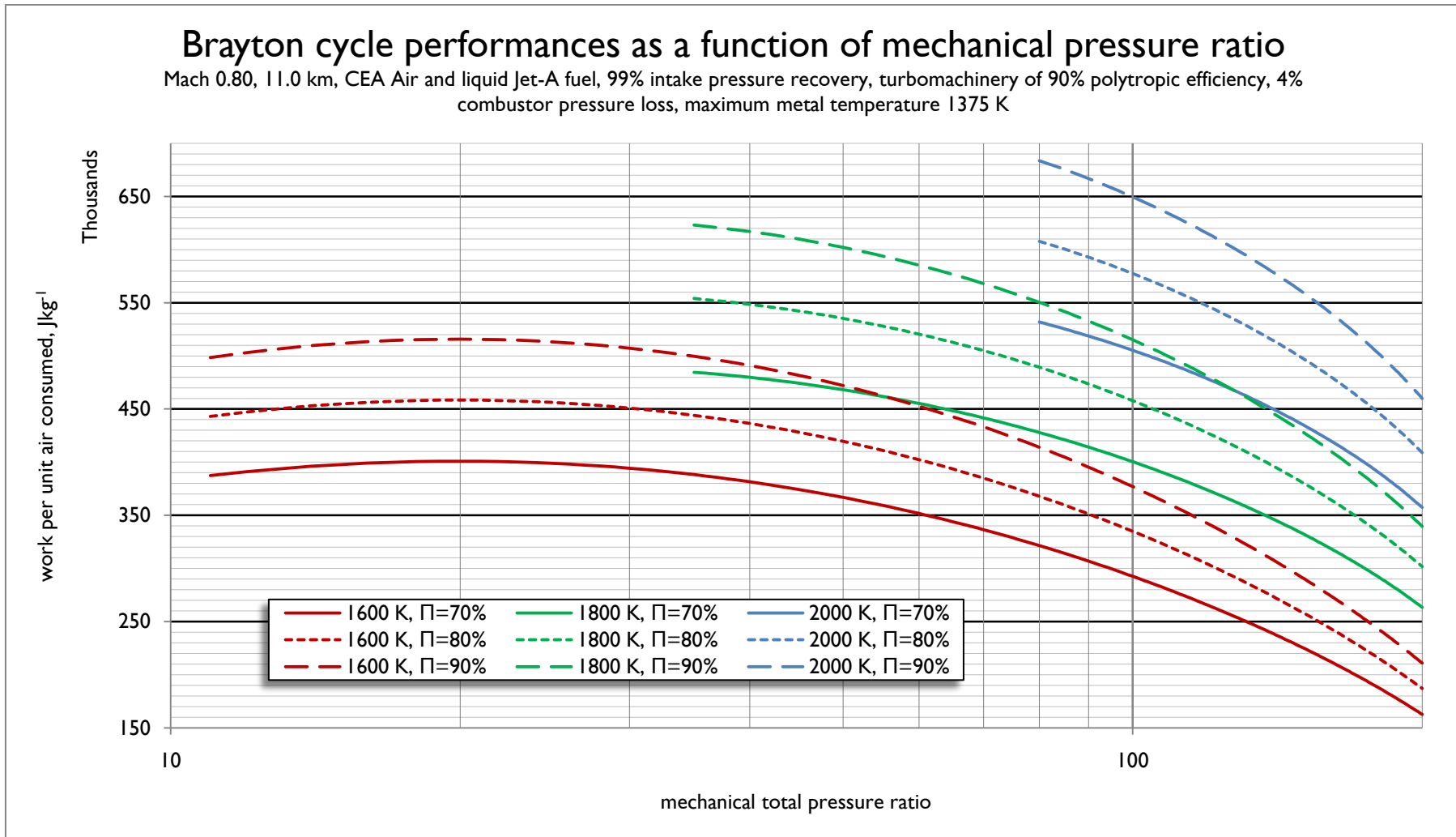


Figure 15 – Brayton cycle performances with respect to core air consumption; Mach 0.80, 11 km.

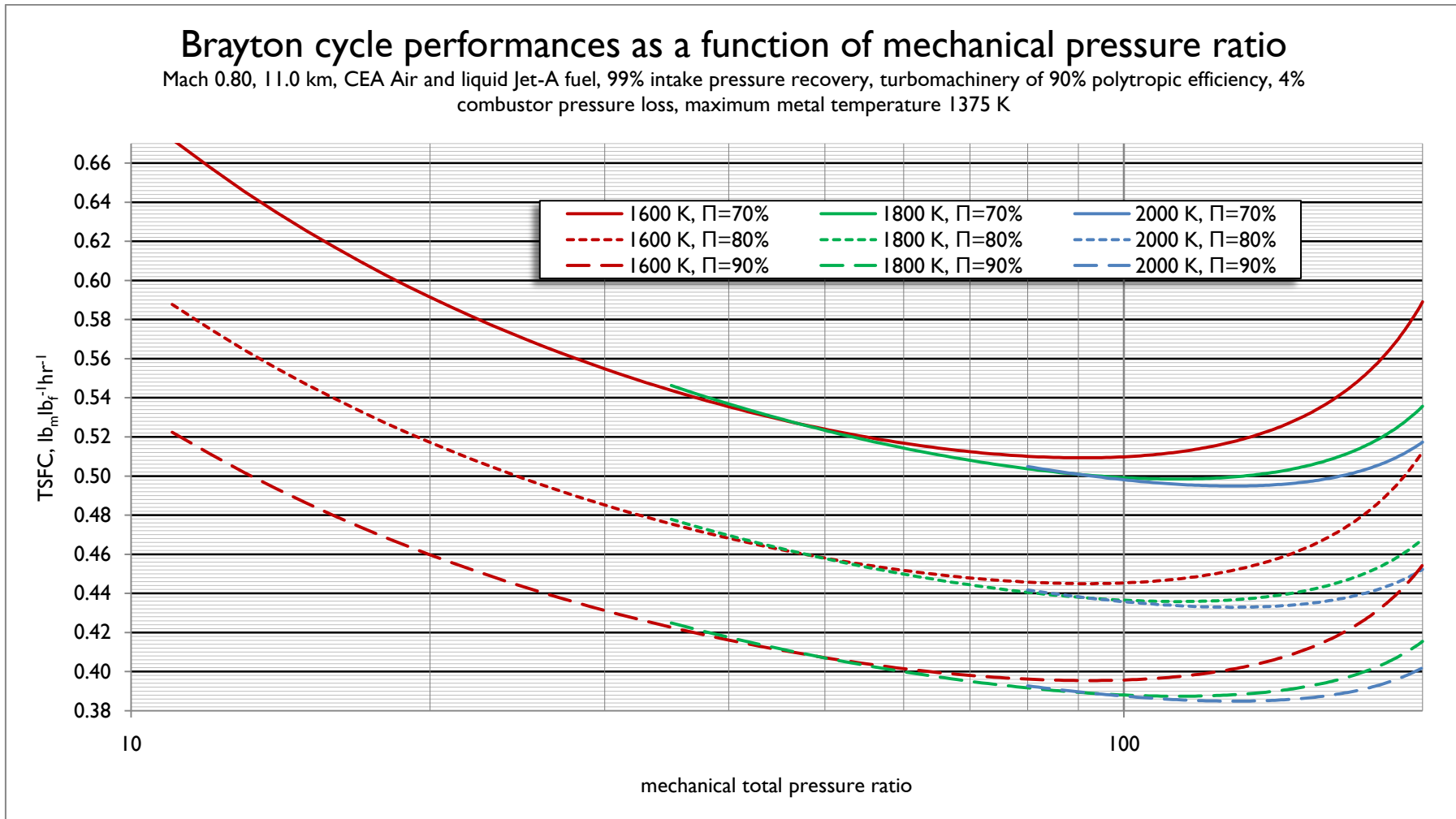


Figure 16 - Brayton cycle TSFC performances, Mach 0.80, 11 km

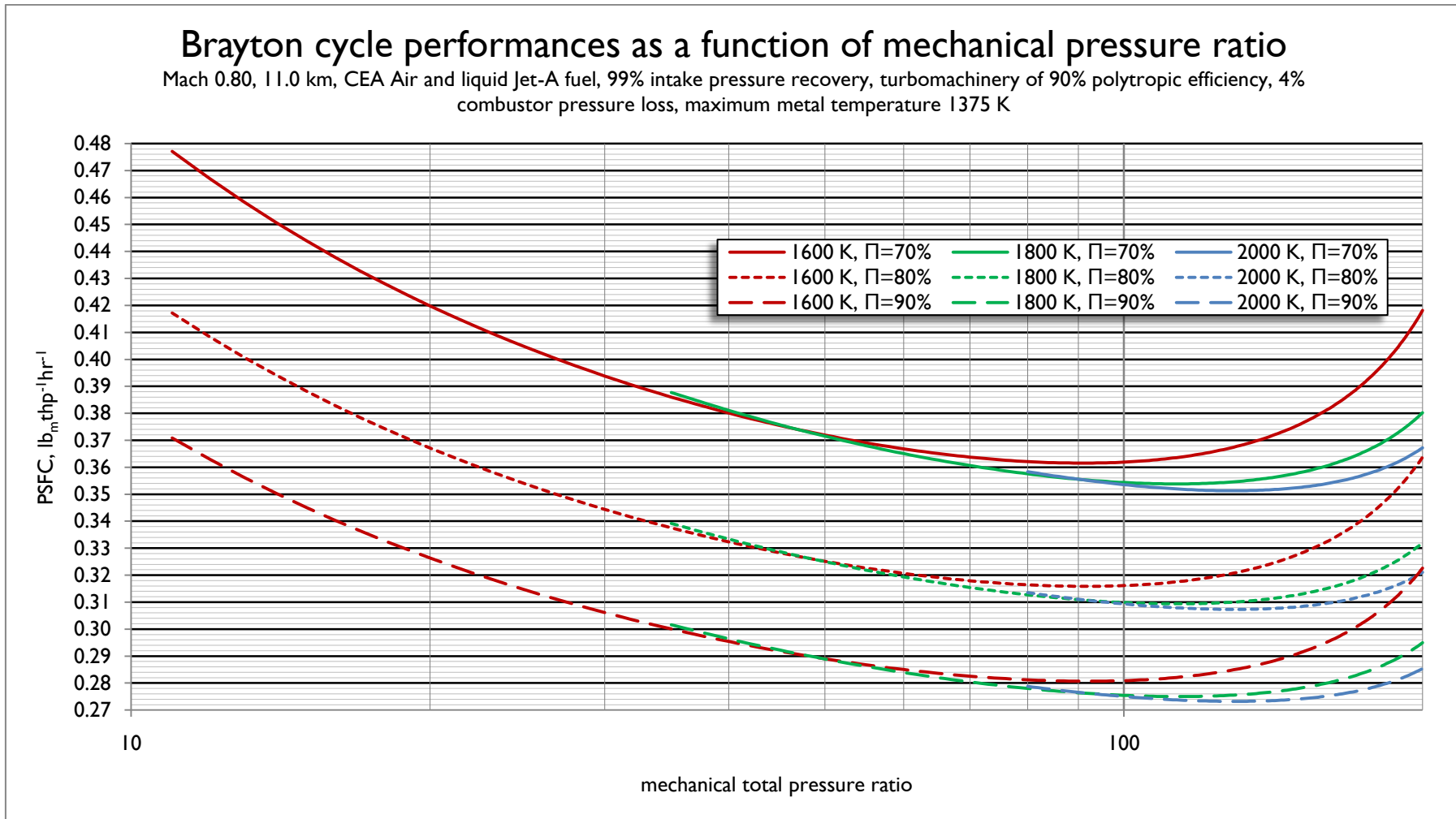


Figure 17 - Brayton cycle tPSFC performances, Mach 0.80, 11 km

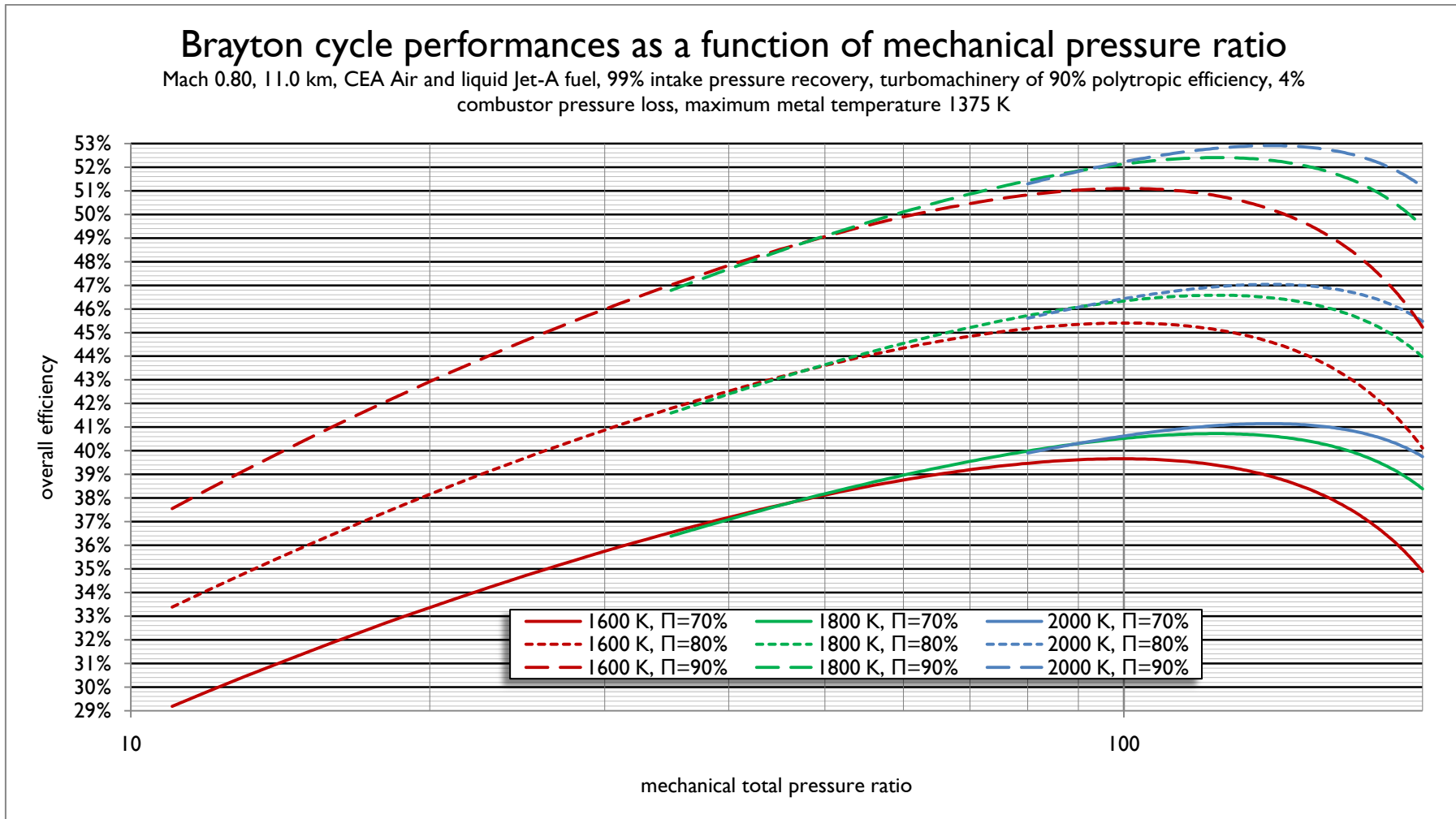


Figure 18 - Brayton cycle overall thermal efficiency performances, Mach 0.80, 11 km

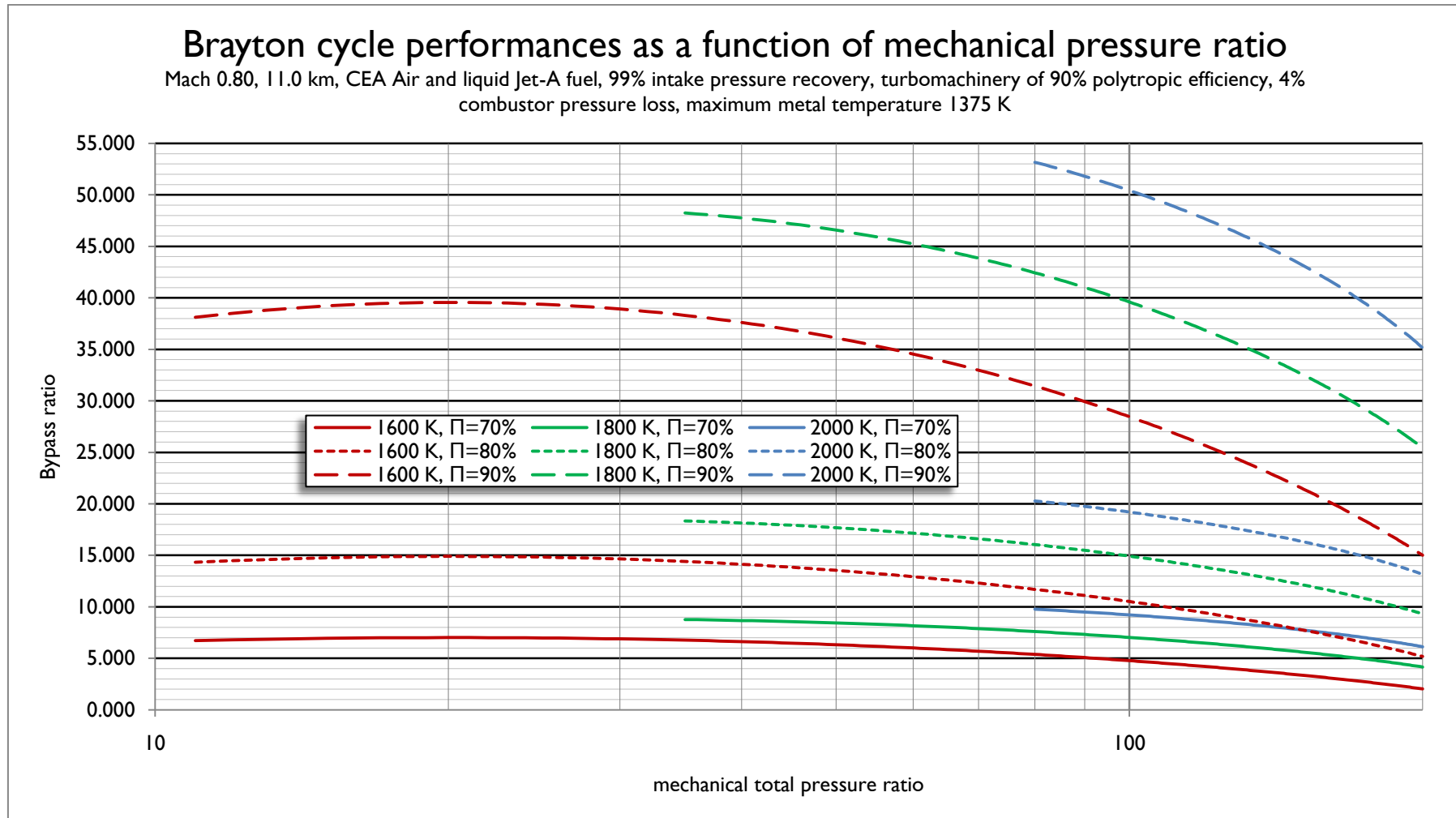


Figure 19 - Brayton cycle optimum bypass ratio, Mach 0.80, 11 km

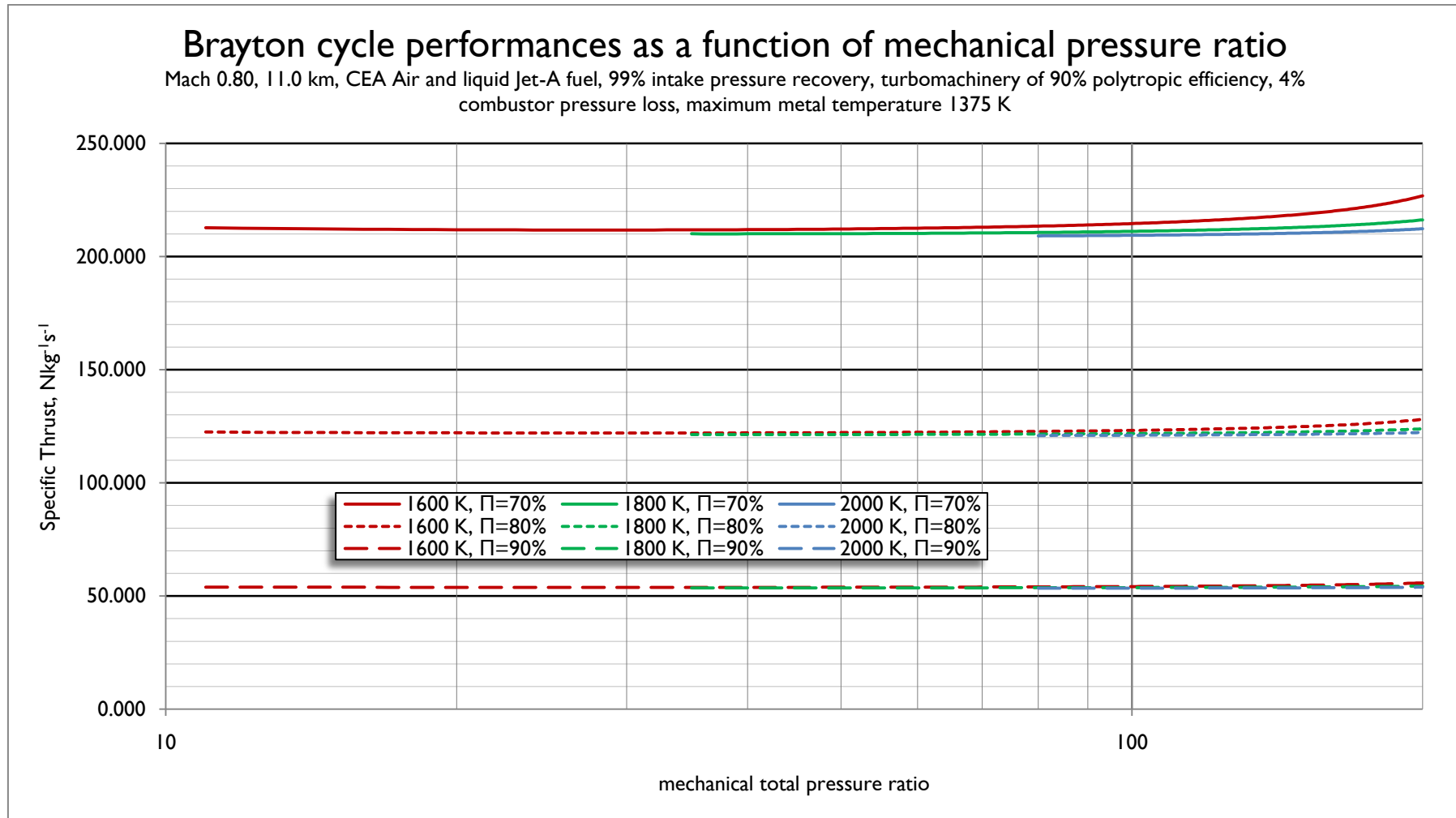


Figure 20 - Brayton cycle overall specific thrust, Mach 0.80, 11 km

Mach 2.0, 18000 m altitude

Several interesting trends emerge at Mach 2.0. Turning initially to Figure 21 on page 127, the pure turbojet achieves maximum performance with respect to specific fuel consumption at low values of peak cycle temperature, because its overall propulsive efficiency varies inversely with its specific thrust (see Figure 22, page 128).

Even with high component efficiencies, the peak cycle temperature for specific fuel consumption is quite surprisingly low.

The turbofan propulsive efficiency standard of 90% is decidedly optimistic; it was selected on the basis that Hooker's autobiography credits Olympus 593 with a propulsive efficiency of approximately 80%.

The vertical TSFC lines are produced when the enthalpy remaining after the gas generator turbine falls to a level insufficient to support the operation of the requested turbofan cycle. This naturally coincides with the point at which the TSFC of the turbofan equals that of the equivalent pure turbojet cycle.

It may be seen that the specific thrust of the turbofan actually falls slightly as the peak cycle temperature is increased; this is due to the fact that the increasing core specific power is able to support an higher bypass ratio, the bypass stream having a lower specific thrust than the core stream for reasons already discussed; this trend would probably still hold, albeit to a slightly reduced degree, were a mixed exhaust system to be modelled, because increasing bypass ratio would tend to reduce the overall exhaust static temperature, thereby reducing the overall jet velocity associated with any given expansion ratio.

The overall efficiency is naturally inverse to the TSFC, and proportional to the work per unit fuel flow, as displayed in Figure 25 on page 131, with the caveat that, as at Mach 0.80, there is some small variation in the fuel heating value as a function of the compressor delivery parameters and T_4 . It is interesting to note that there is relatively little difference in overall efficiency from the Mach 0.80 case when equivalent propulsive efficiency standards are set.

What difference there is may be attributed to differences in component efficiency. Although the intake efficiency is nominally lower, at 94.1% in the

Mach 2.0 case, this is more than offset by the increased ram pressure. Therefore, the effective polytropic efficiency of the whole compression system (i.e. the intake and mechanical compressor in combination) is higher than that in the subsonic case, which allows a slightly higher overall efficiency to be achieved. This highlights how substantial an achievement Concorde's intake represented, given that it is still able to out-compete a mechanical compressor of 90% polytropic efficiency.

As it is unlikely that an open-rotor propulsor configuration would be seriously considered for a supersonic aeroplane, Figure 24 is perhaps only of academic interest.

Unsurprisingly, the optimum bypass ratio is far lower at Mach 2.0 than at Mach 0.80 due to the greatly increased power required to drive the bypass flow.

It is worth observing that these results only consider the internal flow; it is likely that the specific thrust for minimum mission fuel burn would be somewhat higher than that indicated by the code, because of the drag and weight of the engine nacelle. However, this sort of wider trade study is beyond the scope of this thesis.

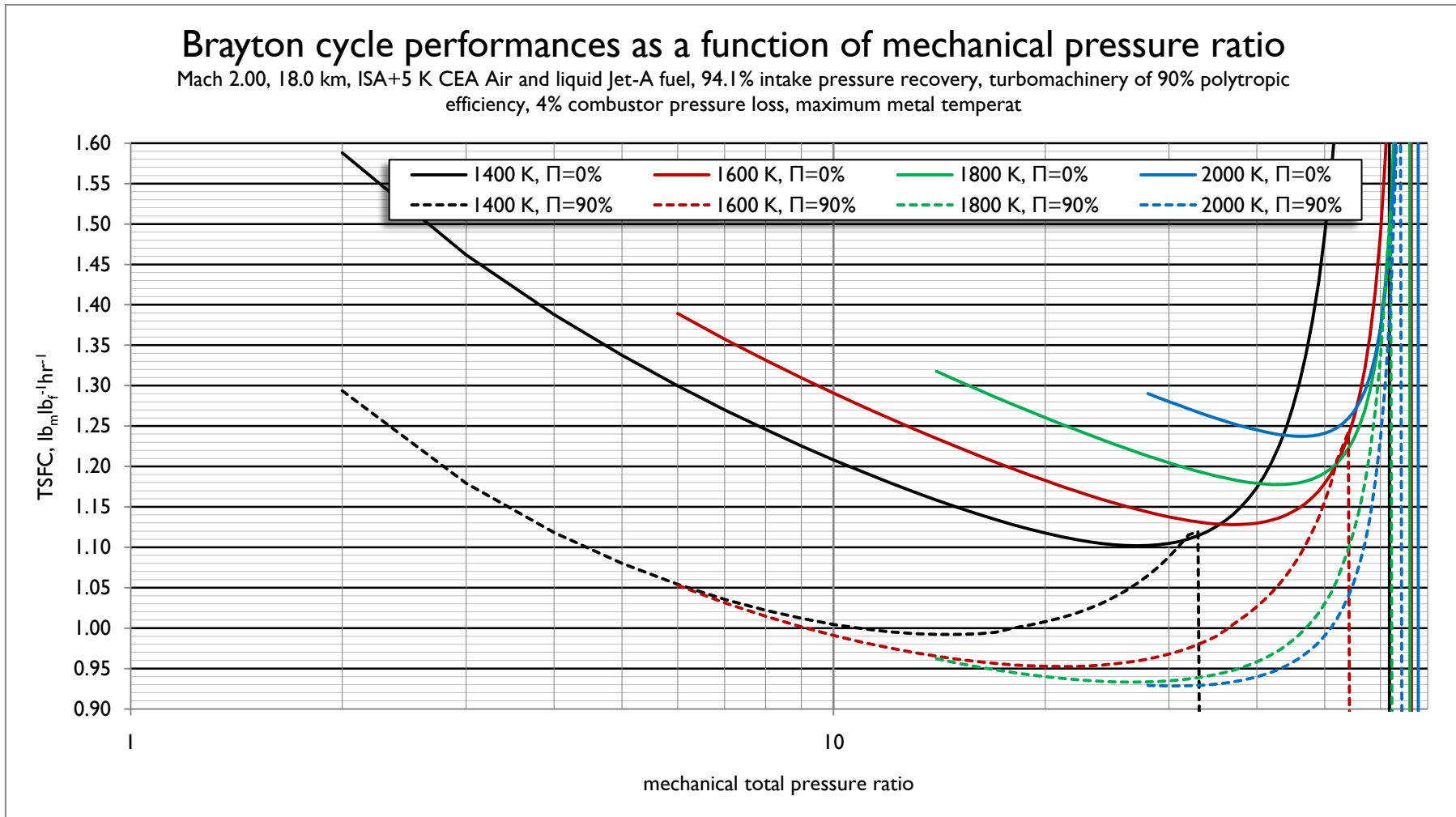


Figure 21 - Brayton cycle performances Imperial TSFC, Mach 2.0, 18 km

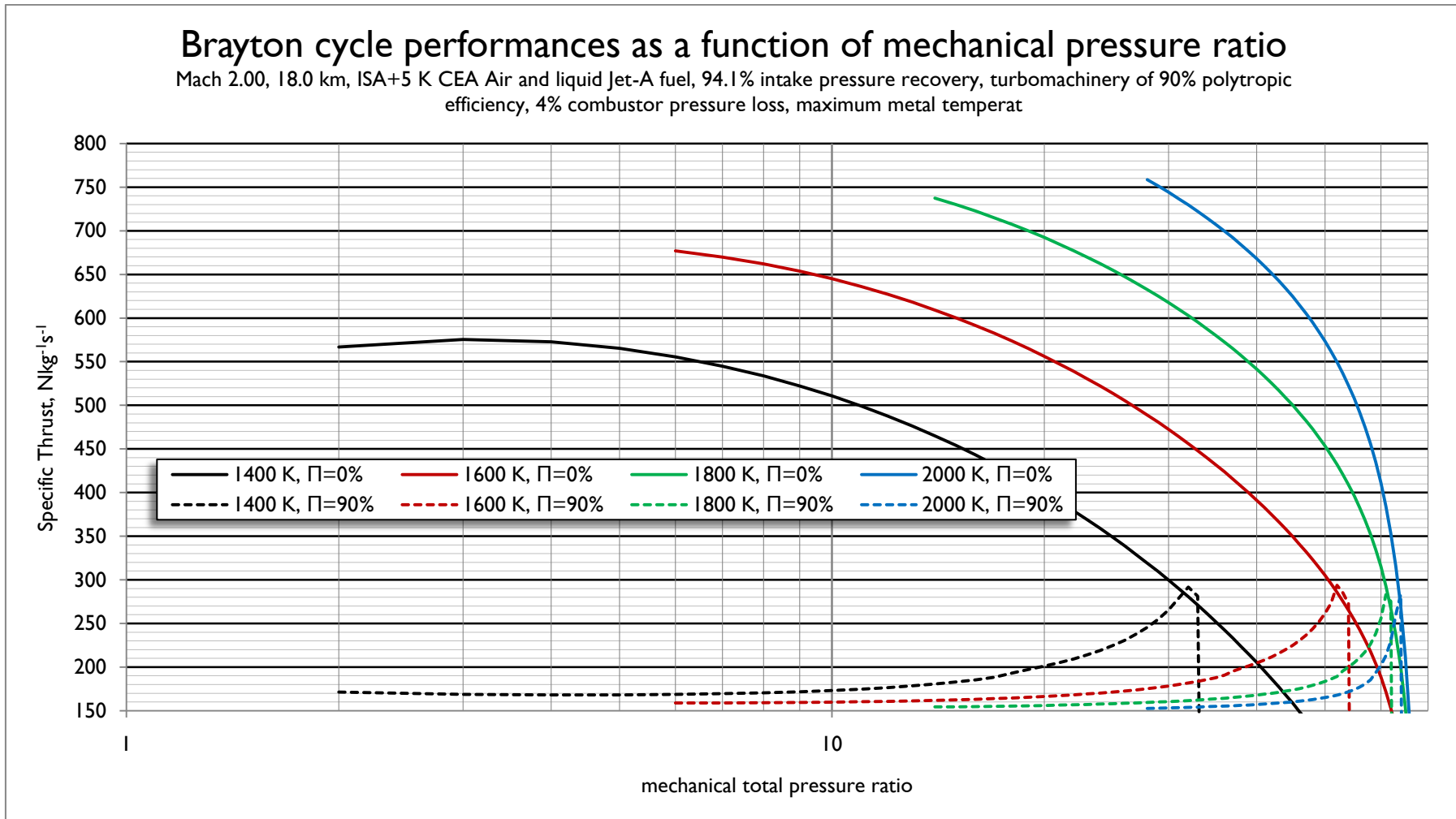


Figure 22 - Brayton cycle specific thrust, Mach 2.0, 18 km

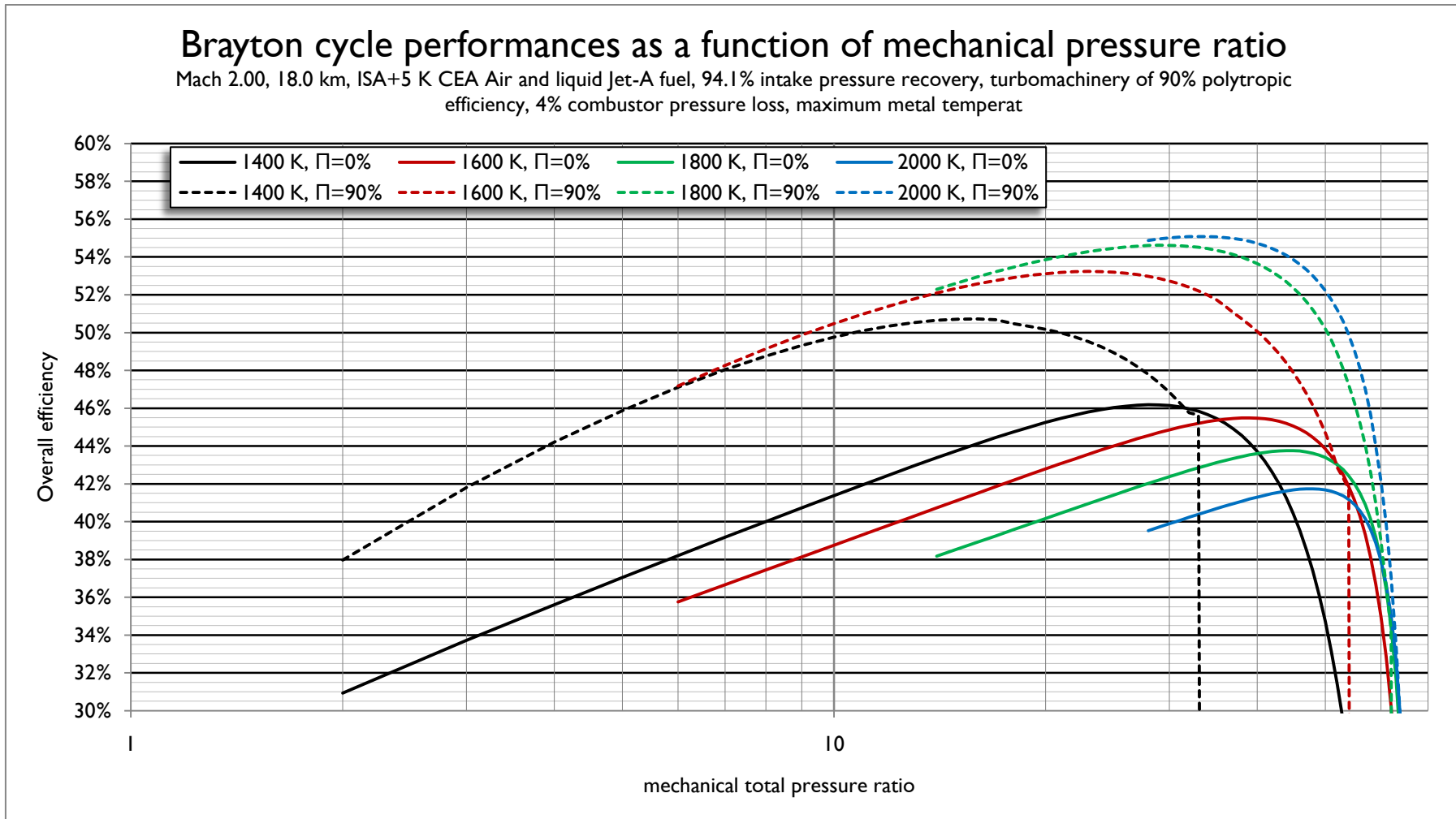


Figure 23 - Brayton cycle overall efficiency, Mach 2.0, 18 km

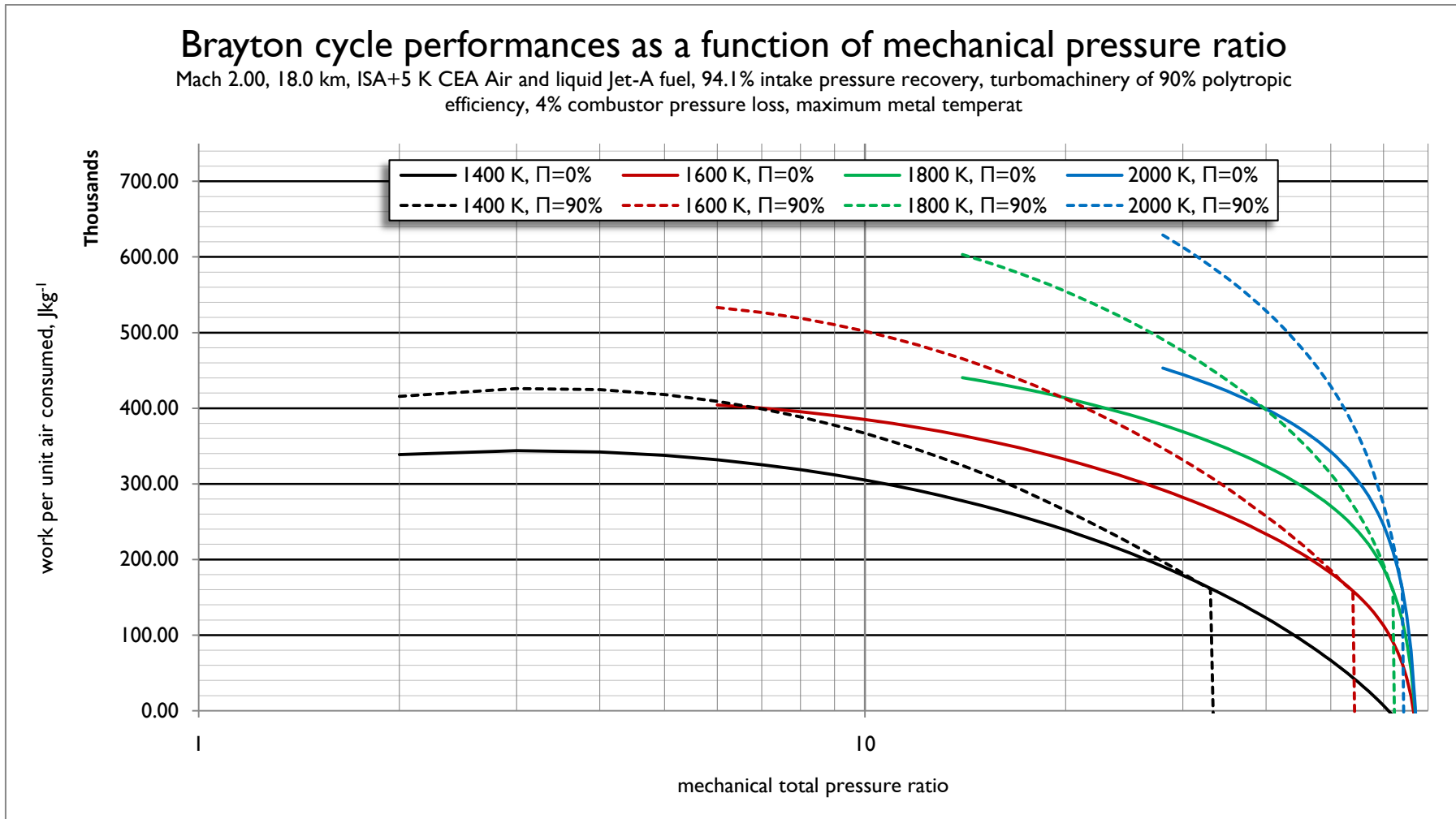


Figure 24 - Brayton cycle performances with respect to core air consumption, Mach 2.0, 18 km

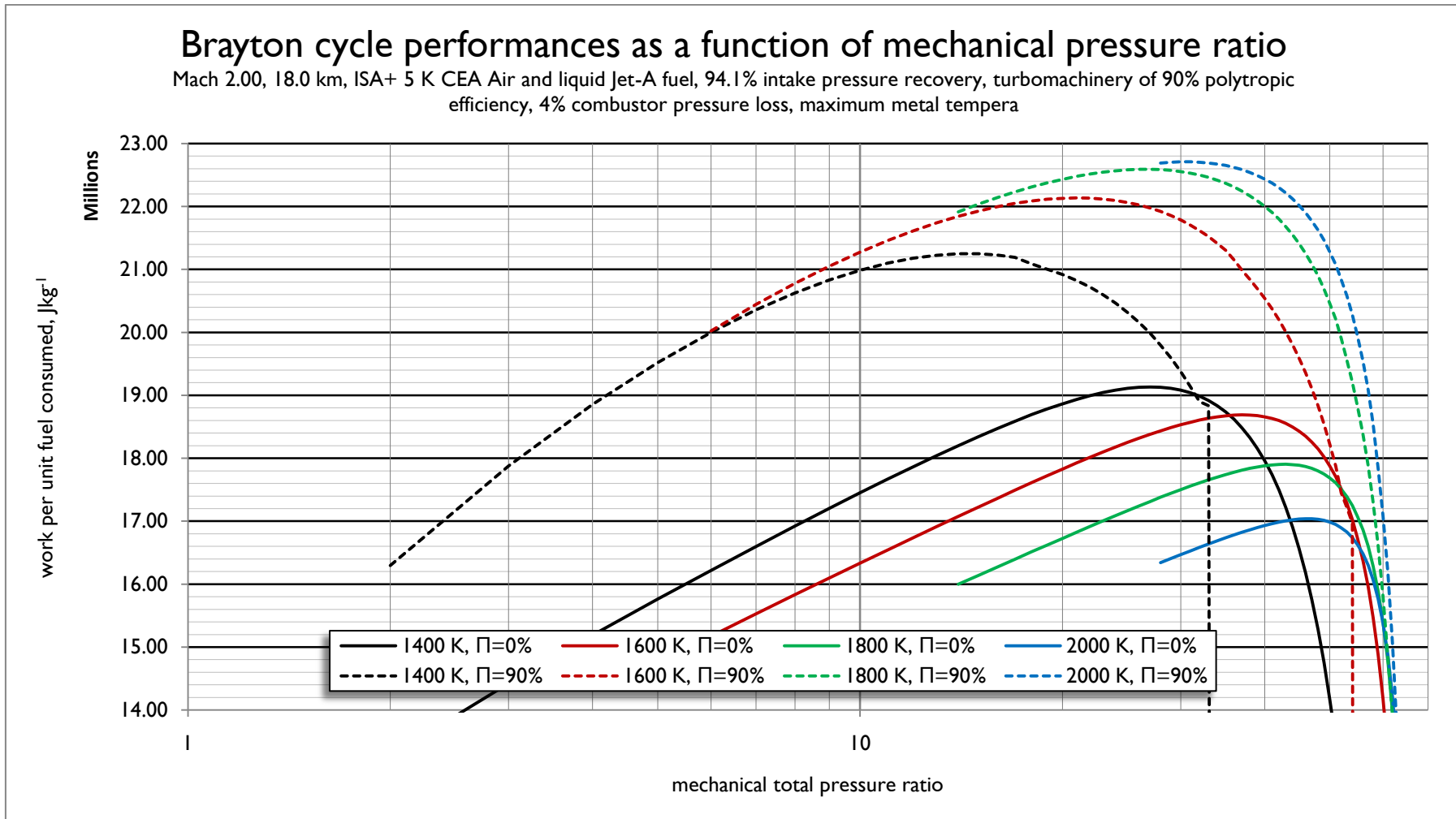


Figure 25 - Brayton cycle performances with respect to fuel consumption, Mach 2.0, 18 km

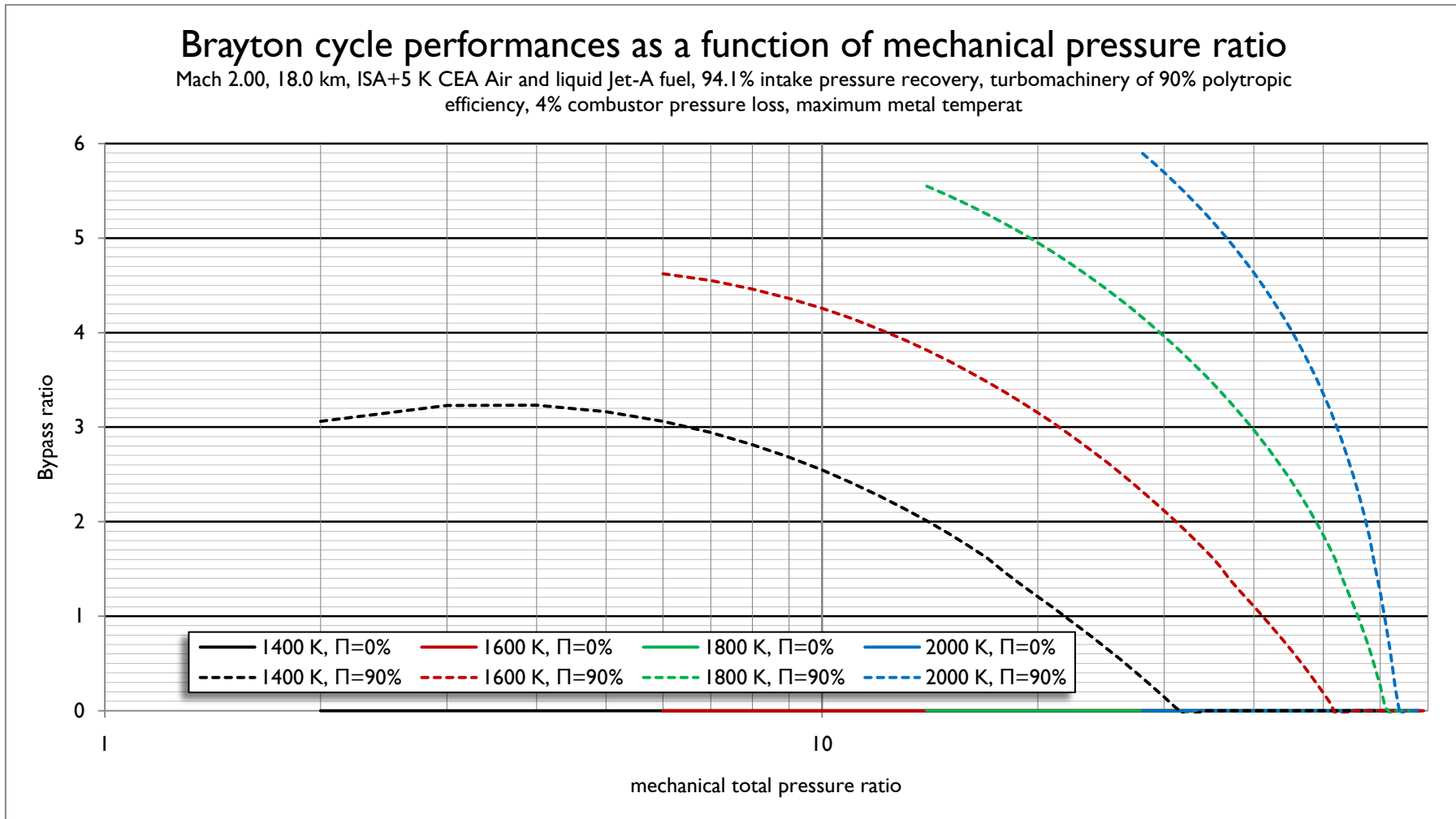


Figure 26 - Brayton cycle optimum bypass ratio, Mach 2.0, 18 km

Stationary power

The stationary Brayton cycle might be used for industrial power generation, or possibly as a prime-mover for low speed vehicles. Lower temperatures are considered than for aircraft propulsion, because there are considerable economic advantages available to engines able operating without cooling, not only due to their inherently lower first cost, but also due to their greater tolerance to ash. This allows cheaper fuel to be used.

Had further time been available, additional fuels would have been investigated, most obviously heavier hydrocarbons and natural gas.

It is expected that the basic trends associated with Jet A would extend to these other fuels, though there would be differences in detail.

Engine performance is considered at sea level on a standard day, and at 4 km altitude, the highest altitude at which it is imagined that a stationary engine might be operated. Had further time been available, higher ambient temperatures would also have been investigated.

Firstly, looking at Figure 27 on page 134, it is apparent that the optimum pressure ratio is considerably higher than for the aero-engines, due to the absence of intake ram. Fuel consumption is reduced at higher altitude due to the reduction in ambient temperature. The absolute value of PSFC is somewhat lower than the tPSFC figures attained by the aero-engines because this analysis accounts all power turbine work as useful work. The actual efficiency with which that power turbine work is produced is probably slightly lower than would be the case for the aero-engines, because intake ram is generally recovered at a higher equivalent polytropic efficiency than may be attained by mechanical compression.

Engine performances with respect to air consumption are not especially surprising; increasing the peak cycle temperature naturally increases both the maximum specific power and the pressure ratio at which this is attained. Perhaps the most interesting characteristic made apparent by Figure 28 (page 135) is therefore the way in which the output appears to “fall off a cliff” at high pressure ratio. This is caused by the rapid increase in cooling airflow requirements as T_3 approaches the maximum metal temperature.

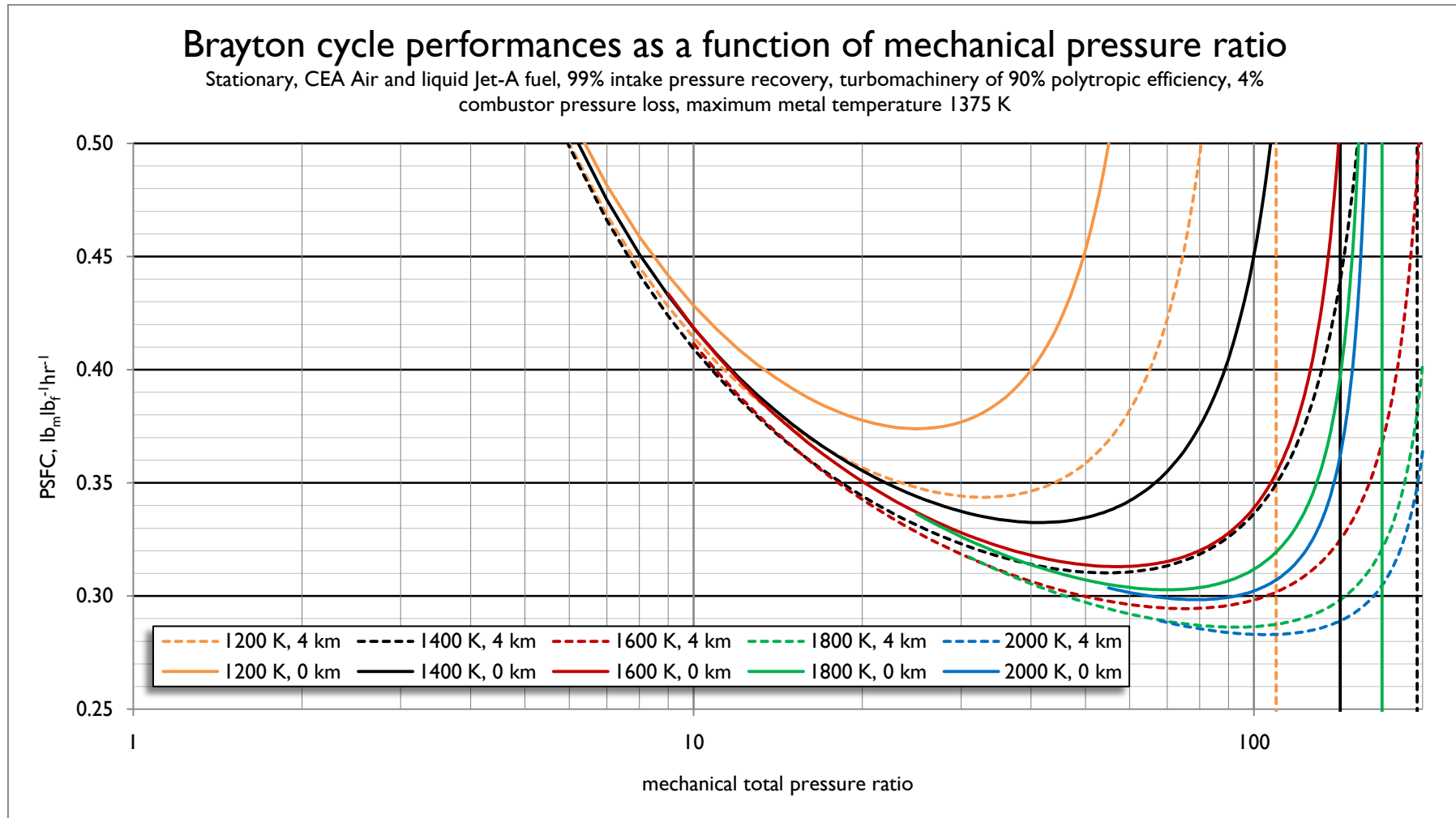


Figure 27 - Stationary Brayton cycle PSFC

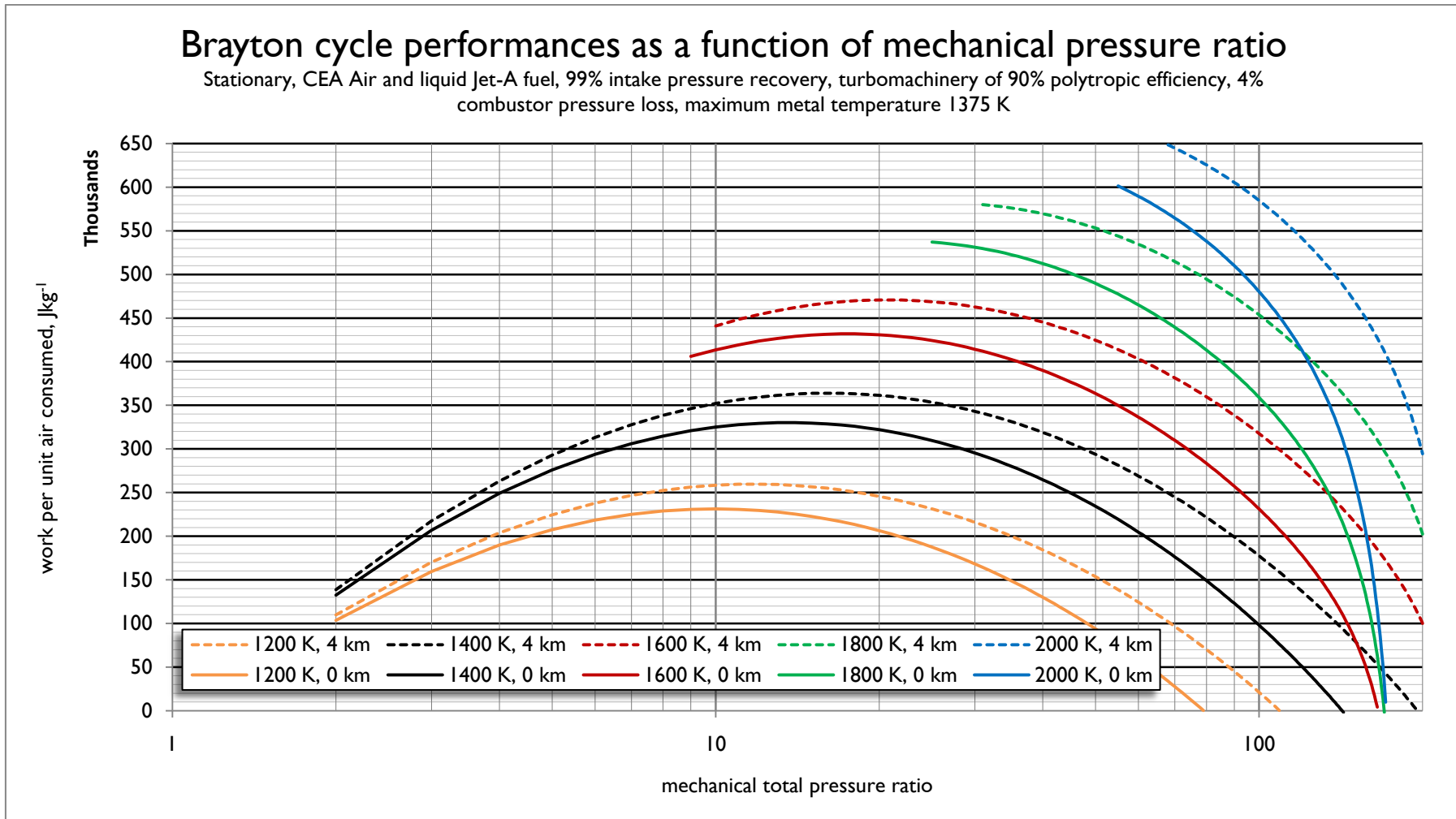


Figure 28 - Stationary Brayton cycle performances with respect to air consumption

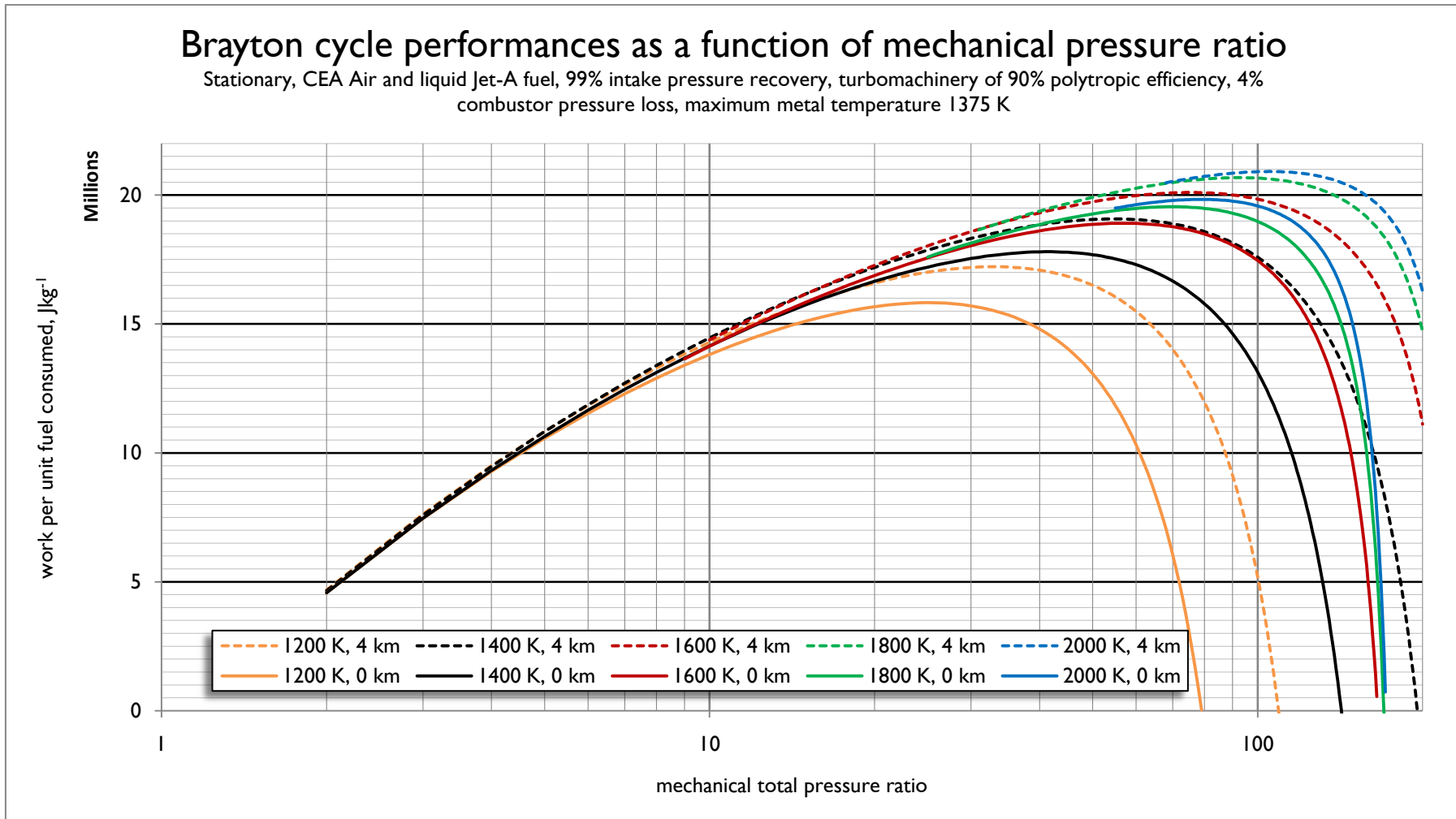


Figure 29 - Stationary Brayton cycle performances with respect to fuel consumption

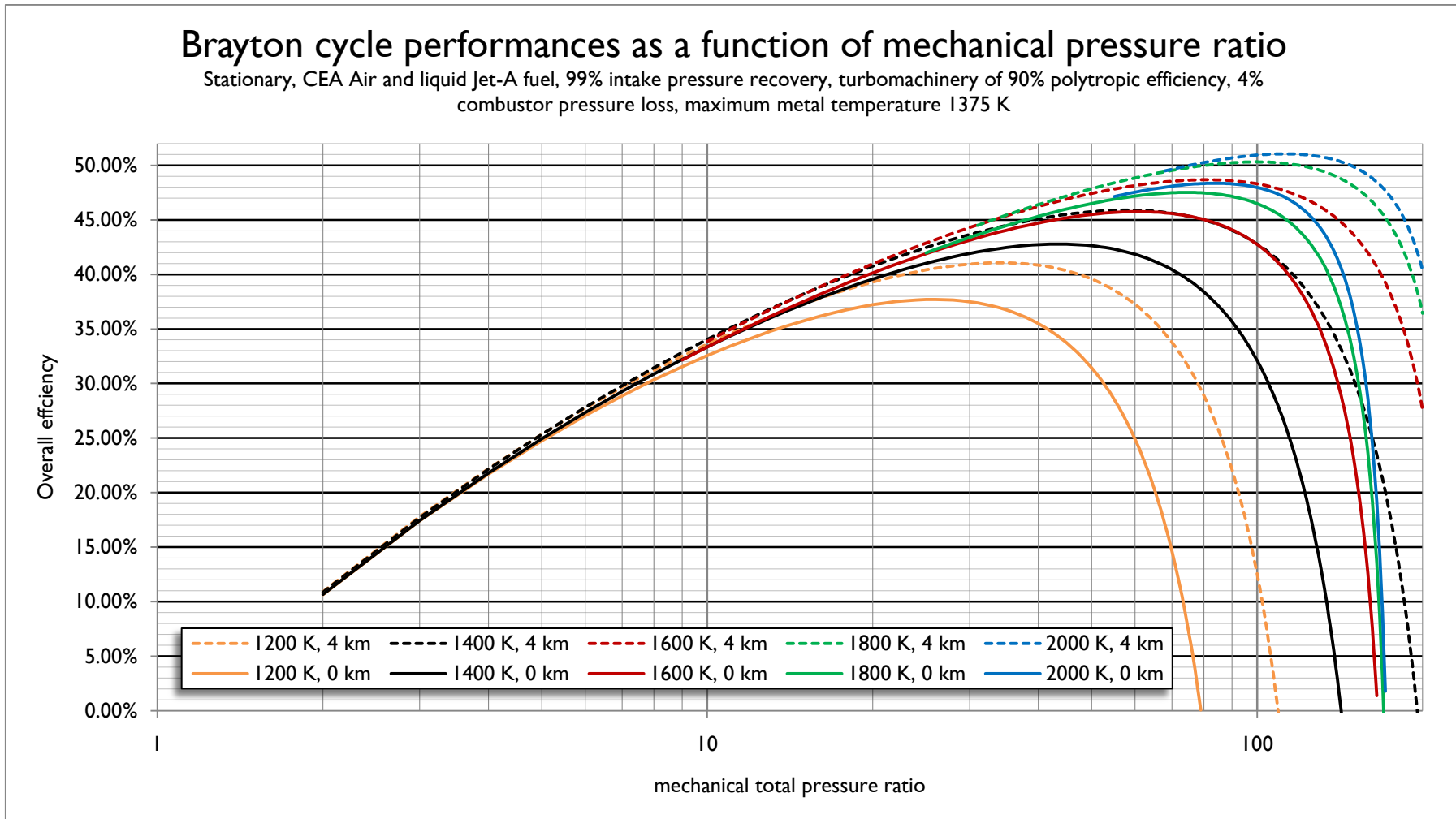


Figure 30 - Stationary Brayton cycle overall efficiency

Thermodynamic surfaces

A note on Maxwell and the origin of thermodynamic surfaces

In 1874, Maxwell sculpted a thermodynamic surface to represent the properties of a water-like substance. He did this in response to a paper by Gibbs.

(Wikipedia, 2011B). This surface may be thought of as a physical representation of a subset the Bridgman equations.

A fourth dimension might be represented by colouring the surface, and a fifth by producing a number of surfaces, and animating them.

Having described the performance of a thermodynamic cycle in terms of the geometry of a multi-dimensional surface, it follows that if such a surface is comprehensive, any thermodynamic surface of that type must be represented by a point on that surface.

This further implies that if an engine is moved away from its design point (by changing ambient or control parameters), it must describe a line on this surface.

Having described the geometrical rules governing movement on the thermodynamic surface associated with a thermodynamic cycle, these rules may be used to constrain (and thus simplify) the process of finding the off-design performance of a given engine (if the surface is comprehensive, then all engines following the cycle it concerns are described, and therefore finding the performance of a real engine comes down to removing "virtual" engines rather than calculating "real" cases).

Discussion

The ExcelCEA code offers a wide range of possibilities for modelling a variety of thermodynamic cycles. The large quantities of data produced by the model could allow engine cycles to be analysed in considerable detail.

The large amount of data produced poses interpretational and visualisation challenges, but there are perhaps worse problems than an excess of data!

The primary limitation associated with the use of CEA is the imposition of total chemical equilibrium; this is explored in *Appendix A – CEA input and output files illustrating the extreme reversibility associated with equilibrium chemistry assumptions* on page 146. This means that topics such as combustion efficiency and emissions cannot be explored in a satisfactory manner without considerable further work.

The primary advantage of the ExcelCEA model is its general nature.

Comparison with Kurzke's conclusions

The results of the Brayton cycle analysis presented in this thesis would appear to be in good general agreement with those presented by Kurzke in his 2003 paper *Achieving maximum thermal efficiency with the simple gas turbine cycle*.

It is hoped that small differences in the results will be found to be due to the increased accuracy of the ExcelCEA model.

POSSIBILITIES FOR FURTHER INVESTIGATION

Modelling of additional processes

At the time of writing, the ExcelCEA code only considers those processes required to model the Brayton-cycle gas-turbine engine as described above. Modelling further processes would allow further thermodynamic cycles to be modelled.

Apart from the obvious attraction of modelling some additional cycle, the primary advantage of extending the code in this manner would be that it would facilitate a truly fair comparison between thermodynamic cycles, using consistent modelling assumptions.

Capacity to handle additional phases

At present, the code is unable to handle non-gaseous phases of matter. This precludes the general modelling of *e.g.* Rankine cycle steam engines. It also complicates the modelling of engines burning certain potentially attractive fuels, such as Boron, whose products of combustion tend to condense during expansion.

Extension of the *thermo.lib* database

Although a large number of chemical species are contained within CEA's thermo.lib database, the scope of the code could be extended, and its fidelity improved, by the addition of further chemical species. The procedures for doing this have been described by Gordon & McBride in their description of the CEA code, and therefore there should be almost no technical risk associated with this work, although it would undoubtedly be somewhat tedious.

Additional thermodynamic cycles

The further work outlined above would facilitate the consideration of additional thermodynamic cycles.

Rational automated searches for novel thermodynamic cycles

Having developed the capability to model additional cycles, the next level of abstraction is to modify the structure of the cycles themselves in the same way that component performances are currently iterated in the ExcelCEA code.

Thus, whereas the code presently searches for the "best" Brayton cycle, it would be possible to instead search for the "best" thermodynamic cycle composed of any of the processes that the code is capable of modelling.

Such meta-analysis would be extremely computationally expensive, but may well be feasible with modern high-performance computers.

Extension of the ExcelCEA code to off-design-point cases

There are two potential approaches to off-design modelling using ExcelCEA.

The first option would be the conventional approach, solving the matching equations at the primary code's runtime.

However, a second option would be to calculate the off-design performance of real engines by post-processing of the output of a design-point solution. This is possible because the design-point case considers all combinations of

component efficiencies. Therefore the task of finding the off-design trajectory of an engine along the thermodynamic surface describing its cycle is effectively a search problem.

It may be that this search problem is computationally cheaper in the long-term than the conventional approach.

Another application of this search-based approach to off-design performance analysis might be engine health management.

The known design parameters of the engine would serve to limit the search space to "adjacent" engines. The task of diagnosing the causes of engine performance degradation is then essentially one of searching for a point on the thermodynamic surface which matches the measured performance parameters of the engine in question.

The advantage of this approach is its generality; given sufficient data, it should be possible to infer component performances for new engines without the need to for example train a neural network or evolve a genetic algorithm based upon service experience.

PUBLICATION

Moxon, M., Cranfield University (2010) *Gas Generator*. UK Patent number GB2468143A. [Assigned to Rolls-Royce]

REFERENCES

Anderson, J. D. (2006) *Hypersonics and High-Temperature Gas Dynamics*. Virginia: AIAA.

Bridgman, P.W. (1914) *A Complete Collection of Thermodynamic Formulas*. *Physical Review* **3** (4): 273–281. [Bibcode 1914PhRv...3..273B](#).
[doi:10.1103/PhysRev.3.273](#).

Casey, M.V. (2007) *Accounting for losses and definitions of efficiency in turbomachinery stages*. [Proceedings of the Institution of Mechanical Engineers, Part A: Journal of Power and Energy, Volume 221, Number 6 / 2007](#), pages 735-743, DOI: 10.1243/09576509JPE459.

Eames, D.J.H. (2006) *Short Haul Civil Tiltrotor Contingency Power System Preliminary Design*. NASA/CR-2006.214059. Available from:
<http://gltrs.grc.nasa.gov/reports/2006/CR-2006-214059.pdf> (Accessed 21/06/2011)

Feynman, R.P. (1986). Appendix F - Personal observations on the reliability of the Shuttle. NASA, available from:
<http://science.ksc.nasa.gov/shuttle/missions/51-l/docs/rogers-commission/Appendix-F.txt>

Goodger, E.M.(2000). *Transport Fuels Technology*. Margate: Thanet Press for Landfall Press.

Google (2011) *Google Ngram*, available from:
http://ngrams.googlelabs.com/graph?content=Joule+cycle%2COtto+cycle%2CDiesel+cycle%2CRankine+cycle%2CBrayton+cycle&year_start=1890&year_end=2008&corpus=1&smoothing=5 (accessed 23/01/2011)

Gorden, S. & McBride, B. J. (1994) NASA RP 1311, *Computer Program for Calculation of Complex Chemical Equilibrium Compositions and Applications. I. Analysis*, available from:

<http://www.grc.nasa.gov/WWW/CEAWeb/RP-1311.pdf> (accessed 20/02/2011)

Hofstadter, D. R. (1979) *Gödel, Escher, Bach: An eternal golden braid*. Harmondsworth: Penguin Books.

Hooker, S. G. (1984) *Not Much of an Engineer*. Shrewsbury: Airlife.

Kerrebrock, J. L. (1992) *Aircraft Engines and Gas Turbines*. 2nd edition. Cambridge, MA: MIT Press.

Krase, W. H. (1979) *ERICSSON CYCLE GAS TURBINE POWERPLANTS*. Rand Report R-2327, Available from:

<http://www.rand.org/pubs/reports/2006/R2327.pdf> (Accessed 20/07/2011)

Kuentzmann, P. & Falempin, F. (2002) *Ramjet, Scramjet & PDE, an Introduction*. Available from <http://www.onera.fr/conferences/ramjet-scrumjet-pde/> (accessed 20/07/2011)

Kurzke, J. (2003) *Achieving maximum thermal efficiency with the simple gas turbine cycle*. Available from:

http://www.mtu.de/en/technologies/engineering_news/development/Kurzke_Achieving_maximum_thermal_efficiency_en.pdf (accessed 23/02/2011)

M2dude (2010) *Olympus 593-610-14-28 Performance data*. Available from <http://www.pprune.org/tech-log/423988-concorde-question-13.html#post5918963> (accessed 19/07/2011).

McBride, B. J. & Gordon, S. (1996) NASA RP1311, *Computer Program for Calculation of Complex Chemical Equilibrium Compositions and Applications. II. Users Manual and Program Description*, available from:

<http://www.grc.nasa.gov/WWW/CEAWeb/RP-1311-P2.pdf> (accessed 23/02/2011)

Moore, G. E. (1965) Cramming more components onto integrated circuits. *Electronics, Volume 38 number 8*. Available from:

ftp://download.intel.com/museum/Moores_Law/Articles-Press_Releases/Gordon_Moore_1965_Article.pdf

Moran, M. J., Shapiro, H. N. (2006) *Fundamentals of Engineering Thermodynamics*, 5th edition, Chichester: John Wiley.

Murrell, J. (2008) *A Very Brief History of Thermodynamics*, available from: http://www.sussex.ac.uk/chemistry/documents/a_thermodynamics_history.pdf (accessed 05/02/2011)

NATO, (2007) *RTO-TR-AVT-036 Performance Prediction and Simulation of Gas Turbine Engine Operation for Aircraft, Marine, Vehicular, and Power Generation*. ISBN 978-92-837-0061-6. Available from: <http://www.rta.nato.int/pubs/rdp.asp?RDP=RTO-TR-AVT-036> (accessed 04/03/2011)

Oxford English Dictionary (2011) Thermodynamics. Available from: <http://oxforddictionaries.com/definition/thermodynamics> (accessed 12/07/2011)

Saravanamuttoo, H. I. H., Rogers, G. F. C., Cohen, H. (2001) *Gas Turbine Theory*. 5th ed. Pearson Education:Harlow.

Seddon, J. M. & Goldsmith, E. L. (1999) *Intake Aerodynamics*. 2nd edition. Oxford: Blackwell Sciences.

Walsh, P. P. & Fletcher, P. (2004) *Gas Turbine Performance*. 2nd edition. Oxford: Blackwell Sciences.

Wikipedia (2011A) *Lenoir Cycle*. Available from: http://en.wikipedia.org/wiki/Lenoir_cycle (accessed 12/07/2011)

Wikipedia (2011B) *Maxwell's thermodynamic surface*. Available from: http://en.wikipedia.org/wiki/Maxwell%27s_thermodynamic_surface (accessed 24/06/2011)

Wikipedia (2011C) *Transistor Count*. Available from: http://en.wikipedia.org/wiki/Transistor_count (accessed 21/07/2011)

Wintenberger, E. & Shepherd, J. E. (2005) *Thermodynamic Cycle Analysis for Propagating Detonations*. Available from:

<http://www.galcit.caltech.edu/EDL/publications/reprints/FickettJacobsCycle.pdf> (accessed 20/07/2011)

WolframAlpha (2011) *Stirling Cycle*. Available from

<http://www.wolframalpha.com/input/?i=Stirling+cycle> (Accessed 20/07/2011)

Zehe, M. J. (2010 A) *What is CEA?*, available from:

<http://www.grc.nasa.gov/WWW/CEAWeb/ceaWhat.htm> (accessed 20/02/2011)

Zehe, M. J. (2010 B) *CEA History*, available from:

<http://www.grc.nasa.gov/WWW/CEAWeb/ceaHistory.htm> (accessed 20/02/2011)

BIBLIOGRAPHY

Jean-Baptiste Michel*, Yuan Kui Shen, Aviva Presser Aiden, Adrian Veres, Matthew K. Gray, William Brockman, The Google Books Team, Joseph P. Pickett, Dale Hoiberg, Dan Clancy, Peter Norvig, Jon Orwant, Steven Pinker, Martin A. Nowak, and Erez Lieberman Aiden*. *Quantitative Analysis of Culture Using Millions of Digitized Books*. **Science** (Published online ahead of print: 12/16/2010)

Cranfield University. (2009) *The Prescribed Form for the Presentation of Theses*. Available from:

<http://www.cranfield.ac.uk/library/cranfield/documents/prescribedform0109.pdf> (accessed 23/01/2011)

Oxford Dictionaries Online, (2011) <http://oxforddictionaries.com/>

APPENDICES

Appendix A – CEA input and output files illustrating the extreme reversibility associated with equilibrium chemistry assumptions

A four species model of air evaluated at 2000 K, 10^5 Pa

Product mass fractions have been highlighted.

NASA-GLENN CHEMICAL EQUILIBRIUM PROGRAM CEA2, MAY 21, 2004
 BY BONNIE MCBRIDE AND SANFORD GORDON
 REFS: NASA RP-1311, PART I, 1994 AND NASA RP-1311, PART II, 1996

problem case= Steady_Flow_Combustor_|_Steady_Flow_Combustion_fixed_Total_T

hp p,bar=1, t,k=2000

reac

oxid Air t,k=2000

```

output trace=1.e-15 massf short transport
plot p t rho h u g s son
NCOL=20
end

```

```

WARNING!! AMOUNT MISSING FOR REACTANT 1.
PROGRAM SETS WEIGHT PERCENT = 100. (REACT)

```

THERMODYNAMIC EQUILIBRIUM COMBUSTION PROPERTIES AT ASSIGNED
PRESSURES

CASE = Steady_Flow_Com

REACTANT	WT FRACTION (SEE NOTE)	ENERGY KJ/KG-MOL	TEMP K
Air	1.0000000000000000	56469.5398151951012550	2000.0000000000000000

O/F= 0.0000000000000000 %FUEL= 100.0000000000000000 R, EQ. RATIO= 0.0015205319478539
 PHI, EQ. RATIO= 0.0000000000000000

THERMODYNAMIC PROPERTIES

P, BAR	1.0000000000000000
T, K	1980.1365497225706349
RHO, KG/CU M	0.1759096532720050

H, KJ/KG	1949.5706986444588438
U, KJ/KG	1381.0970637986647489
G, KJ/KG	-15812.9944695818194300
S, KJ/(KG)(K)	8.9703738717993584
M, (1/n)	28.9615280900403640
(dLV/dLP)t	-1.0000684621018425
(dLV/dLT)p	1.0020016203056588
Cp, KJ/(KG)(K)	1.3294385362980232
GAMMAS	1.2767214046745530
SON VEL, M/SEC	851.9286693149671237

TRANSPORT PROPERTIES (GASES ONLY)
 CONDUCTIVITY IN UNITS OF MILLIWATTS/(CM)(K)

VISC, MILLIPOISE	0.6910487554290171
------------------	--------------------

WITH EQUILIBRIUM REACTIONS

Cp, KJ/(KG)(K)	1.3294384110995707
CONDUCTIVITY	1.2336838551219640
PRANDTL NUMBER	0.7446857277053881

WITH FROZEN REACTIONS

Cp, KJ/(KG)(K)	1.2490512758576078
CONDUCTIVITY	1.1505340594362528
PRANDTL NUMBER	0.7502214493948671

MASS FRACTIONS

*Ar	0.0129159855888602
*CO	7.5720578898097401D-007
*CO2	4.8349780856493690D-004
*N	2.8772046124319455D-010
*NO	0.0073822765470936
NO2	2.0157274904001598D-005
NO3	3.7694543499786946D-011
*N2	0.7517311600504026
N2O	6.0764000016582201D-007
N2O3	4.8144008921296126D-013
N3	1.4671742245636806D-015
*O	1.4365664158798173D-004
*O2	0.2273219012438914
O3	8.3688178918876199D-009

* THERMODYNAMIC PROPERTIES FITTED TO 20000.K

NOTE. WEIGHT FRACTION OF FUEL IN TOTAL FUELS AND OF OXIDANT IN TOTAL OXIDANTS

Output file demonstrating equilibrium cooling of the products of the above reactions

Product mass fractions have been highlighted.

NASA-GLENN CHEMICAL EQUILIBRIUM PROGRAM CEA2, MAY 21, 2004
 BY BONNIE MCBRIDE AND SANFORD GORDON
 REFS: NASA RP-1311, PART I, 1994 AND NASA RP-1311, PART II, 1996

problem case= Steady_Flow_Combustor_|_Steady_Flow_Combustion_fixed_Total_T

hp p,bar=1, t,k=288

reac

oxid Ar	, wt= 0.0129159855888602	t,k=288
oxid CO	, wt= 7.5720578898097401E-007	t,k=288
oxid CO2	, wt= 4.8349780856493690E-004	t,k=288
oxid N	, wt= 2.8772046124319455E-010	t,k=288
oxid NO	, wt= 0.0073822765470936	t,k=288
oxid NO2	, wt= 2.0157274904001598E-005	t,k=288
oxid NO3	, wt= 3.7694543499786946E-011	t,k=288
oxid N2	, wt= 0.7517311600504026	t,k=288
oxid N2O	, wt= 6.0764000016582201E-007	t,k=288
oxid N2O3	, wt= 4.8144008921296126E-013	t,k=288
oxid N3	, wt= 1.4671742245636806E-015	t,k=288
oxid O	, wt= 1.4365664158798173E-004	t,k=288
oxid O2	, wt= 0.2273219012438914	t,k=288
oxid O3	, wt= 8.3688178918876199E-009	t,k=288

output trace=1.e-15 massf short transport
plot p t rho h u g s son

NCOL=20
end

THERMODYNAMIC EQUILIBRIUM COMBUSTION PROPERTIES AT ASSIGNED
PRESSURES

CASE = Steady_Flow_Com

REACTANT	WT FRACTION (SEE NOTE)	ENERGY KJ/KG-MOL	TEMP K
Ar	0.0129159854765452	-210.9806912500000067	288.0000000000000000
CO	7.5720578239645667D-007	-110830.9426749548147200	288.0000000000000000
CO2	4.8349780436053206D-004	-393884.5446296971058500	288.0000000000000000
N	2.8772045874123221D-010	472469.0192344780080000	288.0000000000000000
NO	0.0073822764828987	90968.0775594199803890	288.0000000000000000
NO2	2.0157274728717776D-005	33817.2767692177803840	288.0000000000000000
NO3	3.7694543172002373D-011	70656.6278780730790460	288.0000000000000000
N2	0.7517311535134916	-295.5908165084421739	288.0000000000000000
N2O	6.0763999488190025D-007	81210.2877959285106040	288.0000000000000000
N2O3	4.8144008502644993D-013	85894.9902800272539030	288.0000000000000000
N3	1.4671742118054129D-015	435635.0938473441638100	288.0000000000000000
O	1.4365664033877092D-004	248952.2934619995649000	288.0000000000000000
O2	0.2273218992671434	-297.9477281554356409	288.0000000000000000
O3	8.3688178191139736D-009	141402.7852364885038700	288.0000000000000000

O/F= 0.0000000000000000 %FUEL= 100.00000000000000 R, EQ. RATIO= 0.0015205318961876
 PHI, EQ. RATIO= 0.0000000000000000

THERMODYNAMIC PROPERTIES

P, BAR 1.0000000000000000
 T, K 312.5947519028580359
 RHO, KG/CU M 1.1144406093201455
 H, KJ/KG 10.1845398838290055
 U, KJ/KG -79.5465764840536309
 G, KJ/KG -2150.3935112600456705
 S, KJ/(KG)(K) 6.9117540777373510

 M, (1/n) 28.9651159580815829
 (dLV/dLP)t -0.999999998206626
 (dLV/dLT)p 0.999999984314979
 Cp, KJ/(KG)(K) 1.0054890173073159
 GAMMAS 1.3995517250043570
 SON VEL, M/SEC 354.3773958638400359

TRANSPORT PROPERTIES (GASES ONLY)

CONDUCTIVITY IN UNITS OF MILLIWATTS/(CM)(K)

VISC, MILLIPOISE 0.1933284444182592

WITH EQUILIBRIUM REACTIONS

Cp, KJ/(KG)(K) 1.0054890051825225
 CONDUCTIVITY 0.2724321581403039
 PRANDTL NUMBER 0.7135340650624969

WITH FROZEN REACTIONS

Cp, KJ/(KG)(K)	1.0054890051825225
CONDUCTIVITY	0.2724321581403039
PRANDTL NUMBER	0.7135340650624969

MASS FRACTIONS

*Ar	0.0129159854765453
*CO2	4.8468752692076719D-004
*NO	1.0403741357273225D-015
NO2	3.7978544106660819D-010
*N2	0.7551836879656890
*O2	0.2314156390308439

* THERMODYNAMIC PROPERTIES FITTED TO 20000.K

NOTE. WEIGHT FRACTION OF FUEL IN TOTAL FUELS AND OF OXIDANT IN TOTAL OXIDANTS

It may be seen from the above that all of the dissociation reactions produced by heating the 4-species “CEA air” to 2000 K have been reversed in the cooling process (the tiny fractions of NO and NO₂ remaining in the second output file are simply the equilibrium concentrations of those chemicals associated with dry air at 288 K and 10⁵ Pa).

Appendix B – the author's Patent

TITLE: GAS GENERATOR

DESCRIPTION

TECHNICAL FIELD

The present invention relates generally to gas generators and more particularly, but not exclusively, to gas generators for use in aero engines.

BACKGROUND ART

FLIGHT magazine, February 22, 1945, page 210 suggests the combination of a two-stroke piston engine with a gas turbine. The former is used as a gas generator, its exhaust gases being used to drive a gas turbine.

The piston engine is an example of a positive displacement motor, i.e. a motor in which a volume of fluid (in this case an air/fuel mixture) is trapped and the pressure of the fluid then used to generate an output torque. The gas turbine, in contrast, is an example of a dynamic (also known as "kinetic") motor in which there is no trapping of fluid, the output torque resulting instead from the motion of the fluid.

By their nature, positive displacement devices are capable of much greater pressure ratios than dynamic devices. As noted in the FLIGHT article, the positive displacement piston engine enables gases to be burned at high temperature and pressure before being led to the turbine. This, the article notes, gives better results than either the piston engine or the turbine alone as far as fuel consumption is concerned. No detail that might enable such a combination to be implemented in practice is provided in the FLIGHT article, however. This is understandable given that gas turbine technology was in its infancy at the time it was written.

US5692372 discloses an aircraft compound cycle propulsion engine having a fan and a core - gas generator - engine. The core engine comprises three rotary internal combustion engines of the Wankel type. These positive

displacement motors are fed with air by a dynamic (also known as "kinetic") axial compressor which is driven by the engines via a first shaft. The combustion products of the engines drive an axial flow power turbine (a dynamic or "kinetic" motor) which in turn drives the fan via a second shaft.

Gas generator assemblies of the free piston, positive displacement, internal combustion type are known, for example, from WO1980/000730 and from IEEE Transactions on Control Systems Technology, Volume 10, Issue 2, March 2002, pages 177-190, the latter disclosing a free-piston diesel engine.

The present invention has as an objective an improvement in the efficiency of gas generators over a range of operating conditions.

DISCLOSURE OF INVENTION

According to the present invention, there is provided:

a gas generator comprising:

a positive displacement gas motor configured to allow ingress of gas into the motor, to thereafter supply energy to the gas and thereafter allow egress of gas from the motor, the motor having a valve for controlling said egress; and

a compressor driven by the motor and configured to supply pressurised gas for ingress into the motor;

characterised by

a valve controller for controlling the valve such that the speed of the motor is independent of variation in the supply of energy to the gas.

By controlling the valve, it is possible to maintain a constant motor speed even when the supply of energy (e.g. fuel flow) to the gas varies. This allows the motor and compressor to continue to operate at their most efficient speed (at which the compressor is properly matched to the positive displacement motor) while enabling a variation in the gas generator output by varying the supply of energy.

For example, if the energy input is increased (e.g. by increasing the amount of fuel added to the air in each cycle), the valve can be adjusted to exhaust the chamber earlier in the cycle such that the energy used in driving the piston and thus the compressor remains the same. As a result, the speed of the compressor remains the same (preferably at its optimum operating speed) while the energy in the exhaust gases increases.

The positive displacement gas motor may comprise a chamber, a supply of energy to the gas in the chamber, a piston configured to move relative to the chamber under the action of the gas; and a valve for controlling the egress of gas from the chamber.

The piston may be configured to reciprocate in the chamber under the action of the gas. Such an arrangement enables higher compression than in the Wankel type engine employed in the aforementioned US5692372.

In particular, both piston and chamber may be of cylindrical form, enabling the kind of high compression known from conventional internal combustion engines.

Where the piston and chamber are cylindrical, the valve may comprise a sleeve moveable relative to a port in the chamber.

The supply of energy may be by way of fuel introduced into the gas in the chamber and then burnt. Combustion may be initiated by compression ignition.

Alternatively, energy may be introduced to the gas by means of a heat exchanger in the chamber.

The gas generator may comprise multiple pistons moving in multiple respective chambers.

The compressor may be a dynamic device (in contrast to a positive displacement compressor), in particular an axial or centrifugal flow compressor.

The present invention also provides an engine comprising a gas generator as set out above together with a turbine configured to be driven by the gas from the gas generator.

The turbine may drive a fan, which may be ducted or unducted.

The fan may be located upstream of the compressor and feed the compressor with air.

Alternatively the fan may be located downstream of the compressor. This may enable a shorter connection between the turbine and the fan.

Multiple chambers may be arranged radially about a central point. The resulting circular form may be more easily packaged with a fan and an aerodynamic compressor.

The present invention also provides a method of gas generation comprising:

providing a positive displacement gas motor configured to allow ingress of gas into the motor, to thereafter supply energy to the gas and thereafter allow egress of gas from

the motor, the motor having a valve for controlling said egress; and

providing a compressor driven by the motor and configured to supply pressurised gas for ingress into the motor; and

controlling the valve such that the speed of the motor is independent of variation in the supply of energy to the gas.

BRIEF DESCRIPTION OF DRAWINGS

An embodiment of the invention will now be described by way of example with reference to the accompanying drawings, in which:

Figure 1 is a block diagram of an aero engine according to a first embodiment of the present invention;

Figure 2 is a schematic view of the positive displacement gas motor used in the embodiment of figure 1;

Figure 3 is a block diagram of a stationary engine according to a second embodiment of the present invention.

DETAILED DESCRIPTION OF SPECIFIC EMBODIMENTS

Figure 1 is a block diagram of an aero engine 10 according to an embodiment of the present invention and

incorporating a gas generator 15 comprising a positive displacement gas motor 30 and a compressor 20.

Air entering the engine (indicated at 15) first undergoes steady flow compression by compressor 20 before being supplied (as indicated at 25) to positive displacement gas motor 30.

Within the gas motor 30, the air undergoes non-flow compression (indicated by process step 35) followed by heat addition at substantially constant volume (indicated by process step 40) followed by non-flow expansion (indicated by process step 45). Work is extracted during the non-flow expansion to drive the compressor via shaft 70.

Gas generated by gas generator 15 (as indicated at 50) is fed to turbine 55 where it undergoes steady flow expansion, exiting the turbine as indicated at 60. The turbine 55 drives a fan 65 which, in the embodiment shown, is of the rear-mounted unducted type.

Figure 2 is a schematic diagram of the positive displacement gas motor 30, which comprises a piston 100 configured to move relative to a chamber 110. In the embodiment shown, piston 100 reciprocates in the chamber 110 and is connected via connecting rod 120 to crankshaft 130 which in turn drives the compressor as indicated at 70 in

figure 1. Piston 100 and chamber 110 are both cylindrical and of circular cross-section.

Ingress of air to the chamber (as indicated at 25) takes place through an inlet valve 140, which is then closed and the air in the chamber compressed by the upward (as seen in figure 2) stroke of piston 100. This positive displacement, non-flow compression (process step 35 in figure 1) is followed by energy addition, e.g. by the addition of heat by compression ignition of fuel in the chamber. This occurs towards the end of the upward stroke of the piston and towards the beginning of the downward stroke, i.e. at substantially constant chamber volume (process step 40 in figure 1). Positive displacement, non-flow expansion of the heated gas then follows on the downward stroke of the piston (process step 45 in figure 1), the work done by the gas being transmitted solely to crankshaft 130 until such time as egress of the heated gas from the chamber is allowed (as indicated at 50) by opening exhaust valve 145.

The operation of exhaust valve 145 is controlled by valve controller 150 such that the speed of the motor 30 is independent of variation in the supply of energy to the gas, the exhaust valve timing being controlled such that sufficient work is extracted during the non-flow expansion of

the gas to power the compressor 20 and the motor 30 while retaining the maximum possible energy in the exhaust gases.

Accordingly, if greater exhaust gas energy is required, e.g. to increase the speed of turbine 55 and its associated fan 65, the amount of fuel added to the air in each cycle can be increased (e.g. by a fuel pump feeding a fuel injector, not shown). This increase in gas energy results in the work necessary to drive the motor and compressor at their most efficient ("matched") speed being achieved earlier in the expansion stroke. Accordingly, the valve controller 150 can open the exhaust valve 145 earlier in the expansion stroke, resulting in the exhaust gas having higher energy. It will be appreciated that the rotational speed and power output of the gas generator comprising compressor 20 and motor 30 can be varied independently, which is not the case with a conventional gas turbine. This allows scope for optimisation, and therefore possible further improvement in off-design performance.

The valve controller 150 may be an active electrical or pneumatic system (rather than fixed gearing) and may be linked to the management computer for the engine as a whole.

Valve 145 may be a sleeve valve moveable relative to a port in the chamber, the simplified ductwork enabled by such

an arrangement enhancing the overall volumetric efficiency of the gas generator.

Higher power density is achieved by the use of a two-stroke cycle, while the use of compression ignition may allow the use of widely-available fuel such as "Jet A", which is cheaper and more readily available than Avgas. Jet A has a low octane number, but a reasonable cetane number, and therefore is far better suited to compression ignition. Moreover, spark ignition engines suffer from limited practical overall pressure ratio due to pre-ignition and/or detonation of the charge, thus limiting their efficiency. In non-aerospace applications, compression ignition engines are inherently better suited to burning alternative fuels.

To facilitate starting of a gas motor using compression ignition, a suitably sized starter may be employed to bring the gas generator up to sufficiently high speed as to ensure successful compression ignition. Alternatively/in addition, an auxiliary source of ignition may be provided such as an electrically heated glow-plug. It will be appreciated that limitations on the available starting measures may limit the geometric compression ratio of the gas motor.

Although only a single piston/chamber combination is shown in figure 2, the gas motor may comprise multiple pistons and chambers, in which case a common rail fuel

injection system may be used, providing reliability and improved atomisation at high pressure ratios.

Arranging multiple pistons and chambers radially about a central point simplifies the packaging of the engine since the compressor and power turbine are typically circular in cross-section.

As regards the compressor 20, it will be appreciated that this helps reduce the physical size of the motor 30. Where a two-stroke piston engine is used, the compressor also allows for adequate scavenging. The compressor 20 may be powered by the motor by means of a step-up gearbox (not shown) having a ratio between 2 and 3. For steady flow compression, a dynamic rather than positive displacement compressor is used, which for aeronautical applications may be an axial flow compressor. However, the final stage or stages of the compressor may use centrifugal flow to isolate the compressor from the piston engine downstream. The pressure ratio across the compressor may be around 10.

As regards the turbine 55, this has - unlike the compressor - no mechanical drive connection with the gas motor 30. Rather, it is fed by the exhaust gas (as indicated at 50 in figure 1). Turbine 30 may have several stages and may drive contra-rotating open rotors 65 at the back of the engine, downstream of the compressor. The ultra-high bypass

ratios enabled by such an arrangement are suited to the gas generator machine when used as an aero engine core. They may also enable a shorter connection between the turbine and the fan. The rotational speed of the power turbine may be governed by a control system using variation of the pitch of the open rotors. It may also be advantageous to gear the drive from the turbine to the fan. An alternative, more conventional, arrangement has a ducted fan at the front of the engine, upstream of the compressor and feeding the latter with air.

Typically, for a twin-engined aircraft having a mass of 10^5 kg and a target Lift:Drag ratio of 20:1, the thrust requirement is around 25 kN per engine. Assuming a cruise speed of 220 m/s, this equates to 5.5 MW of thrust power.

Figure 3 is a block diagram of a second embodiment of the present invention for stationary applications. As with the first embodiment, it incorporates a gas generator 15 comprising a positive displacement gas motor 30 and a compressor 20 driven by the motor. Without the packaging requirements of an aero engine, the choice of compressor design is less restricted and geometries other than radial may be used for the gas motor.

In the stationary application shown, gas egress 50 is used to drive a gas turbine 200 having an output shaft 210

which may in turn drive, for example, a generator (not shown).

Gas exhausting from the turbine (as indicated at 60) can further be passed through an exhaust heat recovery unit 220, as known per se from conventional gas turbines in combined cycle plants.

Moreover, the gas generator according to the present invention is also applicable to plant where there is no combustion, energy generation being instead e.g. by nuclear means, in which case heat transfer to the gas in the chamber may be by means of a heat exchanger. In such circumstances, the gas may be held in a closed circuit, being fed back to the compressor following egress from the turbine or exhaust heat recovery unit.

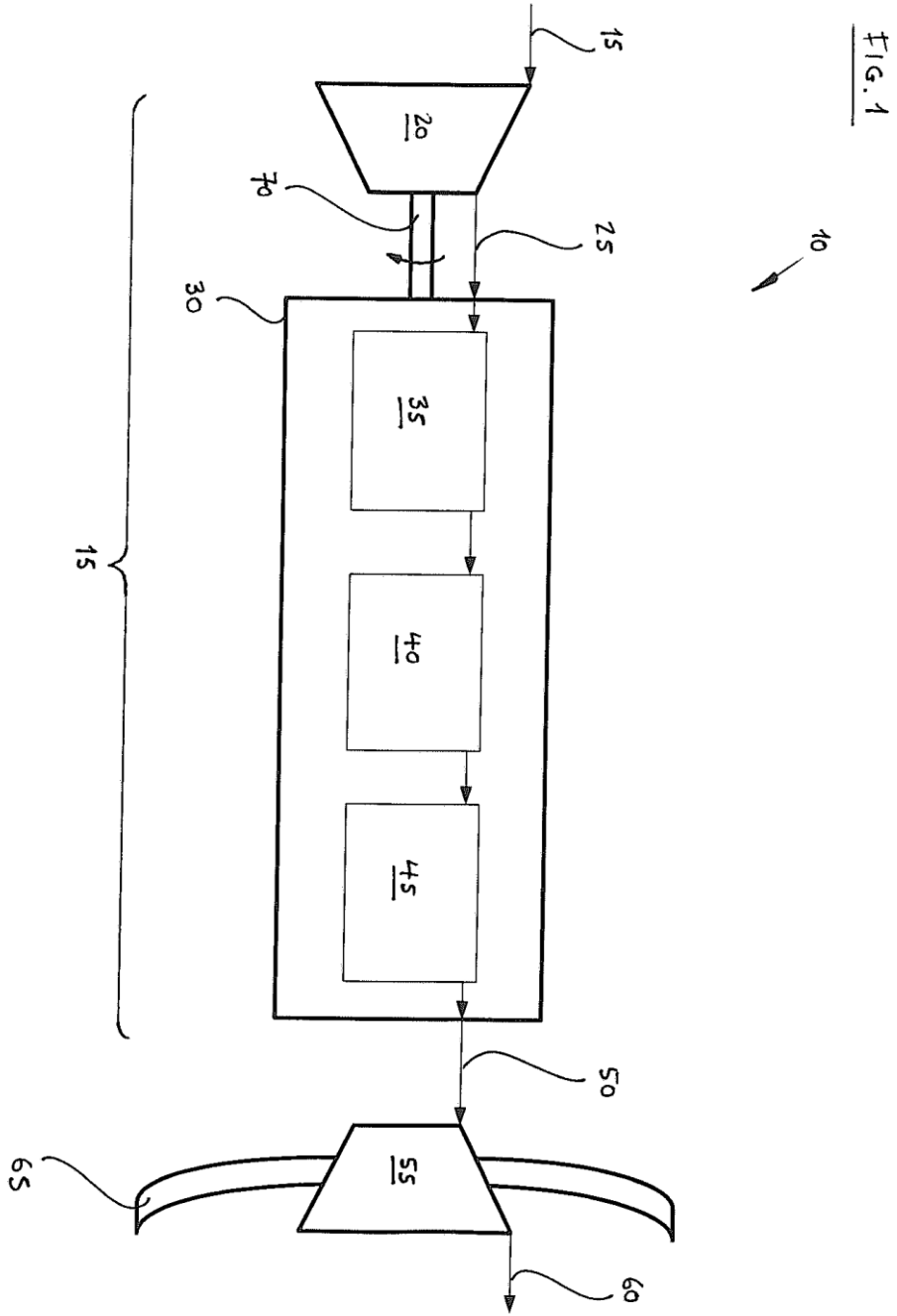
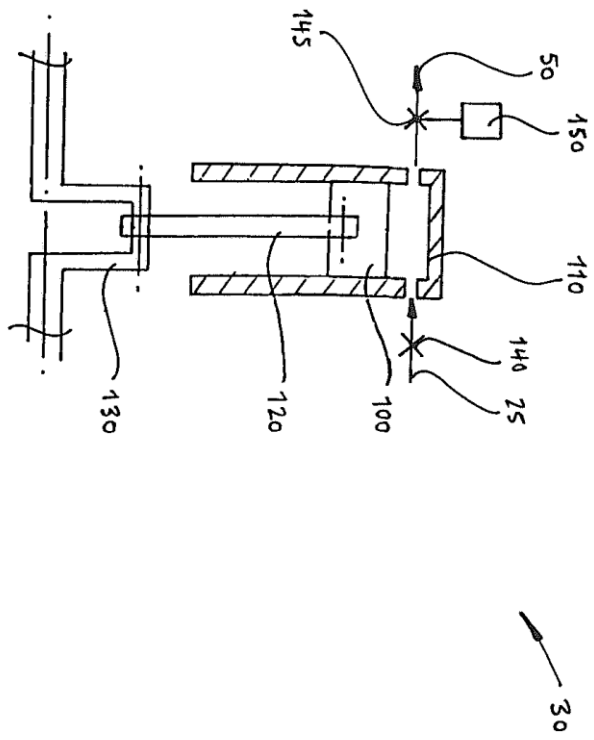


FIG. 2



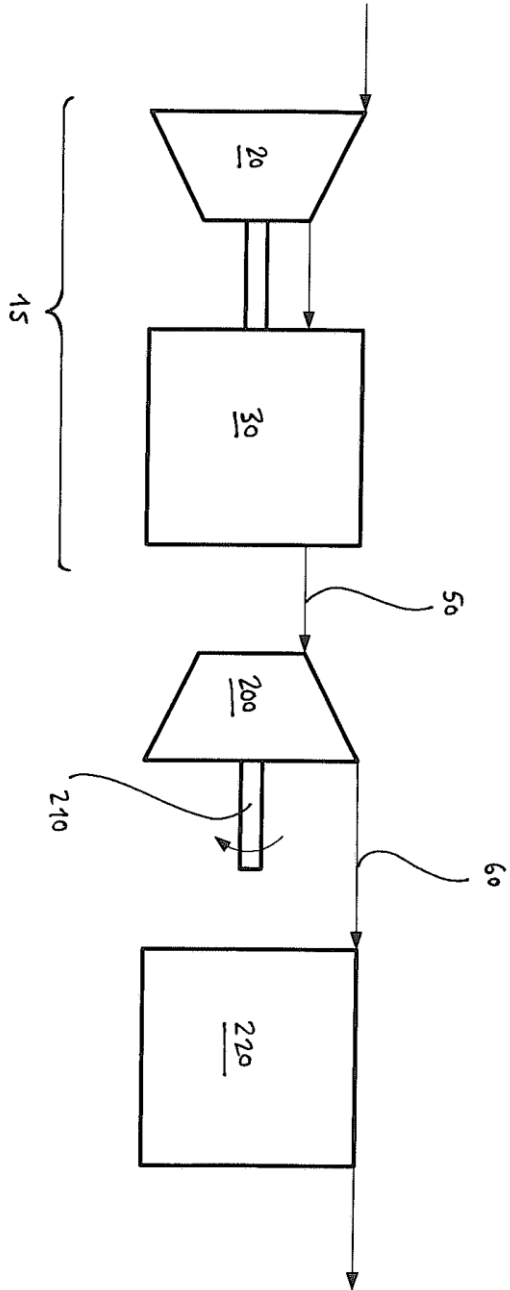


FIG. 3